UNIVERSITY OF COPENHAGEN
FACULTY OF SCIENCE

Master's thesis

# Charge bond order in kagome metals

Eva López Rojo

Advisor: Brian Møller Andersen

Submitted: June 16, 2023

# Abstract

The vanadium kagome metals $AV_3Sb_5$ have been the subject of extensive research since their synthesis in 2019, both theoretically and experimentally. Due to the unique geometry of the kagome layer, their electronic structures exhibit flat bands, van Hove singularities and Dirac cones, making them an excellent platform for investigating the interplay between correlation effects, geometric frustration, and topology. Notably, all three compounds are found to enter a charge density wave phase at high temperature, which breaks translational symmetry generating a 2x2x2 supercell. Additionally, this phase is also reported to break time reversal symmetry and exhibit a giant anomalous Hall effect despite the absence of long-range magnetic order. The focus of this thesis lies in the study of the emergence of said charge density wave phase from electronic interactions. A nearest-neighbour Hubbard model on the kagome lattice is presented, which is decoupled using a Hubbard-Stratonovich transformation. Within mean-field theory, the Ginzburg-Landau free energy is analyzed to determine the potential order parameters of the symmetry-broken phase.

# Acknowledgements

I would like to start by thanking Brian Møller Andersen for supervising me during this year, whose easygoing and kind nature makes it a pleasure to work with. Furthermore, I want to thank Morten Holm Christensen for guiding me through the entirety of this project, sitting with me through very long meetings and always being willing to answer all of my questions. I am extremely grateful for his patience and for the immense knowledge I have gained from him. More generally, I would like to thank the entirety of the CMT group for creating such a friendly and relaxed environment, and for making me feel so welcomed.

Secondly, I want to thank Sofie Castro Holbæk and Luca Buiarelli for being the best office mates. Your passion for physics is contagious, creating the perfect environment for the long days we spent in the office, which did not feel so long anymore. More importantly, their support on a personal level was essential, allowing me to put things into perspective and push through the most challenging times of this project. The later statement I would like to extend to Qiyu Liu and Madalena Branco. All of them have made me grow incredibly during these two years, and I will always be in awe of my luck of finding them. I will keep these memories and friendships regardless of wherever we end up.

Last, but certainly not least, I would like to thank my parents. Muchas gracias por el apoyo económico, pero sobre todo moral que me habeís brindado durante estos dos años. Sin vosotros, nada de esto hubiese sido posible. Gracias por haber creido en mi, sobre todo cuando más lo necesitaba, y por siempre ser una inspiración y mis modelos a seguir.

# Contents

# Chapter 1

# Introduction

The familily of kagome metals $AV_3Sb_5$, where A stands for the alkali atom cesium, potasium and rubidium, where first synthesised in 2019 [1]. The kagome layer, which is formed by the vanadium atoms, provides these compounds with exotic properties that still make them a trending subject in current research. Their band structure shows Dirac cones, flat bands and van Hove singularities, meaning the existence of potential interplay between topologically nontrivial surface states and substantial electron correlation effects [2].

More importantly for this project, they are found to undergo a charge density wave phase at high temperature. It is in this phase that superconductivity settles at much lower temperatures. The symmetry of the Cooper pairing is crucial to understanding the mechanism that drives superconductivity in this materials, reason why it is a focal point of current experimental and theoretical discussions [3]. The possibility of this family of materials hosting a wide range of unconventional superconducting states is still subject to discussion, both in experimental and theoretical settings, including $d+id$ chiral superconductivity and $f-$wave spin triplet, although the common $s$-wave superconductivity is still a potential option [4]. Therefore, understanding the charge density wave could also aid in determining the symmetry of the Cooper pairing.

The origin of the charge density wave phase still remains an open question. The Fermi level is found to be remarkably close to the van Hove singularity, point at which the Fermi surface is hexagonal. As a result, and due to the *pure* character of the van Hove singularity, nesting effects promote bond orders, and more generally, can trigger a multitude of competing instabilities [5, 6]. This is the reasoning behind the widespread belief that the charge density wave is and instability driven by the electronic degree of freedom. However, there is no direct evidence of such a statement, and it is most probable that is it a coupling between the phonons and the electrons which are behind this instability.

Given this introduction, the rest of the document is organized as follows: The next chapter will dive a bit deeper in the $AV_3Sb_5$ metals and the main experimental evidence that have been found so far, focusing specially in the charge density wave phase. Chapter 3 will present a simple nearest-neighbour tight-binding model, which will aid on the understanding of the main features of the kagome lattice. Chapter 4 gives an overview of some the theoretical approaches that have been presented so far in the literature with the aim of modelling the charge density wave in these materials. Chapter 5 shows the model and the microscopic approach that was chosen to tackle the problem in this thesis, presenting the mean-field solutions. Chapter 6 will continue this discussion, delving into the free energy

expression and the second order term of its perturbative expansion. Finally, this work will be wrapped up by the conclusions is Chapter 7, accompanied by an outlook into possible ways of continuing with this research.

# Chapter 2

# $AV_3Sb_5$ kagome metals

Gathering the fundamental results of the extensive research that has been done in the recent years regarding the $AV_3Sb_5$ compounds has been undertaken before in the literature, for instance in the review papers [4] and [3]. This chapter will follow this same line of work, attempting to do an overview of the most relevant experimental findings regarding these materials for the present project.

The compounds $AV_3Sb_5$, where A stands for the alkali atoms Cs, K and Rb, form a layered structure, where the Vanadium atoms arrange in the kagome lattice structure, as shown in Fig. 2.1. The antimony atoms fill the center of the V hexagons, as well as form a honeycomb lattice both above and below this layer. Finally, a triangular layer of the alkali atoms completes the structure. Such arrangement has six-fold rotational symmetry, three mirror planes and inversion symmetry, making it belong to the $P6/mmm$ space group. The associated point group symmetry of the center point (also called $\Gamma$ point) is $D_{6h}$ and the Brillouin zone (BZ) is just an hexagonal prism. The point group symmetry is translated into the reciprocal space, making it possible to define certain points in this space that are invariant under the symmetry operations. These points define a so called high-symmetry line, as it is depicted in Fig. 2.2(c).

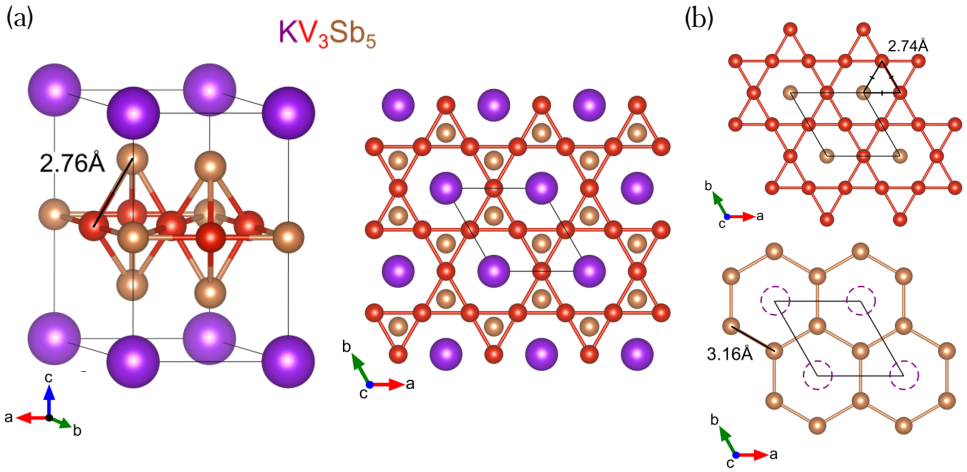


Figure 2.1: (a) Crystal structure of the $AV_3Sb_5$ compounds, in particular for A=K, accompanied by the top-down view. (b) Decomposition of the structure into the kagome and honeycomb layers of the vanadium and antimony atoms, respectively. Figures from Ref. [7].

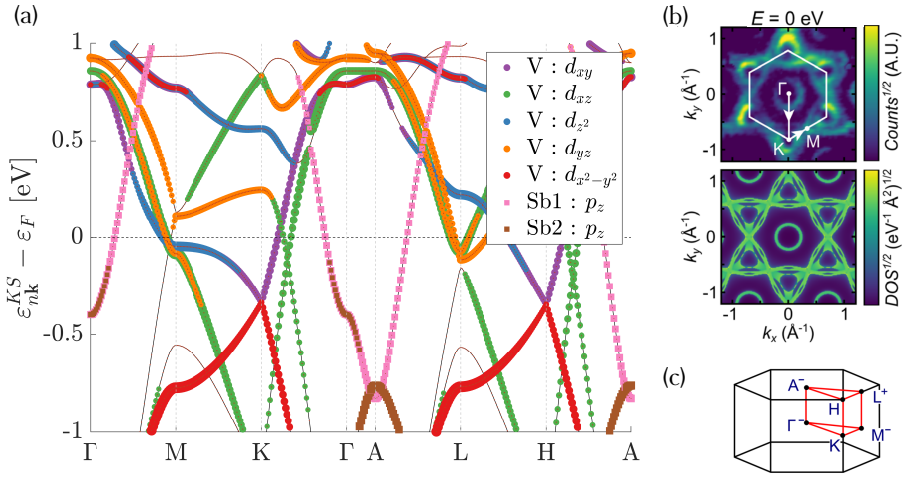


Figure 2.2: (a) Energy bands from DFT calculations [9]. The different colors mark the orbital projections of the wavefunctions. (b) Comparison of the Fermi surface of $CsV_3Sb_5$ from ARPES data and DFT calculations [8], which show great agreement with each other. The hexagonal Brillouin zone is superimposed on the ARPES data. (c) Three-dimensional BZ of the $P6/mmm$ space group, highlighting the high symmetry line along which the energy bands are calculated [8].

The electronic nature of the compounds have been studied through density functional theory (DFT) calculations and angle-resolved photoemission spectroscopy (ARPES) measurements. As one can see from Fig. 2.2(a), there are multiple multiple band crossings around the Fermi level. Around Γ there is an electron-like parabolic band, that appears as a circular electron pocket in the Fermi surface (Fig. 2.2(b)). From the orbital projections it is apparent that it originates from the antimony $p_z$ orbitals. The Fermi contours near the first BZ boundary at the $M$ and $K$ points are dominated by the vanadium atoms. At the $K$ point there is a Dirac cone associated with the vanadium $d_{xy}$ and $d_{x^2-y^2}$ orbitals. Connected to it there is a van Hove (vH) point very close to the Fermi level at the $M$ point. Also at the $M$ point and only slightly further from the Fermi level there is a second vH point associated with the vanadium $d_{xz}$ and $d_{yz}$ orbitals. Both ARPES and DFT calculations show very little dispersion along $k_z$ of the Fermi surfaces [8], hinting at the quasi-2D nature of these materials.

Said quasi-2D character can be further confirmed by electrical resistivity measurements. Fig. 2.3(a) presents its temperature dependence, which shows that the out-of-plane resistivity is around 600 times larger than the in-plane data. Additionally, a kink can be observed at around 94K for $CsV_3Sb_5$. This kink is accompanied by a sharp peak in the heat capacity data at this same temperature, as shown in Fig. 2.3(b), indicating that the phase transition that the system is undergoing is of first order. The other two compounds are also found to undergo the same phase transition, but at around 78K and 103K for the potasium [7] and rubidium [10] compounds, respectively.

Before analyzing further the charge density wave, let us discuss the electrical resistivity measurements at lower temperatures. The zero-field curve in Fig. 2.3(c) shows a broad transition at around 2.5K, which is suppressed by the addition of a magnetic field, hallmark of superconductivity. The corresponding phase transitions for $KV_3Sb_5$ and $RbV_3Sb_5$ happen at around 0.93K and 0.92K, respectively.

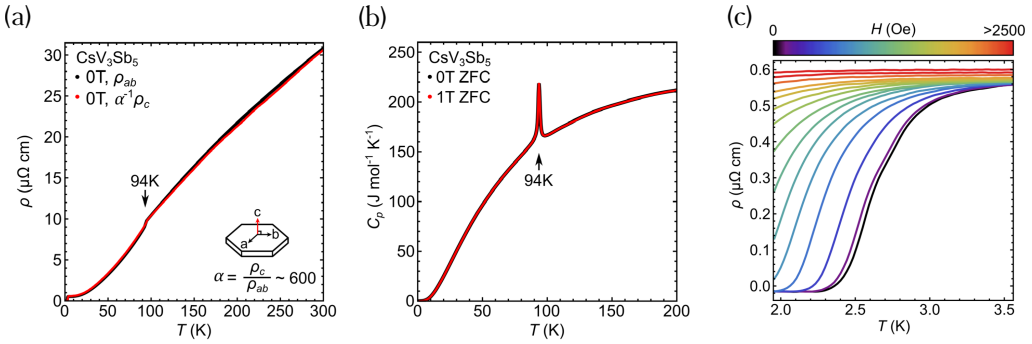


Figure 2.3: Temperature dependent data of (a) the electrical resistivity in and out-of-plane, showing the strong anisotropy and a kink at around 94K, (b) the heat capacity with and without an applied magnetic field, showing a peak at this same temperature and (c) of the electrical resistivity at low temperatures, also as a function of applied magnetic field, showcasing the onset of superconductivity at around 2.5K. All three measurements belong to $CsV_3Sb_5$. Figures from Ref. [8].

Elastic neutron scattering [1] and muon spin spectroscopy [11] show evidence of the absence of long-range magnetic order, meaning that phase transition that occurs at 78-105K derives primarily form the charge degree of freedom. Scanning tunneling microscopy (STM) measurements performed on the antimony surface [12] reveal that upon lowering the temperature across the critical temperature of the phase transition the unit cell gets enlarged in both in-plane directions, as depicted in Fig. 2.4(a)-(b). This phase of matter, which involves a redistribution of the charge that breaks translational symmetry is denominated charge density wave (CDW). Said $2 \times 2$ in-plane modulation is further observed in the Fourier transformed topographic images, where six additional peaks appear additional to those from the primary lattice structure. The modulation wavevectors, which correspond to 1/2 of the Bragg peaks, correspond to the momenta of the three $M$-points that can be defined in the hexagonal BZ. STM also shows an energy gap opening around the Fermi energy of around 50meV [12], which also disappears above the transition temperature (Fig. 2.4(c)). Furthermore, there seems to be a momentum structure of the gap function [13]. As it can be observe in Fig. 2.4(d), there is a gap opening around the BZ boundary but it disappears near the $\Gamma$ point. While the in-plane modulation is widely established, the modulation in the $c$ direction is still debated: there is experimental evidence for both $2 \times 2 \times 2$ [14] and $2 \times 2 \times 4$ [2] charge modulations.

Additionally, the low temperature spectroscopic data of the charge modulation vector peaks at zero field are reported to show strong anisotropy in their intensity in all three compounds [12, 15, 16]. A chirality can thus be defined in the direction form the lowest to the highest vector peaks, as showed in Fig. 2.5(a) for $KV_3Sb_5$. This chirality can be switched by an applied magnetic field along the $c$ axis [12], changing from anticlockwise to clockwise upon changing the magnetic field orientation. This suggest the breaking of the time-reversal symmetry in the CDW phase, specially intriguing given the lack of long-range magnetic order previously mentioned. Stronger evidence for the time-reversal Symmetry breaking (TRSB) is found in the zero-field muon spin relaxation ($\mu$SR) spectroscopy measurements [17]. As depicted in Fig. 2.5(b), the temperature dependence of the muon spin relaxation rates show a noticeable increases immediately after crossing the CDW transition temperature, indicating the existence of internal magnetic fields.

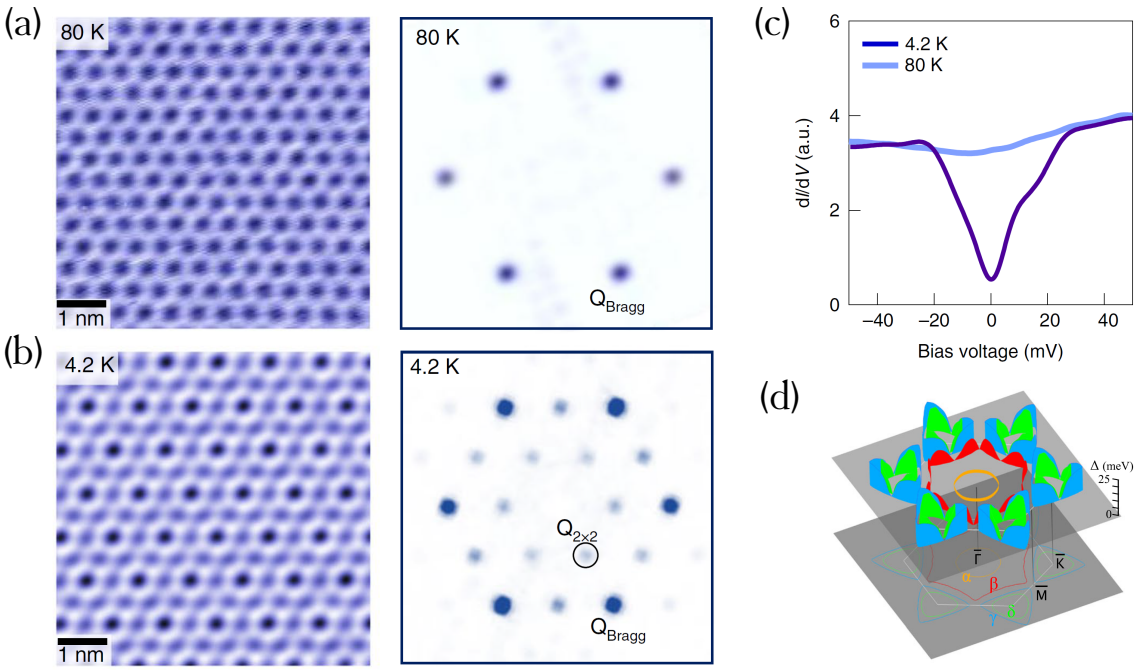


Figure 2.4: STM topographic images and their Fourier transform of the antimony surface above (a) and below (b) the transition temperature, showcasing the $2 \times 2$ charge modulation. Figures from Ref. [12]. (c) Spectroscopic imaging data of the energy gap for the antimony surface. Figure from Ref. [12]. (d) 3D plot of the Fermi surface and momentum dependent structure of the energy gap at 5K. Figure from Ref. [13]. All data presented correspond to the compound $KV_3Sb_5$.

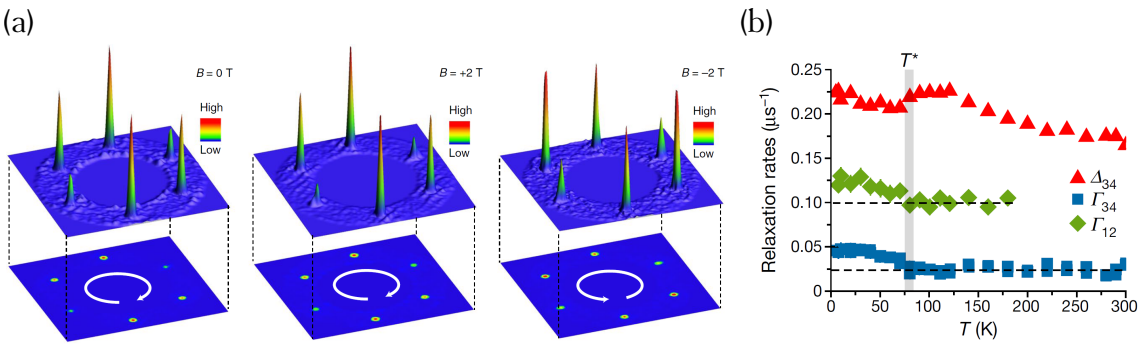


Figure 2.5: (a) Spectroscopic data for $KV_3Sb_5$ of the CDW vector peaks with and without the presence of an applied magnetic field, showing the ability to switch the chirality with said magnetic field. Figure from Ref. [12]. (b) Temperature dependence of the relaxation rates from $\mu$SR experiments in $KV_3Sb_5$. Figure from Ref. [17].

# Chapter 3

# The kagome lattice and the tight-binding model

Given the experimental evidence that the physical properties of $AV_3Sb_5$ are primarily determined by its two-dimensional structure, and in particular by the vanadium kagome layer, a first natural step in the study of these materials is to construct a simple model that solely accounts for this layer. Consequently, in this chapter a nearest-neighbour one-orbital tight-binding model will be formulated. Despite its simplicity, it still showcases the main features of the band structure, which will be key to the discussion of the charge density wave phase in these materials. However, prior to that it is needed to outline the basic features of the lattice, both in real and momentum space.

## 3.1 The kagome lattice

The kagome lattice, as shown schematically in Fig. 3.1, is a two-dimensional tripartite lattice. This allows to divide the lattice in three subsets, which will be denoted by $A$, $B$ and $C$. The unit cell and its corresponding primitive lattice vectors are also depicted in the figure. When assuming the distance between unit cells to be one, these vectors take the values

$$\vec{t}_1 = (1, 0) \qquad \vec{t}_2 = \left(\frac{1}{2}, \frac{\sqrt{3}}{2}\right). \tag{3.1}$$

Taking the site $A$ to be the origin of the unit cell, the basis vectors, which position the three sites in the unit cell, are

$$\vec{d}_A = (0, 0)\ , \qquad \vec{d}_B = \frac{1}{2}\vec{t}_2\ , \qquad \vec{d}_C = \frac{1}{2}\vec{t}_1\ , \tag{3.2}$$

and the vectors that connect two sites $\vec{a}_{\alpha\beta} = \vec{d}_\beta - \vec{d}_\alpha$ are

$$\vec{a}_{AB} = \frac{1}{2}\vec{t}_2\ , \qquad \vec{a}_{AC} = \frac{1}{2}\vec{t}_1\ , \qquad \vec{a}_{BC} = \frac{1}{2}(\vec{t}_2 - \vec{t}_1)\ . \tag{3.3}$$

Given the translational symmetry of the real-space lattice, it becomes convenient to work in momentum space, where one can define the reciprocal lattice. The definition of the reciprocal lattice vectors can be derived by their relation to the primitive lattice vectors $\vec{g}_i \cdot \vec{t}_j = 2\pi\delta_{ij}$, which are

$$\vec{g}_1 = 2\pi\left(1, -\frac{1}{\sqrt{3}}\right)\ , \qquad \vec{g}_2 = 2\pi\left(0, \frac{2}{\sqrt{3}}\right)\ . \tag{3.4}$$

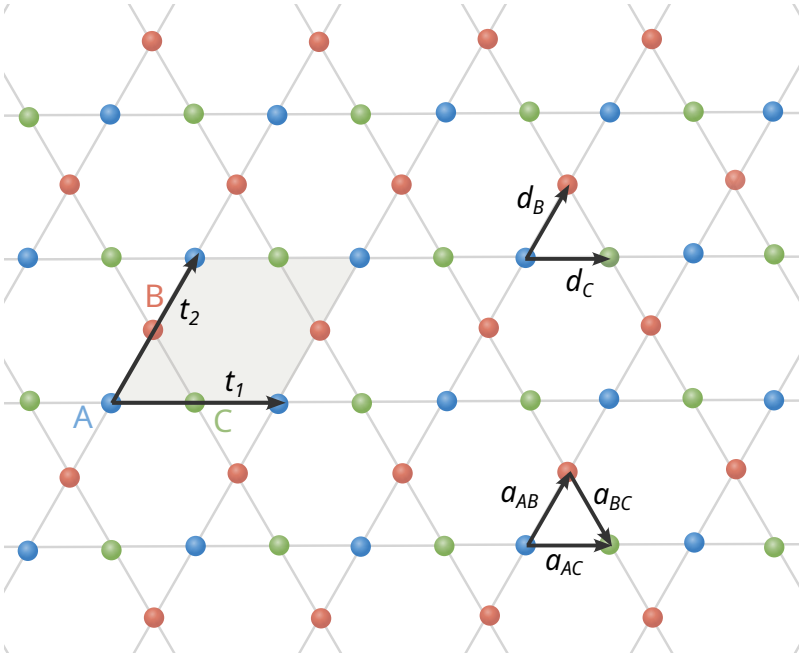


Figure 3.1: Representation of the kagome lattice in real space. The three different subsets of lattice sites are labeled by $A, B$ and $C$ and colored in blue, orange and green respectively. The primitive lattice vectors $\vec{t}_i$ are included and the unit cell that they define is shaded in gray.

The spacial modulations driven by momenta that only differ an integer number of reciprocal lattice vectors $\vec{g}_i$ are equivalent. Therefore, it is possible to restrict oneself to a section of the momentum space such that all the momenta inside produce spacial modulations that are unique, and which constructs the first Brillouin Zone (BZ). The high symmetry points of the kagome lattice are the $\Gamma$ point, in the center of the hexagonal BZ, the $M$ points at the center of the edges, and the $K$ points, located at the vertices. The reciprocal lattice and the high symmetry line are depicted in Fig. 3.2(a).

The three independent $M$-points that can be defined in the first BZ, and which will henceforth be referred to as $M_1$, $M_2$ and $M_3$, are defined by the vectors:

$$\vec{Q}_1 = \frac{1}{2}\vec{g}_1 \ , \qquad \vec{Q}_2 = \frac{1}{2}\vec{g}_2 \ , \qquad \vec{Q}_3 = -\frac{1}{2}(\vec{g}_1 + \vec{g}_2) \ , \tag{3.5}$$

respectively. One could have equivalently defined the $M$-points to be those located in the opposite edges of the hexagonal BZ, since they are connected by reciprocal lattice vector. As a result, the $M$-vectors verify $\vec{Q}_i \equiv -\vec{Q}_i$, and are represented in Fig. 3.2(b).

Having presented the basics of the kagome lattice, we are now prepared to dive into the setup of the tight-binding model.

## 3.2 Nearest-neighbour tight-binding model

The kinetic energy portion of the non-interacting Hamiltonian corresponding to the electrons on the lattice can be described by a tight-binding model. In its simplest form, this Hamiltonian allows hopping between nearest neighbours with a hopping amplitude $t > 0$

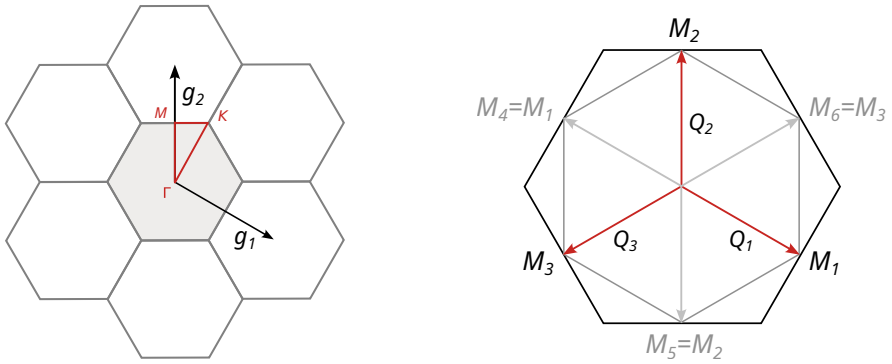


(a) (b)

Figure 3.2: (a) Reciprocal lattice of the real space kagome lattice. $\vec{g}_i$ are the reciprocal lattice vectors, in gray the first Brillouin Zone is shaded and in red the high-symmetry points and line are displayed. (b) Representation of the $M$ points and their respective vectors in the first BZ.

that is equal between all sites. Each atom in the unit cell has four nearest neighbours: the other two atoms in the unit cell, and two in the adjacent unit cells.

In its second-quantized form, the tight-binding Hamiltonian can be written in terms of the fermionic creation and annihilation operators, $c^\dagger_{\vec{R}\sigma\alpha}$ and $c_{\vec{R}\sigma\beta}$, as follows:

$$H_{TB} = -t \sum_{\vec{R}\sigma} \sum_{\alpha\neq\beta} \left( c^\dagger_{\vec{R}\sigma\alpha} c_{\vec{R}\sigma\beta} + c^\dagger_{\vec{R}\sigma\alpha} c_{\vec{R}-2\vec{a}_{\alpha\beta}\sigma\beta} \right) - \mu \sum_{\vec{R}\sigma\alpha} c^\dagger_{\vec{R}\sigma\alpha} c_{\vec{R}\sigma\alpha}. \tag{3.6}$$

Here, $\vec{R}$ represents the unit cell, $\sigma$ denotes the spin, and $\alpha, \beta$ the sublattice site within the unit cell. This means that the site $\alpha$ in the unit cell $\vec{R}$ is located at the position $\vec{R} + \vec{d}_\alpha$. A neighbour $\beta$ of this site located in a different unit cell is connected to it by the vector $\vec{a}_{\beta\alpha} = -\vec{a}_{\alpha\beta}$. Therefore, its position will be $\vec{R} + \vec{d}_\alpha - \vec{a}_{\alpha\beta} = \vec{R} - 2\vec{a}_{\alpha\beta} + \vec{d}_\beta$, consequently belonging to the unit cell $\vec{R} - 2\vec{a}_{\alpha\beta}$. The first term in the Hamiltonian is then the intra-cell hopping while the second term the inter-cell. Hereafter, the spin degree of freedom will be implicitly summed over.

The solution to the Hamiltonian is most easily achieved by going to momentum space, given that the electronic wave functions in the lattice are modulated by plane waves. Considering periodic boundary conditions and a system with $\mathcal{N}$ unit cells, the Fourier transform of the annihilation operator is $c_{\vec{R}\alpha} = \frac{1}{\sqrt{\mathcal{N}}} \sum_{\vec{k}} e^{i\vec{k}\cdot\vec{R}} c_{\vec{k}\alpha}$ and the Hamiltonian then becomes:

$$\begin{aligned} H_{TB} &= -t \sum_{\vec{k}} \sum_{\alpha\neq\beta} c^\dagger_{\vec{k}\alpha} \left( 1 + e^{-2i\vec{k}\cdot\vec{a}_{\alpha\beta}} \right) c_{\vec{k}\beta} - \mu \sum_{\vec{k}\alpha} c^\dagger_{\vec{k}\alpha} c_{\vec{k}\alpha} \\ &= -\sum_{\vec{k}} \begin{pmatrix} c^\dagger_{\vec{k}A} & c^\dagger_{\vec{k}B} & c^\dagger_{\vec{k}C} \end{pmatrix} \begin{pmatrix} \mu & t(1+e^{-2i\vec{k}\cdot\vec{a}_{AB}}) & t(1+e^{-2i\vec{k}\cdot\vec{a}_{AC}}) \\ t(1+e^{2i\vec{k}\cdot\vec{a}_{AB}}) & \mu & t(1+e^{-2i\vec{k}\cdot\vec{a}_{BC}}) \\ t(1+e^{2i\vec{k}\cdot\vec{a}_{AC}}) & t(1+e^{2i\vec{k}\cdot\vec{a}_{BC}}) & \mu \end{pmatrix} \begin{pmatrix} c_{\vec{k}A} \\ c_{\vec{k}B} \\ c_{\vec{k}C} \end{pmatrix}, \end{aligned} \tag{3.7}$$

where $\mu$ is the chemical potential.

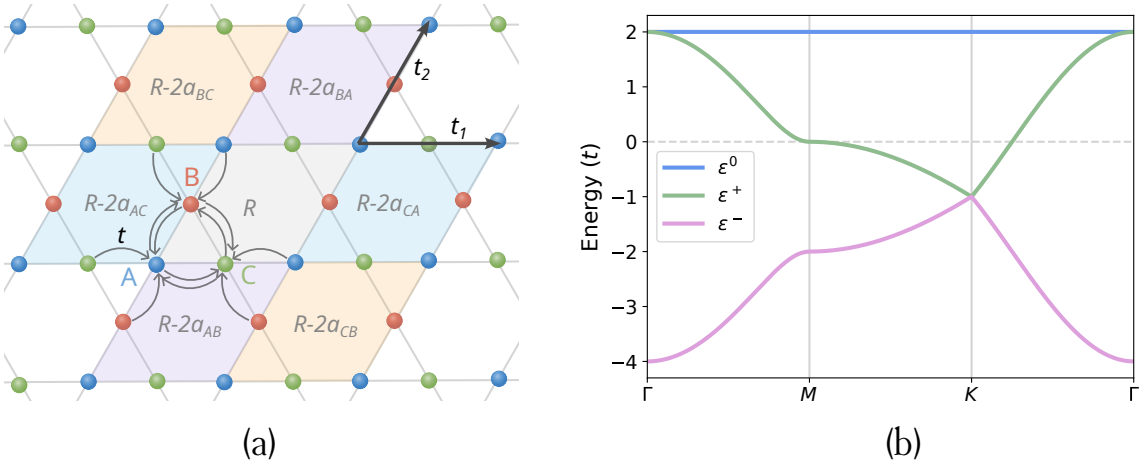


Figure 3.3: (a) Pictorial representation of the hoppings in the nearest-neighbours tight-binding model. (b) Energy bands for the nearest-neighbor tight-binding model for hopping amplitude $t = 1$ and setting the chemical potential $\mu = 0$.

Since the Hamiltonian is block-diagonal in momentum space, it is sufficient to diagonalize one of these blocks. This can be done analytically, yielding three eigenvalues that represent the three energy bands:

$$\varepsilon^0(\vec{k}) = 2t - \mu \tag{3.8a}$$

$$\varepsilon^{\pm}(\vec{k}) = t\left(-1 \pm \sqrt{3 + 2\cos\left(2\vec{k}\cdot\vec{a}_{AB}\right) + 2\cos\left(2\vec{k}\cdot\vec{a}_{AC}\right) + 2\cos\left(2\vec{k}\cdot\vec{a}_{BC}\right)}\right) - \mu. \tag{3.8b}$$

The energy bands along the high symmetry line shown in Fig 3.2(a) are plotted in Fig. 3.3.$\varepsilon^0$ is a flat band, which means that there is no energy dispersion. Its origin is in the wave-function localization due to destructive intereference in the lattice. $\varepsilon^{\pm}$ present two noteworthy features that can also be identified in the DFT calculations of the energy bands of $AV_3Sb_5$: a Dirac cone at the $K$ point and two saddle points at the $M$ point. These two saddle points are van Hove singularities, since at these points the density of states has a logarithmic divergence, as shown in Appendix A.1.

The FS at the van Hove points is a regular hexagon with its vertices on the $M$ points of the first BZ, making nesting effects relevant at these points. Nesting happens when a translation by a certain wavevector $\vec{Q}$ (the nesting vector) leaves the energy spectrum invariant. In other words, $\xi_{\vec{k}} \approx \xi_{\vec{k}+\vec{Q}}$ over a large region of the BZ [18]. A k-point along an edge of this hexagon is related to another k-point in the opposite edge. The vector that connects them is the same for every k-point along a certain edge, so it is the nesting vector.

Three nesting vectors can be defined (Fig. 3.4(a)), and it can be shown that the nesting vectors are equivalent to the $M$-vectors defined previously. This is proven graphically in Fig. 3.4(b). For example, one can look at the vector $\vec{Q}_1$, that connects the points marked in the figure by the yellow and blue crosses. However, the points marked by the blue and the green crosses are equivalent because they are connected by a reciprocal lattice vector. Consequently, the vector that connects the yellow and green crosses (the nesting vector) must be equivalent to the vector that connects the yellow and blue crosses (the $M$-vector).

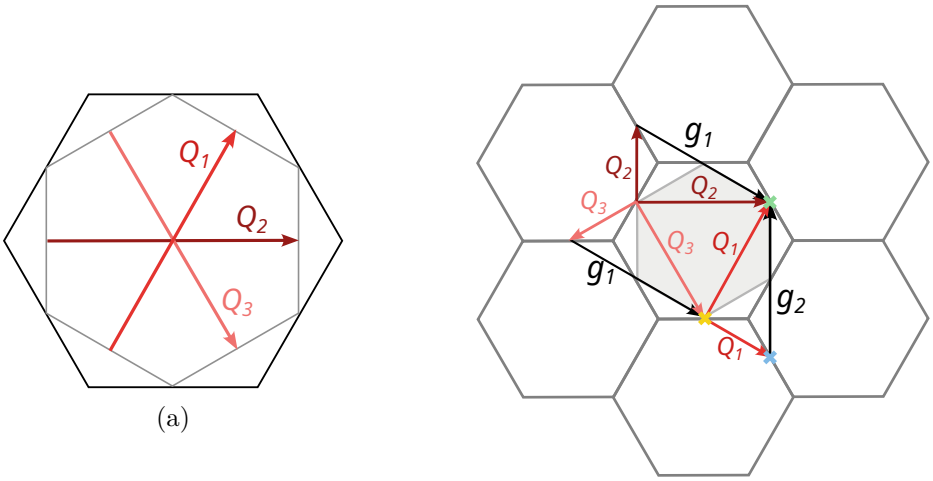


(a) (b)

Figure 3.4: (a) Representation of the Fermi surface at the van Hove points in gray and the three nesting vectors that connect the edges of the hexagonal FS. (b) Graphical proof that the three nesting vectors are equivalent to the three M-vectors.

Since the regions that are connected by the nesting vectors are part of the FS, and the only possible excitable states at low energies lie close to it, any excitation that happens through a wavevector equal to the nesting vector will excite a significantly larger amount of states compared to excitations with any other wavevector. Indeed, the Lindhard response function:

$$\chi_0(\vec{q}) = \sum_{\vec{k}} \frac{f(\varepsilon_{\vec{k}}) - f(\varepsilon_{\vec{k}+\vec{q}})}{\varepsilon_{\vec{k}} - \varepsilon_{\vec{k}+\vec{q}}}, \tag{3.9}$$

will diverge when $\vec{q}$ is one of the nesting vectors. As a result, orders where the wavevector matches the nesting vector will be favored by nesting.

One can wonder what does this modulation mean in real space. Let us consider an order that is modulated by $\vec{Q}_1$, $\Delta_{\vec{Q}_1}$. Fourier transforming to real space, we have $\Delta_{\vec{Q}_1} = \frac{1}{\sqrt{\mathcal{N}}} \sum_{\vec{R}} e^{-i\vec{Q}_1 \cdot \vec{R}} \Delta_{\vec{R}}$, where $\vec{R}$ is the location of the unit cell. This vector can be written in terms of the primitive lattice vectors, $\vec{R} = n\vec{t}_1 + m\vec{t}_2$, and recalling that $\vec{Q}_1 = \frac{1}{2}\vec{g}_1$, $\vec{Q}_1 \cdot \vec{R} = n\pi$. Thus,

$$\Delta_{\vec{Q}_1} = \frac{1}{\sqrt{\mathcal{N}}} \sum_{nm} e^{-in\pi} \Delta_{n\vec{t}_1 + m\vec{t}_2} = \frac{1}{\sqrt{\mathcal{N}}} \sum_{m} \left( \Delta_{m\vec{t}_2} - \Delta_{\vec{t}_1 + m\vec{t}_2} + \Delta_{2\vec{t}_1 + m\vec{t}_2} - ... \right)$$

This means that there is a phase modulation of $\pi$ in the direction of $\vec{t}_1$, doubling the unit cell in this direction, as represented pictorially in Fig. 3.5. Following an analogous reasoning, the order associated to $\vec{Q}_2$ is modulated along $\vec{t}_2$ and the one associated to $\vec{Q}_3$ is modulated along $\vec{t}_1 + \vec{t}_2$.

Additionally, it is relevant to study what kind of order is favoured by the nesting effects at the vH point that is close to the Fermi level. To do this, one should wonder what is the electron distribution within the real space lattice when such a modulation is happening.

When diagonalizing the non-interacting Hamiltonian, the eigenvectors

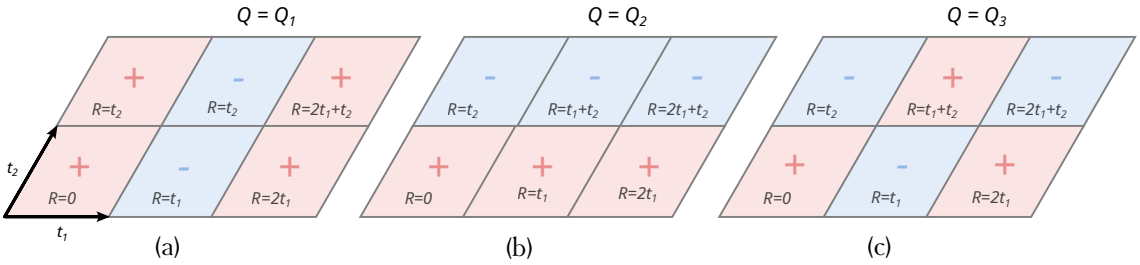


Figure 3.5: Representation of the modulation of the order in the direction of $\vec{t}_1$, $\vec{t}_2$ and $\vec{t}_1 + \vec{t}_2$, respectively. Even if the modulation along $\vec{t}_1 + \vec{t}_2$ appears to double the unit cell in both directions, a new unit cell can be defined so that the doubling only occurs in one direction.

$u_\eta(\vec{k}) = (u_{A\eta}(\vec{k}), u_{B\eta}(\vec{k}), u_{C\eta}(\vec{k}))^T$ are obtained, where $\eta$ is the band index and $\eta = +1$ corresponds to the band that features the upper vH point. $|u_{\alpha+}(\vec{k})|^2$ will represent the probability of finding the electron at each of the sublattice sites $\alpha$ when the measured momentum of the electron is $\vec{k}$. Projecting these sublattice weights along the Fermi surface one obtains Fig. 3.6(a)-(b). From these plots, one can highlight three aspects: (1) only one sublattice site is present at each of the $M$-points, giving the name of *pure-type* to this vH singularity; (2) the nesting vectors are always connecting two different sites; and (3) at each of the BZ edges there is always a sublattice site that is absent. All of this is translated into the fact that nesting effects enhance bond orders between two sites, allowing to relate a certain bond to a certain nesting vector when sitting exactly at the upper vH point: $\vec{Q}_1$ enhances bond orders between sites $A$ and $B$, $\vec{Q}_2$ between $A$ and $C$ and $\vec{Q}_3$ between $B$ and $C$.

One can compare this to what happens at the lower vH point, achieved with a chemical potential $\mu = -2$. At this point the FS is exactly the same, but nesting in this case will promote a different type of order. The sublattice weights plotted along the FS are shown in Fig. 3.6(c)-(d). This singularity is said to be *mixed-type*, since there are two sites with equal weights at each of the $M$-points. Along both of the edges that are connected by a nesting vector there is always a site that is equally present, which means that site orders will be the ones enhanced by nesting in this case.

Looking at Fig. 3.3, one might notice that the energy bands for the kagome lattice in the tight-binding model resemble very much those of the honeycomb lattice, with which it shares the hexagonal symmetry. Indeed, they are identical except for the absence of the flat band. Additionally, the FS at the saddle points is as well a regular hexagon, in which nesting effects are also present. However, the pure and mixed type flavor of the vH points is unique to the kagome lattice, which makes it special in this sense, and which is the source of many of the exotic properties of the kagome based materials.

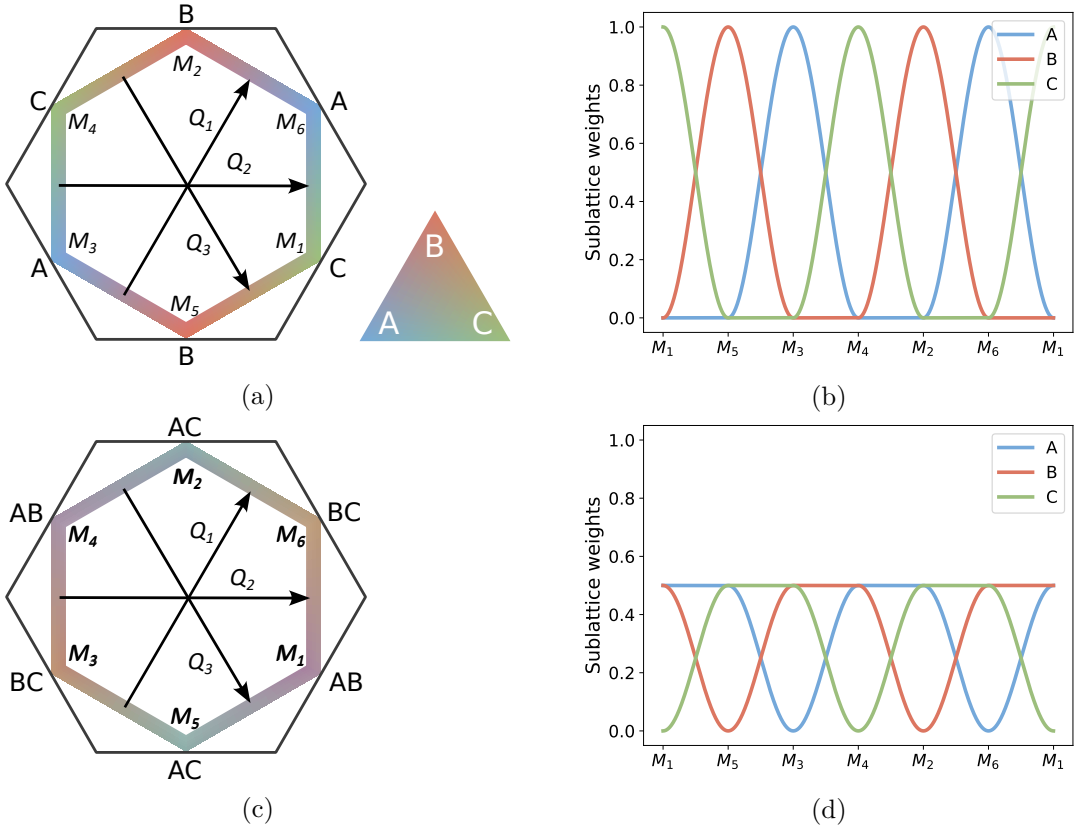


Figure 3.6: Sublattice weights projected onto the FS at the uppper (a)-(b) and lower (c)-(d) vH points, highlighting the fact that the upper vH point is sublattice pure, so that the Bloch states are supported exclusively on one kagome sublattice at every M-point.

# Chapter 4

# Theory of the charge density wave phase

As briefly described in Chapter 2, all the $AV_3Sb_5$ metals enter a phase referred to as charge density wave at temperatures around 90K, which causes a breaking of the translational symmetry of the lattice. This symmetry breaking is sometimes found to be accompanied by two others: rotational and time-reversal, both of which are not always found to emerge at the same temperature as the CDW. The task of theoretically modeling this puzzling order has been undertaken multiple times, but a theory in which a CDW phase that captures all the experimental data from the microscopic point of view is yet lacking. The purpose of this chapter is to introduce the main known features of the theory of CDW in these compounds, along with some of the approaches taken in the literature, which will motivate the approach taken in this project and which is laid out in the next two chapters.

## 4.1 The origin of charge density wave in $AV_3Sb_5$

The formation of a charge density wave order involves the formation of a condensate of particle-hole pairs modulated by a non-zero momentum vector that causes a breaking of the translational symmetry of the real-space lattice. The emergence of this phase can be driven by either an electronic instability, a softening of the phonon modes, or a coupling between both effects.

DFT calculations [19, 20] on the phonon band structure of the pristine lattice show a soft acoustic phonon modes at the $M$ and $L$ points, as depicted in Fig. 4.1(a). This can be seen by the phonon frequencies becoming imaginary (in the figure presented at negative for easier visualization), indication of the strong lattice instability. The $M$-point phonon modes mostly cause an in-plane displacement of the vanadium atoms in the kagome layer that creates two distinct patterns shown in Fig. 4.1(b)-(c): Star of David (SoD) and trihexagonal (TrH), also referred to as inverse Star of David. Both of them cause a doubling of the unit cell in the two in plane directions. The optimized SoD and TrH structures are found to be stable (Fig. 4.1(b)-(c)) and reduce the total energy. In all three compounds the TrH structure is found to have lower energy, as it can be seen from Fig. 4.1(d). The doubling in the unit cell in the out-of-plane direction is given by the phonon mode at the $L$-point. A $\pi$ phase shift between TrH layers is found to be the most favorable [20]. Additionally to the discussed phonon modes, [21] also finds an instability in the $U$-line that connects the $M$ and $L$ points, which would match the $2 \times 2 \times 4$ unit

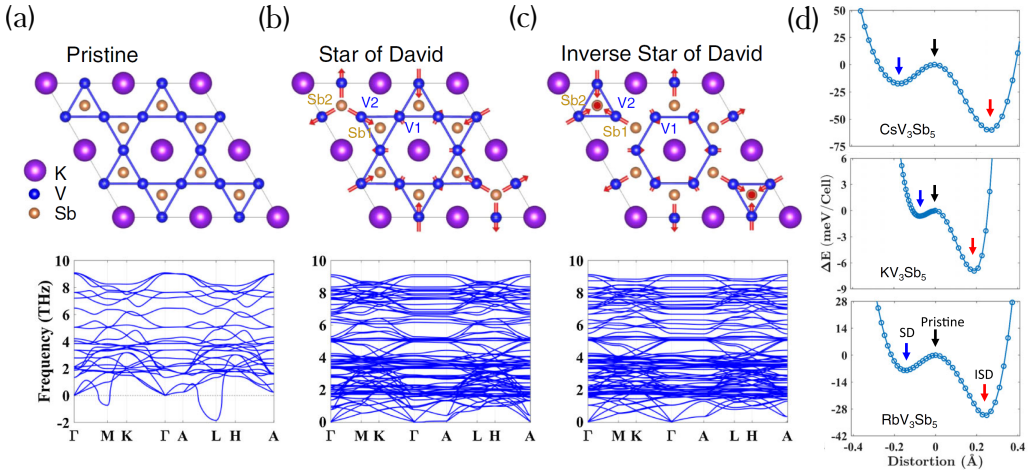


Figure 4.1: Crystal structures and the corresponding phonon dispersions for the pristine (a), Star of David (b), and Inverse Star of David lattices. (d) Total energy profiles of the three kagome metals, where spin-orbit coupling has been considered. All figures from Ref. [19].

cell modulation reported in [2]. In all three instabilities the main displacements occur on the vanadium atoms in the kagome layer, and all of them have the same in-plane vector modulation. This suggest that the interaction with the electronic degrees of freedom might play an important role in the instability.

In fact, the charge density wave phase is commonly regarded as an extension of the Peierls instability: in a one-dimensional electron gas, nesting of the Fermi surface causes a logarithmic divergence in the bare electronic susceptibility, which causes a redistribution of the charge, making the lattice unstable. Hence, an acoustic phonon mode becomes unstable at a momentum equal to the nesting vector, which is exclusively driven by the electronic instability. A derivation of the Peierls instability can be found in Appendix A.4. As discussed in the previous chapter, the Fermi surface structure of the kagome layer at the van Hove singularity prompt the appearance of nesting effects along the $M$-vectors, which coincides with the vectors along which the charge orders. Indeed, the static particle-hole susceptibility

$$\chi_0(\vec{Q}) = -\frac{1}{\beta}\sum_n \int_{\vec{k}} G_0(\vec{k}; i\omega_n) G_0(\vec{k}+\vec{Q}; i\omega_n) \ , \tag{4.1}$$

is shown to have a double logarithmic divergence, both from the van Hove singularity and from Fermi surface nesting, when considering a saddle-point-like dispersion relation in the vicinity of the $M$-points [22]. In (5.29), $G_0(\vec{k}; i\omega_n)$ is the bare Green function, $\int_{\vec{k}} = \int d^2k/(2\pi)^2$, and $\sum_n$ denotes the sum over the fermionic Matsubara frequencies $\omega_n = (2n+1)\pi/\beta$. This is a promising reasoning for the instability being induced by the electronic structure. However, direct evidence is still lacking.

## 4.2 Patch model and Ginzburg-Landau free energy

Given that it is expected that the fermions around these saddle points will dominate the response, patch models have been used several times to study the electronic instabilities of the kagome plane [5, 23, 24]. They assume that the collective electronic behaviour of

the system is determined by the saddle points at the three $M$-points and the interactions between them. A patch around the $\Gamma$ point can also be included in this model [23], which comes from the antimony $p_z$ orbital, but for the present discussion it will be omitted.
In this context, the non interaction Hamiltonian is taken to be

$$H_0 = \sum_{\alpha} \sum_{|\vec{q}|<\Lambda} c^{\dagger}_{\alpha\vec{q}} (\varepsilon_{\alpha}(\vec{q}) - \mu)\, c_{\alpha\vec{q}} \,, \tag{4.2}$$

where $\varepsilon_{\alpha}(\vec{q})$ are the saddle-point-like dispersion relations at the $M$-points at the upper van Hove singularity. Since the tight-binding model in Section 3.2 presented saddle points at the $M$-point, said dispersion relation can be taken to be the Taylor expansion of $\varepsilon^{+}$ (the upper vH point) (4.3) around the three $M$-points:

$$\varepsilon^{+}(\vec{Q}_1 + \vec{k}) \approx \frac{t}{2}\left(q_x^2 - \sqrt{3} q_x q_y\right) \equiv \varepsilon_1(\vec{q}) \tag{4.3a}$$

$$\varepsilon^{+}(\vec{Q}_2 + \vec{k}) \approx \frac{t}{4}\left(-q_x^2 + 3 q_y^2\right) \equiv \varepsilon_2(\vec{q}) \tag{4.3b}$$

$$\varepsilon^{+}(\vec{Q}_3 + \vec{k}) \approx \frac{t}{2}\left(q_x^2 + \sqrt{3} q_x q_y\right) \equiv \varepsilon_3(\vec{q}) \,, \tag{4.3c}$$

where $\vec{q}$ is a small momentum measured from the corresponding $M$-point with a cutoff radius $\Lambda$. [1]. The annihilation and creation operators have two relevant degrees of freedom here, in addition to the spin: the sublattice index $\alpha$ and the small momentum $\vec{q}$ measured from the corresponding $M$-point of the patch. Given the pure character of the vH singularity, a one-to-one correspondence between the sublattice sites and the patches around the $M$-points can be established, allowing for the combination of both in the sublattice index $\alpha$.

Within this framework, all the possible electron-electron interactions between these patches are considered, so that the interaction Hamiltonian is [5]

$$\begin{aligned} H_{int} = \frac{1}{2\mathcal{N}} \sum_{|\mathbf{q}_1|,\ldots,|\mathbf{q}_4|<\Lambda} \Big[ \sum_{\alpha\neq\beta} (g_1 c^{\dagger}_{\alpha\mathbf{q}_1\sigma} c^{\dagger}_{\beta\mathbf{q}_2\sigma'} c_{\alpha\mathbf{q}_3\sigma'} c_{\beta\mathbf{q}_4\sigma} + g_2 c^{\dagger}_{\alpha\mathbf{q}_1\sigma} c^{\dagger}_{\beta\mathbf{q}_2\sigma'} c_{\beta\mathbf{q}_3\sigma'} c_{\alpha\mathbf{q}_4\sigma} + \\ + g_3 c^{\dagger}_{\alpha\mathbf{q}_1\sigma} c^{\dagger}_{\alpha\mathbf{q}_2\sigma'} c_{\beta\mathbf{q}_3\sigma'} c_{\beta\mathbf{q}_4\sigma}) + \sum_{\alpha} g_4 c^{\dagger}_{\alpha\mathbf{q}_1\sigma} c^{\dagger}_{\alpha\mathbf{q}_2\sigma'} c_{\alpha\mathbf{q}_3\sigma'} c_{\alpha\mathbf{q}_4\sigma} \Big] \,. \end{aligned} \tag{4.4}$$

The listed interactions correspond to interpatch exchange ($g_1$), interpatch ($g_2$) and intrapatch ($g_4$) density-density, and umklapp ($g_3$) scatterings. A graphical representation of the considered BZ and the interaction between patches is shown in Fig. 4.2.

Since the charge density wave phase is a particle-hole condensate that causes the redistribution of the charge along the $M$-vectors, the order parameters of this phase will have three components $\alpha = 1, 2, 3$, associated to $\vec{Q}_1$, $\vec{Q}_2$ and $\vec{Q}_3$, respectively. These OP will be in general complex, so that one can define two sets of OP [5]:

$$N_{\alpha} = \frac{G_{rC}}{2\mathcal{N}} \sum_{\vec{q}} \left\langle c^{\dagger}_{\beta\vec{q}}\, c_{\gamma\vec{q}} + c^{\dagger}_{\gamma\vec{q}}\, c_{\beta\vec{q}} \right\rangle \,, \tag{4.5}$$

[1] In [5] a more general version of the dispersion relations is taken, in which perfect nesting is not assumed, and the shape of the saddle point is determined by two parameters. Nevertheless, the following discussion does not rely on this perfect nesting or the lack thereof, so the expressions in (4.3) will be used.

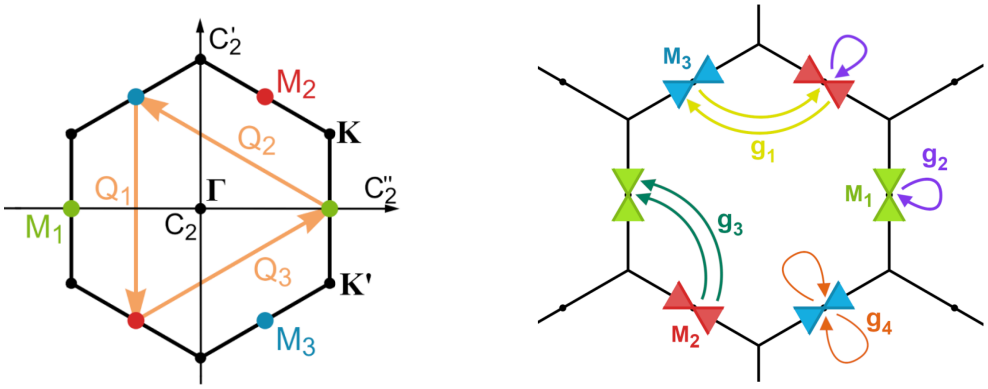


(a) (b)

Figure 4.2: Pictorial representation of the first BZ (a), with the three distinct $M$-points and the nesting vectors, and of the interactions between patches (b) as defined in (4.4). Notice that their definition of the kagome lattice corresponds to a reflection across the y axis, followed by a 30° clockwise rotation respect to the definitions shown in Chapter 3. Figure from Ref. [5]

with $\alpha \neq \beta \neq \gamma$, corresponding to what is referred to as a real charge density wave phase (rCDW), and

$$\phi_\alpha = \frac{G_{iC}}{2i\mathcal{N}} \sum_{\vec{q}} \left\langle c^\dagger_{\beta\vec{q}}\, c_{\gamma\vec{q}} - c^\dagger_{\gamma\vec{q}}\, c_{\beta\vec{q}} \right\rangle \ , \tag{4.6}$$

also with $\alpha \neq \beta \neq \gamma$ and corresponding to an imaginary CDW (iCDW). $G_{rC}$ and $G_{iC}$ are the interaction stregths corresponding to the real and imaginary CDW, respectively, and $\mathcal{N}$ is the number of unit cells.

Let us analyze these order parameters and what their physical meaning is. Both order parameters are condensates of a particle and a hole that live in two different patches. Consequently, the associated order in real-space is bonds. Recalling our tight-binding Hamiltonian from Section 3.2, the bond density between nearest-neighbours can be defined as

$$\langle \delta\rho_{\alpha\beta} \rangle = \mathrm{Re}\left[ \left\langle c^\dagger_{\vec{R}\alpha} c_{\vec{R}'\beta} + c^\dagger_{\vec{R}\beta} c_{\vec{R}'\alpha} \right\rangle \right] \tag{4.7}$$

Given the one-to-one correspondence between lattice sites and momentum patches, the fermion located at the lattice site $\alpha$ at the unit cell $\vec{R}$ will be related to the fermions with momentum $\vec{q}$ near $\vec{Q}_\alpha$ as

$$c_{\vec{R}\alpha} = \frac{1}{\sqrt{\mathcal{N}}} \sum_{|\vec{q}|<\Lambda} e^{i\vec{Q}_\alpha \cdot \vec{R}} c_{\alpha\vec{q}} \ , \tag{4.8}$$

so that

$$\begin{aligned} \langle \delta\rho_{\alpha\beta} \rangle =& \frac{1}{\mathcal{N}} \sum_{|\vec{q}|<\Lambda} \mathrm{Re}\left[ e^{-i(\vec{Q}_\alpha \cdot \vec{R} - \vec{Q}_\beta \cdot \vec{R}')} \left\langle c^\dagger_{\alpha\vec{q}}\, c_{\beta\vec{q}} + c^\dagger_{\vec{R}\beta} c_{\vec{R}'\alpha} \right\rangle \right] \\ =& \frac{1}{G_{cR}} \cos\left( \vec{Q}_\alpha \cdot \vec{R} - \vec{Q}_\beta \cdot \vec{R}' \right) N_\gamma \ . \end{aligned} \tag{4.9}$$

On the other hand, as shown in [5], the expectation value of the current on nearest-neighbours bonds is

$$\begin{aligned}\langle j_{\alpha\beta}\rangle &= iet\left\langle c^\dagger_{\vec{R}\alpha}c_{\vec{R}'\beta} - c^\dagger_{\vec{R}'\beta}c_{\vec{R}\alpha}\right\rangle = \frac{iet}{\mathcal{N}}e^{-i(\vec{Q}_\alpha\cdot\vec{R}-\vec{Q}_\beta\cdot\vec{R}')}\sum_{|\vec{q}|<\Lambda}\left\langle c^\dagger_{\alpha\vec{q}}\,c_{\beta\vec{q}} - c^\dagger_{\beta\vec{q}}\,c_{\alpha\vec{q}}\right\rangle \\ &= -\frac{2et}{G_{iC}}e^{-i(\vec{Q}_\alpha\cdot\vec{R}-\vec{Q}_\beta\cdot\vec{R}')}\phi_\gamma\ ,\end{aligned} \tag{4.10}$$

where $t$ is the tight-binding hopping.

Therefore, while the order parameter of the rCDW phase (which is even under time-reversal symmetry) is related to the bond-density modulation, the OP of the iCDW (time-reversal odd) is associated to real-space bond currents. The question now is which configurations of these bond densities and currents are preferred on the CDW phase. To answer it, we can analyze the free energy in the mean field approach. For that purpose, the interaction Hamiltonian, which has a quartic dependence on the fermionic operators, needs to be decoupled. The approach taken is to perform a Hubbard-Stratonovich (HS) transformation within the path integral formalism. In a HS transformation, the decoupling can be done in different channels, depending on the phase of matter that one wishes to explore. Given that here we are focusing on the CDW phase, we want to write (4.4) in terms of the bilinears that would provide the order parameters (4.5) and (4.6) after the mean-field treatement. Consequently, upon defining the bilinears

$$\rho_{rC,\alpha} = \frac{1}{2\mathcal{N}}\sum_{\vec{q}}\left(\bar{c}_{\beta\vec{q}}c_{\gamma\vec{q}} + \bar{c}_{\gamma\vec{q}}c_{\beta\vec{q}}\right)\ , \qquad \rho_{iC,\alpha} = \frac{1}{2i\mathcal{N}}\sum_{\vec{q}}\left(\bar{c}_{\beta\vec{q}}c_{\gamma\vec{q}} - \bar{c}_{\gamma\vec{q}}c_{\beta\vec{q}}\right)\ , \tag{4.11}$$

the interaction Hamiltonian can be written as $H_{int} = H_{rC} + H_{iC}$ with [5]:

$$H_{rC} = -\frac{\mathcal{N}}{2}G_{rC}\sum_\alpha \rho_{rC,\alpha}\rho_{rC,\alpha}\ , \qquad H_{iC} = -\frac{\mathcal{N}}{2}G_{iC}\sum_\alpha \rho_{iC,\alpha}\rho_{iC,\alpha}\ . \tag{4.12}$$

It can be obtained [5] that the interaction strengths of the real and imaginary CDW, respectively, are $G_{rC} = -2g_1 + g_2 - g_3$ and $G_{iC} = -2g_1 + g_2 + g_3$. Notice that the only difference between them is the sign of $g_3$, which is the only interaction that transfers charge between patches. Were this interaction to not exist, the two order parameters would be degenerate.

Having written the Hamiltonian in this form, the HS transformation can be performed in both channels (real and imaginary), which allows integrating out the electrons. Since this process (for a different model) will be the focus of the next chapter, here I will just state the results that can be obtained in the present case. Nonetheless, the detailed derivation can be found in Appendix B.

The effective free energy is found to be

$$\mathcal{F}_E[N,\phi] = -\frac{1}{\beta}\,\mathrm{Tr}\big(\log\big(-\mathcal{G}^{-1}\big)\big) + \frac{\mathcal{N}}{2G_{rC}}\sum_\alpha N_\alpha^2 + \frac{\mathcal{N}}{2G_{iC}}\sum_\alpha \phi_\alpha^2\ , \tag{4.13}$$

where full Green function $\mathcal{G}$ is defined such that

$$\mathcal{G}^{-1} = \begin{pmatrix} i\omega_n - \varepsilon_1(\vec{q}) & \frac{N_3 - i\phi_3}{2} & \frac{N_2 + i\phi_2}{2} \\ \frac{N_3 + i\phi_3}{2} & i\omega_n - \varepsilon_2(\vec{q}) & \frac{N_1 - i\phi_1}{2} \\ \frac{N_2 - i\phi_2}{2} & \frac{N_1 + i\phi_1}{2} & i\omega_n - \varepsilon_3(\vec{q}) \end{pmatrix}\ . \tag{4.14}$$

Said expression can be expanded perturbatively to obtain

$$\begin{aligned} f_{CDW} =& \left(\frac{1}{2G_{rC}} + K_1\right)\sum_\alpha N_\alpha^2 + \left(\frac{1}{2G_{iC}} + K_1\right)\sum_\alpha \phi_\alpha^2 \\ &+ K_2\left(N_1N_2N_3 - N_1\phi_2\phi_3 - N_2\phi_1\phi_3 - N_3\phi_1\phi_2\right) \\ &+ K_4\Big(\sum_\alpha (N_\alpha^2+\phi_\alpha^2)\Big)^2 + (K_3-2K_4)\sum_{\alpha<\beta}\left(N_\alpha^2+\phi_\alpha^2\right)^2\left(N_\beta^2+\phi_\beta^2\right)^2 \\ =& f_{rCDW} + f_{iCDW} + f_{r-iCDW}\ , \end{aligned} \tag{4.15}$$

where the coefficients $K_i$ are only dependent on the temperature and the chemical potential, and whose expressions can be found in Appendix C.6.

Let us start by assuming that the only OP present is the real one. Thus, the free energy is

$$f_{rCDW} = r_N\sum_\alpha N_\alpha^2 + K_2N_1N_2N_3 + K_4\Big(\sum_\alpha N_\alpha^2\Big)^2 + \tilde{K}_3\sum_{\alpha<\beta}N_\alpha^2N_\beta^2\ , \tag{4.16}$$

calling $r_N = \left(\frac{1}{2G_{rC}} + K_1\right)$ and $\tilde{K}_3 = (K_3 - 2K_4)$. The presence of the trilinear term means that there always exist a configuration of $N_\alpha$ in which $K_2N_1N_2N_3 < 0$ regardless of the sign of $K_2$. Thus, this term always lowers the energy of the configuration in which all three components of $N$ are present. If only one component is present, the trilinear term will vanish, being less favorable. The possible configurations that the order parameters can take are obtained by finding the global minima of (4.16). It can be found that the physically relevant solutions of the mean field theory belong to the $3Q_\pm$ or the $1Q$ phases [5]. Let us minimize the energy for the allowed cases.

Starting from the case in which only one component is present, the absence of the trilinear term provides a free energy in the usual Ginzburg-Landau form:

$$(f_{rCDW})^{1Q} = r_NN^2 + K_4N^4\ . \tag{4.17}$$

For the energy to be bounded, $K_4 > 0$. Taking the temperature dependence of the second order term to be $r_N = \alpha_N(T - T_N)$ with $\alpha_N > 0$, the minimization of the free energy respect to $N$ provides that for $T < T_N$

$$N^0 = \pm\sqrt{-\frac{\alpha_N(T-T_N)}{2K_4}}\ , \tag{4.18}$$

so that the free energy is

$$(f_{rCDW})^{1Q} = -\frac{\alpha_N^2(T-T_N)^2}{4K_4}\ , \tag{4.19}$$

which crosses zero at $T = T_N$. As discussed in the previous chapter, an order that is modulated by one of the $M$-vectors will have a phase modulation of $\pi$ along the corresponding primitive vector, which will break both the translational and rotational symmetry of the lattice. The new unit cell becomes a $2 \times 1$ unit cell, as shown in Fig. 4.3, giving it the name *stripe* configuration.

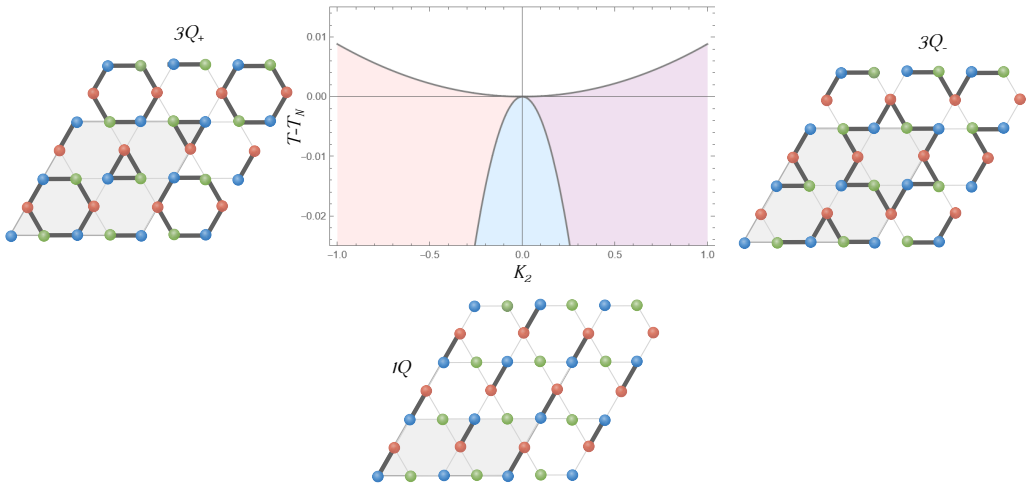


Figure 4.3: Pictorial representation of the $3Q_{\pm}$ and $1Q$ configurations, along with the phase diagram for the rCDW free energy. The corresponding new unit cells are shaded in gray. Notice that the stripe phase breaks the rotational symmetry of the lattice to two-fold and the, and the two $3Q$ phases correspond to a $\pi$ phase shift of one of the components.

Conversely, let us consider the configuration (which will be referred to as 3Q) where all three components are present and have equal magnitude $|N_\alpha| = N$. The trilinear term in the free energy is now present, so that

$$(f_{rCDW})^{3Q} = 3\alpha_N(T - T_N)N^2 + \mathrm{sgn}(N_1N_2N_3)K_2N^3 + 3(3K_4 + \tilde{K}_3)N^4 \ . \tag{4.20}$$

For the energy to be bounded in this case, $u = 3K_4 + \tilde{K}_3 > 0$ is required. By minimizing the free energy, one can obtain

$$N^0 = \frac{\mathcal{K}}{8u} \ , \quad \text{with} \quad \mathcal{K} = -\mathrm{sgn}(N_1N_2N_3)K_2 + \sqrt{K_2^2 - 32u\alpha_N(T - T_N)} \ . \tag{4.21}$$

Since $N = |N_\alpha| > 0$ and $u > 0$, then $\mathcal{K} > 0$. Therefore, we obtain that if $K_2 > 0$, $\mathrm{sgn}(N_1N_2N_3) < 0$ and vice versa, meaning that, as previously argued, the system will always choose a configuration such that the trilinear term is negative. Substituting in the expression for the free energy,

$$(f_{rCDW})^{3Q} = \frac{\mathcal{K}^2}{2048u^3}\left(48u\alpha_N(T - T_N) - |K_2|\mathcal{K}\right) \ , \tag{4.22}$$

which crosses zero at

$$T^{3Q} = \frac{K_2^2}{36\alpha_N u} + T_N \ . \tag{4.23}$$

Consequently, as long as the trilinear term is present ($K_2 \neq 0$), the system will have a preference for entering the $3Q$ phase over the stripe phase. A modulation along the three $M$-vectors will generate a real-space lattice in which the translational symmetry is broken along both directions in the plane, but the six-fold rotational symmetry is preserved. However, depending on the sign of $K_2$, two different $3Q$ configurations are possible: Star of David for $K_2 > 0$ and trihexagonal (or inverse Star of David) for $K_2 < 0$. Both of the $3Q$ patterns are depicted in Fig. 4.3.

At the transition temperature (when $T = T^{3Q}$), the order parameter experiences a jump which is proportional to the trilinear coefficient

$$\Delta N = \frac{K_2}{6u} \ , \tag{4.24}$$

making the phase transition of first order, which matches experiments as discussed in Chapter 2.

This discussion have established that the leading instability corresponds to the $3Q$ phase. However, when $\tilde{K}_3$ (term only present in the $3Q$ phase) is positive, it penalizes the free energy. Accordingly, in the presence of the positive quartic term the stripe phase could appear as a subleading instability that onsets at a temperature $T^{1Q} < T^{3Q}$:

$$T^{1Q} = -\frac{K_2^2}{8\alpha_N u K_3^2}\left[\sqrt{K_4(4K_4+\tilde{K}_3)^3)} + K_4(8K_4+3\tilde{K}_3)\right] + T_N \tag{4.25}$$

A phase diagram for the case in which $\tilde{K}_3 > 0$ is presented in Fig. 4.3. Entering a phase that lowers the rotational-symmetry from six to two-fold at a temperature $T^{1Q} < T^{3Q}$ would actually agree reported experimental data [25].

Let us move on to the the part of the free energy corresponding exclusively to the iCDW. From (4.15),

$$f_{iCDW} = r_\phi \sum_\alpha \phi_\alpha^2 \quad + K_4\Big(\sum_\alpha (\phi_\alpha^2)\Big)^2 + \tilde{K}_3 \sum_{\alpha<\beta} \phi_\alpha^2 \phi_\beta^2 \ , \tag{4.26}$$

with $r_\phi = \frac{1}{2G_{iC}} + K_1$. Note that there is no trilinear term, since time reversal symmetry forbids it. Starting again with the $1Q$ configuration, and assuming $r_\phi = \alpha_\phi(T - T_\alpha)$ with $\alpha_\phi > 0$, the free energy will simply be

$$(f_{iCDW})^{1Q} = \alpha_\phi(T - T_\alpha)\phi^2 + K_4\phi^4 \ . \tag{4.27}$$

For the energy to be bounded $K_4 > 0$, and the minimization of $(f_{iCDW})^{1Q}$ is analogous to the $1Q$ configuration of the rCDW: the free energy crosses zero at $T = T_\alpha$, and in terms of the order parameter $\phi^0 = \pm\sqrt{-\frac{\alpha_\phi(T-T_N)}{2K_4}}$, the free energy becomes

$$(f_{iCDW})^{1Q} = -\frac{\alpha_\phi^2(T - T_\phi)^2}{4K_4} \ . \tag{4.28}$$

The associated real space bond current pattern in the $1Q$ configuration is shown in Fig. 4.4.

For the $3Q$ configuration, with $|\phi_\alpha| = \phi$,

$$(f_{iCDW})^{3Q} = 3\alpha_\phi(T - T_\alpha)\phi^2 + 3(3K_4 + \tilde{K}_3)\phi^4 \ . \tag{4.29}$$

Also in this case $3K_4 + \tilde{K}_3$ needs to be positive for the energy to be bounded. After its minimization one finds that the order parameter is $\phi^0 = \pm\sqrt{-\frac{\alpha_\phi(T-T_\phi)}{2(3K_4+\tilde{K}_3)}}$ and the free energy can be written as

$$(f_{iCDW})^{3Q} = -\frac{\alpha_\phi^2(T - T_\phi)^2}{4K_4 + \frac{4}{3}\tilde{K}_3} \ , \tag{4.30}$$

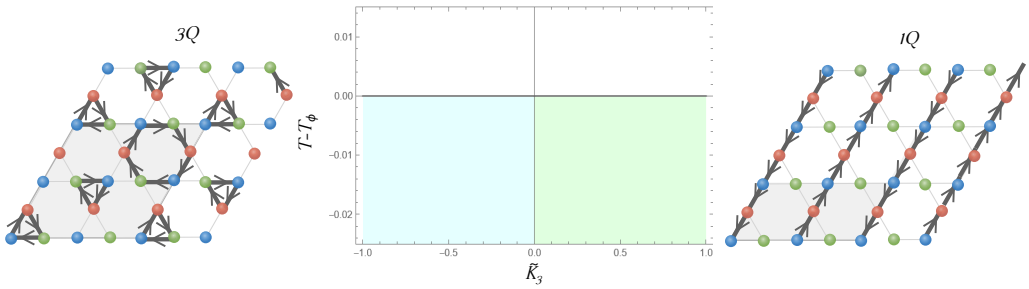


Figure 4.4: Pictorial representation of the $3Q$ and $1Q$ configurations, along with the phase diagram for the iCDW free energy. In gray the new $2 \times 2$ and $2 \times 1$ unit cells are shaded, respectively.

which also crosses zero at $T = T_\phi$. The real-space bond current pattern for the $3Q$ phase is depicted in Fig. 4.4.

Comparing the free energy of both phases shows that the sign of $\tilde{K}_3$ establishes which configuration is preferred: the $3Q$ phase is favorable for $\tilde{K}_3 < 0$ while the $1Q$ is for $\tilde{K}_3 > 0$. When both the real and imaginary CDW order parameters are present, they are coupled by $f_{r-iCDW}$. The treatment of the free energy becomes too complex to perform analytically, but numerical calculations have been performed, also taking into account the orbital degree of freedom [26].

# Chapter 5

# Mean-field theory and broken-symmetry solutions

In Chapter 4, we saw how patch models can be used to model the charge density wave phase, where real and imaginary order parameters were considered. However, these OP would be degenerate unless their interaction strengths were different, relying in the interaction $g_3$ to break said degeneracy. It is not apparent, though, the origin of this interaction from a more general model that starts with the interactions between fermions in real-space. Consequently, it is our goal to study if indeed the real and imaginary order parameters are degenerate, and how the analysis changes when starting from the simplest form of the Hubbard model in the kagome lattice.

## 5.1 Model setup and decoupling of the interactions

For the non-interacting Hamiltonian, we will make use of the nearest-neighbour Hamiltonian developed in Section 3.2. To account for the interactions between the electrons, we will consider an extended Hubbard model, where the on-site repulsion for the electrons on the same lattice site are parametrized by $U$ and the nearest-neighbours repulsion by $V$. If the interaction strengths are assumed to be independent on the lattice sites the interaction Hamiltonian in real space is:

$$H_{int} = H' + H'' \tag{5.1}$$

with

$$H' = U \sum_{\vec{R}\alpha} \sum_{\sigma \neq \sigma'} c^{\dagger}_{\vec{R}\alpha\sigma} c_{\vec{R}\alpha\sigma} c^{\dagger}_{\vec{R}\alpha\sigma'} c_{\vec{R}\alpha\sigma'} \tag{5.2}$$

$$H'' = \frac{V}{2} \sum_{\vec{R}\sigma\sigma'} \sum_{\alpha \neq \beta} \left( c^{\dagger}_{\vec{R}\sigma\alpha} c_{\vec{R}\sigma\alpha} c^{\dagger}_{\vec{R}\sigma'\beta} c_{\vec{R}\sigma'\beta} + c^{\dagger}_{\vec{R}\sigma\alpha} c_{\vec{R}\sigma\alpha} c^{\dagger}_{\vec{R}-2\vec{a}_{\alpha\beta}\beta\sigma'} c_{\vec{R}-2\vec{a}_{\alpha\beta}\beta\sigma'} \right), \tag{5.3}$$

using the same notation as in Section 3.2. The factor $\frac{1}{2}$ in $H''$ has been added to avoid double counting. The interactions considered are drawn in Fig. 5.1.

Fourier transforming, the Hamiltonians become

$$H' = \frac{U}{\mathcal{N}} \sum_{\sigma \neq \sigma'} \sum_{\vec{k}\vec{k}'\vec{q}} \sum_{\alpha} c^{\dagger}_{\vec{k}'\alpha\sigma} c_{\vec{k}'+\vec{q}\alpha\sigma} c^{\dagger}_{\vec{k}+\vec{q}\alpha\sigma'} c_{\vec{k}\alpha\sigma'} \ , \tag{5.4}$$

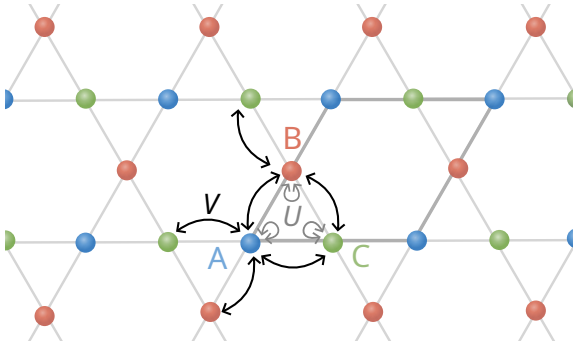


Figure 5.1: Pictorial representation of the nearest-neighbour Hubbard model in the kagome lattice.

and

$$H'' = \frac{V}{2\mathcal{N}} \sum_{\sigma\sigma'} \sum_{\vec{k}\vec{k}'\vec{q}} \sum_{\alpha\neq\beta} \left(1 + e^{-2i\vec{q}\cdot\vec{a}_{\beta\alpha}}\right) c^{\dagger}_{\vec{k}'\beta\sigma} c_{\vec{k}'+\vec{q}\beta\sigma} c^{\dagger}_{\vec{k}+\vec{q}\alpha\sigma'} c_{\vec{k}\alpha\sigma'} \ . \tag{5.5}$$

Here I have used $c_{\vec{R}\alpha} = \frac{1}{\sqrt{\mathcal{N}}} \sum_{\vec{k}} e^{i\vec{k}\cdot\vec{R}} c_{\vec{k}\alpha}$ in order to Fourier transform the fermionic operators. Nevertheless, we have the gauge freedom to use instead $c_{\vec{R}\alpha} = \frac{1}{\sqrt{\mathcal{N}}} \sum_{\vec{k}} e^{i\vec{k}\cdot(\vec{R}+\vec{d}_\alpha)} \tilde{c}_{\vec{k}\alpha}$, which provides the real prefactor $\cos(\vec{q}\cdot\vec{a}_{\beta\alpha})$ in $H''$. While this initially appears to be a better option, the fact that the Fourier-transformed fields are not periodic (e.g. $\tilde{c}_{\vec{k}+\vec{g}_1\alpha} = \frac{1}{\sqrt{\mathcal{N}}} \sum_{\vec{R}} e^{-i(\vec{k}+\vec{g}_1)\cdot(\vec{R}+\vec{d}_\alpha)} c_{\vec{R}\alpha} = e^{-i\vec{g}_1\cdot\vec{d}_\alpha} \tilde{c}_{\vec{k}\alpha}$ while $c_{\vec{k}+\vec{g}_1\alpha} = \frac{1}{\sqrt{\mathcal{N}}} \sum_{\vec{R}} e^{-i(\vec{k}+\vec{g}_1)\cdot\vec{R}} c_{\vec{R}\alpha} = c_{\vec{k}\alpha}$) carries complications further on.

For the study of the interactions, we will work within the path integral formalism, in which, arising from the parallelism to classical mechanics, the partition function of our system can be written as

$$\mathcal{Z} = \int \mathcal{D}[\bar{c}, c] e^{-S[\bar{c},c]} \ . \tag{5.6}$$

The action is defined as

$$S[\bar{c}, c] = \int_0^\beta d\tau \left[ \sum_{\alpha\vec{q}} \bar{c}_{\alpha\vec{k}} \partial_\tau c_{\alpha\vec{q}} + \sum_{\alpha\beta\vec{k}} \bar{c}_{\vec{k}\alpha} h_{\alpha\beta}(\vec{k}) c_{\vec{k}\beta} + H_{int} \right], \tag{5.7}$$

where $h_{\alpha\beta}(\vec{k})$ is the tight-binding Hamiltonian described in (3.7), $\mathcal{D}[\bar{c}, c] \equiv \prod_\lambda d\bar{c}_\lambda dc_\lambda$ is the shorthand notation for the measure of the fermionic operators $c^\dagger, c$, and inside the path integral these operators have been replaced by their associated anticommuting Grassman numbers $\bar{c}, c$.

The principal aim of this project is to obtain the order parameters favored in the ground state of the charge density wave phase. For this purpose, a Hubbard-Stratonovich (HS) transformation will be performed, which will provide an effective action that can be treated within mean-field theory. As briefly mentioned in the previous chapter, the channel in which to perform the HS transformation is dictated by the physical system we wish to describe. Since we want to study the CDW phase, the meaningful channel is one that involves particle-hole bilinears between different sublattice sites. Therefore,

applying the anti-commutation relations of the fermionic operators $\{c^\dagger_{\vec{k}'\beta}, c_{\vec{k}\alpha}\} = \delta_{\vec{k}\vec{k}'}\delta_{\alpha\beta}$ and $\{c_{\vec{k}'\beta}, c_{\vec{k}\alpha}\} = 0$, the Hamiltonian can be rewriten as

$$\begin{aligned} H'' = &- \frac{V}{2\mathcal{N}} \sum_{\sigma\sigma'} \sum_{\vec{k}\vec{k}'\vec{q}} \sum_{\alpha\neq\beta} \left(1 + e^{-2i(\vec{k}'-\vec{k})\cdot\vec{a}_{\beta\alpha}}\right) c^\dagger_{\vec{k}'\beta\sigma} c_{\vec{k}'+\vec{q}\alpha\sigma'} c^\dagger_{\vec{k}+\vec{q}\alpha\sigma'} c_{\vec{k}\beta\sigma} \\ &+ \frac{V}{\mathcal{N}} \sum_{\sigma\sigma'} \sum_{\vec{k}\vec{q}} \sum_{\alpha} c^\dagger_{\vec{k}\alpha\sigma'} c_{\vec{k}\alpha\sigma'}. \end{aligned} \tag{5.8}$$

The last term in the Hamiltonian, that arises from the anticonmutation of the fields, can be simply included with the chemical potential.

However, before continuing with the decoupling of the interaction, it is worth paying greater attention to the two interactions that are part of our Hubbard model, and how they affect bond orders.

### 5.1.1 On site vs. nearest neighbours interactions

The kagome Hubbard model has been extensively discussed in the literature [27, 24, 28], including the discussion of how the two interactions can promote different instabilities. An essential factor of said discussion is a mechanism called *sublattice interference*, which impacts the nesting of the Fermi surface, affecting the possible Fermi surface instabilities [28].

Let us start by looking at the on site interaction ($U$) for an electron filling such that we are at the upper vH point. Going to band space, it is enough to consider the band that is closest to the Fermi level. Therefore, we can redefine the interaction $\tilde{U} = U \sum_{\alpha\eta} u^*_{\alpha\eta}(\vec{k}') u_{\alpha\eta}(\vec{k}'+\vec{q}) u^*_{\alpha\eta}(\vec{k}'+\vec{q}) u_{\alpha\eta}(\vec{k}')$. This interaction vertex is diagonal in the sublattice index. However, if we are to recall the sublattice distribution along the Fermi surface at the upper vH point (Fig. 3.6(a)-(b)), the nesting vectors at the $M$-points only connect different sublattice sites. As a result, the interaction vertex will be small, so that nesting does not enhance the particle-hole pairing for the on-site interaction, which brings the name *sublattice interference* to this effect. On the other hand, as the nearest-neighbour interactions $\tilde{V} = V \sum_{\alpha\beta\eta} u^*_{\beta\eta}(\vec{k}') u_{\beta\eta}(\vec{k}'+\vec{q}) u^*_{\alpha\eta}(\vec{k}'+\vec{q}) u_{\alpha\eta}(\vec{k}')$ are not diagonal in the sublattice index, the sublattice interference effects are reduced, reestablishing the nesting enhancement given by the FS geometry.

In turn, we can wonder what would happen if we were to be at the lower vH point, which is of a mixed type (Fig. 3.6(c)-(d)). In this case, the nesting vectors connect points in which there is same-site contributions. Hence, the on-site interaction will not be as affected by the sublattice interference mechanism, making the interplay between both interaction vertices more complex. Furthermore, the opposite case can be found, for instance, in the honeycomb lattice. As previously mentioned, while possessing the same FS geometry, the sublattice weight distribution along said surface is homogeneous. Hence, sublattice interference effects do not take place at all, making on-site interactions the ones that enhance the pairing, as opposed to long-range interactions.

Apart from the effect of sublattice interference on the nesting effects, one can wonder if these interactions can promote the charge bond orders. For illustrative purposes, let us write the usual (real-space) on-site Hubbard interaction in terms of the charge and spin

densities:

$$H' = \frac{U}{4}\sum_i (n_{i\uparrow} + n_{i\downarrow})^2 - \frac{U}{4}\sum_i (n_{i\uparrow} - n_{i\downarrow})^2$$

The Hubbard model is frequently presented in the context of magnetism, where the HS transformation is done in the spin density channel. The fact that the interaction is attractive means that the RPA susceptibility exhibits the behaviour $\chi_{RPA} \approx (U^{-1} - \chi_0)^{-1}$. Both $U$ and $\chi_0$ are positive magnitudes, so that there will be a point in which they are equal, making the susceptibility diverge, and thus, the system is found to be unstable. However, if one where to do an analogous decoupling in the charge density channel, the repulsive nature of the interaction for this case means that the behaviour of the RPA susceptibility will instead be $\chi_{RPA} \approx (U^{-1} + \chi_0)^{-1}$. Therefore, $U$ will not cause an instability in the charge density channel.

In the present case, from looking at (5.4) and (5.15), we can deduce that the on-site $U$ will not cause an instability in the bond channel.

It is for this reasoning that in the model presented in this work the on-site interactions will be omitted and only the nearest-neighbours interactions will be treated. This allows us to have the sum over the spins to be implicit in the remaining of the study, reducing greatly the calculations.

### 5.1.2 Decoupling of the interactions

Even if we have already established that the decoupling will be done in the bond channel, there is still different choices one can make. Now, the process of starting from a fundamental interaction in real space and only subsequently going to momentum space, means having a momentum-dependent factor in front of the creation/annihilation operators in $H''$. Determining the optimal way of dealing with this factor proved to be a greater challenge than initially anticipated.

One possibility is to include it in the definition of a momentum-dependent interaction $V^{\alpha\beta}(\vec{k}, \vec{k}') = V\left(1 + e^{2i(\vec{k}'-\vec{k})\cdot\vec{a}_{\alpha\beta}}\right)$. However, this would imply the definition of bilinears of the form $n^{\alpha\beta}_{\vec{k},\vec{q}} = c^\dagger_{\vec{k}+\vec{q}\alpha} c_{\vec{k}\beta}$, and having bilinears with four degrees of freedom proved to become burdensome. More importantly, doing the HS transformation with a non-scalar interaction was very intricate and introduces issues when it came to inverting the matrix later on in the process. The alternative is including it in the definition of the bilinears. However, even in that case, we had to deal with the restriction $\alpha \neq \beta$ in the sum over the sites. Initially we thought of dealing with it by including said restriction in the definition of the interaction by defining the interaction matrix $V_{\alpha\beta} = V(1 - \delta_{\alpha\beta})$. This idea was also rejected since this matrix is singular, so that the HS was not allowed to be performed. This can easily be solved, though, by including the factor $(1 - \delta_{\alpha\beta})$ in the definition of the bilinears and having the interaction strength to just be a constant.

An initial guess for including the momentum dependent factor in the definition of the bilinears, was to write it in terms of sines and cosines:

$$\left(1+e^{-2i(\vec{k}'-\vec{k})\cdot\vec{a}_{\beta\alpha}}\right) = 2e^{-i\vec{k}'\cdot\vec{a}_{\beta\alpha}}\cos\left(\vec{k}'\cdot\vec{a}_{\beta\alpha}\right)e^{-i\vec{k}\cdot\vec{a}_{\alpha\beta}}\cos\left(\vec{k}\cdot\vec{a}_{\alpha\beta}\right) \\ -2e^{-i\vec{k}'\cdot\vec{a}_{\beta\alpha}}\sin\left(\vec{k}'\cdot\vec{a}_{\beta\alpha}\right)e^{-i\vec{k}\cdot\vec{a}_{\alpha\beta}}\sin\left(\vec{k}\cdot\vec{a}_{\alpha\beta}\right)\ ,$$

which motivated the definition of the complex bilinears:

$$n_{\vec{q}}^{\alpha\beta} = (1-\delta_{\alpha\beta})\frac{1}{\mathcal{N}}\sum_{\vec{k}} e^{-i\vec{k}\cdot\vec{a}_{\alpha\beta}}\cos\left(\vec{k}\cdot\vec{a}_{\alpha\beta}\right)c^{\dagger}_{\vec{k}+\vec{q}\alpha}c_{\vec{k}\beta}\ , \tag{5.9}$$

$$m_{\vec{q}}^{\alpha\beta} = (1-\delta_{\alpha\beta})\frac{1}{\mathcal{N}}\sum_{\vec{k}} e^{-i\vec{k}\cdot\vec{a}_{\alpha\beta}}\sin\left(\vec{k}\cdot\vec{a}_{\alpha\beta}\right)c^{\dagger}_{\vec{k}+\vec{q}\alpha}c_{\vec{k}\beta}\ , \tag{5.10}$$

As a result, the Hamiltonian could be written as

$$H'' = -V\mathcal{N}\sum_{\vec{q}}\sum_{\alpha\beta}\left[(n_{\vec{q}}^{\alpha\beta})^{\dagger}n_{\vec{q}}^{\alpha\beta} + (m_{\vec{q}}^{\alpha\beta})^{\dagger}m_{\vec{q}}^{\alpha\beta}\right]\ . \tag{5.11}$$

Even if we succeeded in the decoupling with this definition of the bilinears, and we could obtain an expression for the perturbative expansion of the free energy, we found that the order parameters associated to the bilinears were not independent. With the objective of trying to find a set of bilinears that were independent, we tried a different approach, which was to define the complex bilinears:

$$n_{\vec{q}}^{\alpha\beta} = \frac{1}{\mathcal{N}}(1-\delta_{\alpha\beta})\sum_{\vec{k}} c^{\dagger}_{\vec{k}+\vec{q}\alpha}c_{\vec{k}\beta} \quad , \quad m_{\vec{q}}^{\alpha\beta} = \frac{1}{\mathcal{N}}(1-\delta_{\alpha\beta})\sum_{\vec{k}} e^{-2i\vec{k}\cdot\vec{a}_{\alpha\beta}}c^{\dagger}_{\vec{k}+\vec{q}\alpha}c_{\vec{k}\beta}, \tag{5.12}$$

Again, the decoupling process was successful but the results were not easy to interpret since the fields were still coupled and there was not a clear distinction between real and imaginary order parameters. Therefore, the final approach was to divide each of the complex bilinears defined in (5.12) into their real and imaginary parts. Thus, taking $n_{\vec{q}}^{\alpha\beta} = n_{\vec{q}R}^{\alpha\beta} + n_{\vec{q}I}^{\alpha\beta}$ and $m_{\vec{q}}^{\alpha\beta} = m_{\vec{q}R}^{\alpha\beta} + m_{\vec{q}I}^{\alpha\beta}$, the new set of bilinears is:

$$n_{\vec{q}R}^{\alpha\beta} = \frac{1}{2\mathcal{N}}(1-\delta_{\alpha\beta})\sum_{\vec{k}}\left(c^{\dagger}_{\vec{k}+\vec{q}\alpha}c_{\vec{k}\beta} + c^{\dagger}_{\vec{k}\beta}c_{\vec{k}+\vec{q}\alpha}\right) = (n_{\vec{q}R}^{\alpha\beta})^{\dagger} \tag{5.13a}$$

$$n_{\vec{q}I}^{\alpha\beta} = \frac{1}{2\mathcal{N}}(1-\delta_{\alpha\beta})\sum_{\vec{k}}\left(c^{\dagger}_{\vec{k}+\vec{q}\alpha}c_{\vec{k}\beta} - c^{\dagger}_{\vec{k}\beta}c_{\vec{k}+\vec{q}\alpha}\right) = -(n_{\vec{q}I}^{\alpha\beta})^{\dagger} \tag{5.13b}$$

$$m_{\vec{q}R}^{\alpha\beta} = \frac{1}{2\mathcal{N}}(1-\delta_{\alpha\beta})\sum_{\vec{k}}\left(e^{-2i\vec{k}\cdot\vec{a}_{\alpha\beta}}c^{\dagger}_{\vec{k}+\vec{q}\alpha}c_{\vec{k}\beta} + e^{-2i\vec{k}\cdot\vec{a}_{\beta\alpha}}c^{\dagger}_{\vec{k}\beta}c_{\vec{k}+\vec{q}\alpha}\right) = (m_{\vec{q}R}^{\alpha\beta})^{\dagger} \tag{5.13c}$$

$$m_{\vec{q}I}^{\alpha\beta} = \frac{1}{2\mathcal{N}}(1-\delta_{\alpha\beta})\sum_{\vec{k}}\left(e^{-2i\vec{k}\cdot\vec{a}_{\alpha\beta}}c^{\dagger}_{\vec{k}+\vec{q}\alpha}c_{\vec{k}\beta} - e^{-2i\vec{k}\cdot\vec{a}_{\beta\alpha}}c^{\dagger}_{\vec{k}\beta}c_{\vec{k}+\vec{q}\alpha}\right) = -(m_{\vec{q}I}^{\alpha\beta})^{\dagger} \tag{5.13d}$$

The Hamiltonian in (5.15) can be rewritten in terms of these bilinears (as shown in Appendix C.1), yielding

$$H'' = -\frac{V\mathcal{N}}{2}\sum_{\alpha\beta}\sum_{\vec{q}}\left[(n_{\vec{q}R}^{\alpha\beta})^{\dagger}n_{\vec{q}R}^{\alpha\beta} + (n_{\vec{q}I}^{\alpha\beta})^{\dagger}n_{\vec{q}I}^{\alpha\beta} + (m_{\vec{q}R}^{\alpha\beta})^{\dagger}m_{\vec{q}R}^{\alpha\beta} + (m_{\vec{q}I}^{\alpha\beta})^{\dagger}m_{\vec{q}I}^{\alpha\beta}\right]. \tag{5.14}$$

### 5.1.3 Hubbard-Stratonovich transformation

Now, this Hamiltonian is formulated in the "optimal" form to perform the HS transformation in all four channels. Following the standard procedure applied to repulsive interactions, for each of the channels that we wish to decouple in, we will introduce a white noise field $\gamma_{\vec{q}i}^{\alpha\beta}$ with the action $S_{\gamma_i} = -\frac{\mathcal{N}}{2V}\int_0^\beta d\tau \sum_{\vec{q}\alpha\beta} \bar{\gamma}_{\vec{q}i}^{\alpha\beta}\gamma_{\vec{q}i}^{\alpha\beta}$ [1]. Since the correlation functions of these white-noise fields are just a constant, multiplying the original partition function by $\mathcal{Z}_{\gamma_i} = \int \mathcal{D}[\gamma_i] e^{-S[\gamma_i]}$ will just account for a shift in the free energy of our system [2] , leaving its physical properties unchanged. In turn, entangling the two functional integrals will allow for the definition of an effective action that decouples the interactions. Indeed, after introducing a set of variables that are a combination of the white-noise fields and the physical fields (5.13), the quadratic terms in the bilinears are cancelled. These new set of variables $\left(N_{\vec{q}R}^{\alpha\beta}, N_{\vec{q}I}^{\alpha\beta}, M_{\vec{q}R}^{\alpha\beta} \text{ and } M_{\vec{q}I}^{\alpha\beta}\right)$ are often referred to as Weiss fields , and the decoupled interaction Hamiltonian becomes

$$\begin{aligned}\tilde{H}'' = &-\mathcal{N}\sum_{\vec{q}\mu}\left(N_{\vec{q}R}^{\alpha\beta}n_{\vec{q}R}^{\alpha\beta} - N_{\vec{q}I}^{\alpha\beta}n_{\vec{q}I}^{\alpha\beta} + M_{\vec{q}R}^{\alpha\beta}m_{\vec{q}R}^{\alpha\beta} - M_{\vec{q}I}^{\alpha\beta}m_{\vec{q}I}^{\alpha\beta}\right)\\ &+\frac{\mathcal{N}}{2V}\sum_{\vec{q}\mu}\left(\left(N_{\vec{q}R}^{\alpha\beta}\right)^2 - \left(N_{\vec{q}I}^{\alpha\beta}\right)^2 + \left(M_{\vec{q}R}^{\alpha\beta}\right)^2 - \left(M_{\vec{q}I}^{\alpha\beta}\right)^2\right). \end{aligned} \tag{5.15}$$

A detailed derivation of this procedure can be found in Appendix C.1.

Written in this way, it the spirit of the HS transformation is apparent: under the path integral, the interactions can be rewritten in terms of electrons moving in the fluctuating Weiss fields, and these fluctuations are the ones that mediate the interactions between the electrons in this new picture. When the physical fields are prone to enter a broken-symmetry state, the distribution function of the Weiss fields becomes concentrated around a non-zero value, so that they can be identified with the order parameters of the broken-symmetry phase.

Taking into account the expressions of the bilinears, this Hamiltonian is now quadratic in the fermionic operators $c^\dagger, c$, so that the action (5.7) can be written as

$$\begin{aligned}S = \int_0^\beta d\tau \sum_{\alpha\beta}\Bigg[\sum_{\vec{k}\vec{k}'}\bar{c}_{\vec{k}\alpha}\left(\partial_\tau\delta_{\vec{k}\vec{k}'}\delta_{\alpha\beta} + \mathcal{H}_{\alpha\beta}(\vec{k},\vec{k}')[N_R,N_I,M_R,M_I]\right)c_{\vec{k}'\beta}\\ + \frac{\mathcal{N}}{2V}\sum_{\vec{q}\mu}\left(\left(N_{\vec{q}R}^{\alpha\beta}\right)^2 - \left(N_{\vec{q}I}^{\alpha\beta}\right)^2 + \left(M_{\vec{q}R}^{\alpha\beta}\right)^2 - \left(M_{\vec{q}I}^{\alpha\beta}\right)^2\right),\end{aligned} \tag{5.16}$$

where we have defined the effective Hamiltonian

$$\begin{aligned}\mathcal{H}_{\alpha\beta}(\vec{k},\vec{k}')[N_R,N_I,M_R,M_I] =& h_{\alpha\beta}(\vec{k})\delta_{\vec{k}\vec{k}'} - \frac{1}{2}(1-\delta_{\alpha\beta})\Big[N_{\vec{k}-\vec{k}'R}^{\alpha\beta} + N_{\vec{k}'-\vec{k}R}^{\beta\alpha} - N_{\vec{k}-\vec{k}'I}^{\alpha\beta}\\ &+ N_{\vec{k}'-\vec{k}I}^{\beta\alpha} + \left(M_{\vec{k}-\vec{k}'R}^{\alpha\beta} - M_{\vec{k}-\vec{k}'I}^{\alpha\beta}\right)e^{-2i\vec{k}'\cdot\vec{a}_{\alpha\beta}}\\ &+ \left(M_{\vec{k}'-\vec{k}R}^{\beta\alpha} + M_{\vec{k}'-\vec{k}I}^{\beta\alpha}\right)e^{-2i\vec{k}\cdot\vec{a}_{\alpha\beta}}\Big].\end{aligned} \tag{5.17}$$

Consequently, the electronic part of the partition function (5.6) has been reduced to a Gaussian integral, which can be analitically solved, a step which is commonly referred to as *integrating-out the fermions*. Essentially,

[1] Here and in the following, I will use the notation $\bar{\Delta}_{\vec{q}i}^{\alpha\beta}$ to refer to the operator $(\Delta_{\vec{q}i}^{\alpha\beta})^\dagger$ inside the action.

[2] $\mathcal{F} = -T\ln(\mathcal{Z}) = -T\ln\left(\mathcal{Z}\mathcal{Z}_{\gamma_i}\frac{1}{\mathcal{Z}_{\gamma_i}}\right) = -T\ln(\mathcal{Z}\mathcal{Z}_{\gamma_i}) + T\ln(\mathcal{Z}_{\gamma_i})$.

$$\begin{aligned}\mathcal{Z} &\equiv \int \mathcal{D}[N_R, N_I, M_R, M_I] \int \mathcal{D}[c, \bar{c}] e^{-S[c,\bar{c},N_R,N_I,M_R,M_I]} \\ &= \int \mathcal{D}[N_R, N_I, M_R, M_I] e^{-S_E[N_R,N_I,M_R,M_I]},\end{aligned} \tag{5.18}$$

where

$$\begin{aligned}S_E[N_R, N_I, M_R, M_I] = &- \operatorname{Tr}\left(\log\left(\partial_\tau \mathbb{1} + \mathcal{H}[N_R, N_I, M_R, M_I]\right)\right) \\ &+ \frac{\mathcal{N}}{2V} \int_0^\beta d\tau \sum_{\vec{q}} \sum_{\alpha\beta} \left( \left(N^{\alpha\beta}_{\vec{q}R}\right)^2 - \left(N^{\alpha\beta}_{\vec{q}I}\right)^2 + \left(M^{\alpha\beta}_{\vec{q}R}\right)^2 - \left(M^{\alpha\beta}_{\vec{q}I}\right)^2 \right),\end{aligned} \tag{5.19}$$

is the effective action of the Weiss fields.

## 5.2 Mean-field approach

The low-energy physics of the system can be extracted by performing a stationary phase analysis, which will allow the exploration of the broken-symmetry solutions. This is done by seeking the solutions of the saddle-point equations, which for $N_R$ take the form

$$\left.\frac{\partial S_E[N_R, N_I, M_R, M_I]}{\partial N_R}\right|_{N_R = N_R^{(0)}} = 0, \tag{5.20}$$

where $N_R^{(0)}$ constitutes the value at the saddle point. One can define analogous saddle-point equations for the rest of the fields, and they are the foundation of the mean-field approach: if the free energy (proportional to the action) develops a minimum around a non-zero value of the saddle-point solutions, the system enters a spontaneously broken-symmetry state. These mean-field solutions constitute then the order parameters of the broken symmetry state, and they are the starting point around which to compute the fluctuations. Certainly, this approach will be consistent only as long as the fluctuations are not strong enough to destroy the ordered state.

It can be shown (refer to Appendix C.2) that:

$$\left.\frac{\partial S_E}{\partial N^{\alpha\beta}_{\vec{q}R}}\right|_{N_R = N_R^{(0)}} = \mathcal{N}\left\langle n^{\alpha\beta}_{\vec{q}R}\right\rangle + \frac{\mathcal{N}}{V} N^{\alpha\beta(0)}_{\vec{q}R} = 0 \tag{5.21a}$$

$$\Rightarrow \quad N^{\alpha\beta(0)}_{\vec{q}R} = \frac{V}{2\mathcal{N}} \sum_{\vec{k}} \left\langle c^\dagger_{\vec{k}+\vec{q}\alpha} c_{\vec{k}\beta} + \text{H.c.} \right\rangle = (N^{\alpha\beta(0)}_{\vec{q}I})^\dagger, \tag{5.21b}$$

and for the rest of the fields:

$$N^{\alpha\beta(0)}_{\vec{q}I} = \frac{V}{2\mathcal{N}} \sum_{\vec{k}} \left\langle c^\dagger_{\vec{k}+\vec{q}\alpha} c_{\vec{k}\beta} - \text{H.c.} \right\rangle = -(N^{\alpha\beta(0)}_{\vec{q}I})^\dagger \tag{5.21c}$$

$$M^{\alpha\beta(0)}_{\vec{q}R} = \frac{V}{2\mathcal{N}} \sum_{\vec{k}} \left\langle e^{-2i\vec{k}\cdot\vec{a}_{\alpha\beta}} c^\dagger_{\vec{k}+\vec{q}\alpha} c_{\vec{k}\beta} + \text{H.c.} \right\rangle = (M^{\alpha\beta(0)}_{\vec{q}R})^\dagger \tag{5.21d}$$

$$M^{\alpha\beta(0)}_{\vec{q}I} = \frac{V}{2\mathcal{N}} \sum_{\vec{k}} \left\langle e^{-2i\vec{k}\cdot\vec{a}_{\alpha\beta}} c^\dagger_{\vec{k}+\vec{q}\alpha} c_{\vec{k}\beta} - \text{H.c.} \right\rangle = -(M^{\alpha\beta(0)}_{\vec{q}I})^\dagger \tag{5.21e}$$

Considering static configurations $N^{(0)}_{R(I)}(\tau) = N^{(0)}_{R(I)}$, $M^{(0)}_{R(I)}(\tau) = M^{(0)}_{R(I)}$, the effective action can be written in terms of the effective mean-field Hamiltonian $\mathcal{H}_{MF}[N^{(0)}_R, N^{(0)}_I, M^{(0)}_R M^{(0)}_I]$ and the fermionic Matsubara frequencies $i\omega_n$, yielding

$$\begin{aligned} S^{MF}_E = &- \mathrm{Tr}\left(\log\left(-i\omega_n \mathbb{1} + \mathcal{H}_{MF}[N^{(0)}_R, N^{(0)}_I, M^{(0)}_R M^{(0)}_I]\right)\right) \\ &+ \frac{\mathcal{N}\beta}{2V}\sum_{\vec{q}}\sum_{\alpha\beta}\left(\left(N^{\alpha\beta(0)}_{\vec{q}R}\right)^2 - \left(N^{\alpha\beta(0)}_{\vec{q}I}\right)^2 + \left(M^{\alpha\beta(0)}_{\vec{q}R}\right)^2 - \left(M^{\alpha\beta(0)}_{\vec{q}I}\right)^2\right). \end{aligned} \tag{5.22}$$

We can identify the factor inside the logarithm $\left(i\omega_n \mathbb{1} - \mathcal{H}_{MF}(\vec{k}, \vec{k}')\right) = G^{-1}(\vec{k}, \vec{k}'; i\omega_n)$ as the inverse of the propagator of the full system, and it can be split into the sum of two terms: the inverse of the free Green function $G_0^{-1}(\vec{k}; i\omega_n) = \left(i\omega_n \mathbb{1} - h(\vec{k})\right)$, and the scattering potential $\mathcal{V}$. The matrix elements of this last term are

$$\begin{aligned} \mathcal{V}^{\alpha\beta}(\vec{k}, \vec{k}') = \frac{1}{2}(1-\delta_{\alpha\beta})\Big[2\left(N^{\beta\alpha(0)}_{\vec{k}'-\vec{k}R} + N^{\beta\alpha(0)}_{\vec{k}'-\vec{k}I}\right) + e^{-2i\vec{k}'\cdot\vec{a}_{\alpha\beta}}\left(M^{\alpha\beta(0)}_{\vec{k}-\vec{k}'R} - M^{\alpha\beta(0)}_{\vec{k}-\vec{k}'I}\right) \\ + e^{-2i\vec{k}\cdot\vec{a}_{\alpha\beta}}\left(M^{\beta\alpha(0)}_{\vec{k}'-\vec{k}R} + M^{\beta\alpha(0)}_{\vec{k}'-\vec{k}I}\right)\Big]. \end{aligned} \tag{5.23}$$

Here we have used that, for an arbitrary $\vec{q}$, $N^{\beta\alpha(0)}_{-\vec{q}R} = N^{\alpha\beta(0)}_{\vec{q}R}$ and $N^{\beta\alpha(0)}_{-\vec{q}I} = -N^{\alpha\beta(0)}_{\vec{q}I}$, as it is proved in Appendix C.3. In the following, $k$ will denote the four-component momentum $(\vec{k}, i\omega_n)$, and the superscript (0) in the fields will be omitted for the sake of simplicity.

If one where to manipulate the first term in (5.22), so that

$$\mathrm{Tr}\left(\log\left(-G^{-1}\right)\right) = \mathrm{Tr}\big(\log\big(-G_0^{-1} - \mathcal{V}\big)\big) = \mathrm{Tr}\big(\log\big(-G_0^{-1}\big)\big) + \mathrm{Tr}(\log(1 + G_0\mathcal{V})), \tag{5.24}$$

one would see that the fist term in the sum is independent of the Weiss fields. After normalization, it just constitutes the free energy density of the non-interacting system. The second term is associated to the change in the free energy of the fermions due to the Weiss fields, and it can be interpreted as an infinite sum of Feynman diagrams, illustrating the iterative scattering process off the Weiss field.

$$\mathrm{Tr}(\log(1 + G_0\mathcal{V})) = \mathrm{Tr}\left(G_0\mathcal{V} - \frac{1}{2}(G_0\mathcal{V})^2 + \frac{1}{3}(G_0\mathcal{V})^3 - \frac{1}{4}(G_0\mathcal{V})^4 + ...\right). \tag{5.25}$$

In the vicinity of the phase transition, the order parameters are small in comparisson with the temperature, so that it is sensible to do a perturbative expansion of the action in $\mathcal{V}$.

The first term of the expansion, generally known as the Hartree contribution, must vanish. This becomes apparent when remembering that we are expanding around an extremum. Additionally, the interaction line carries zero momentum, and $N_{\vec{q}=0,R(I)} = 0$, $M_{\vec{q}=0,R(I)} = 0$.

The second order term in the expansion is significantly more interesting, and it will be the one in which we will focus on for the remainder of this thesis.

### 5.2.1 Second order term of the perturbative expansion

More specifically, written in terms of its matrix elements,

$$\mathrm{Tr}\big((G_0\mathcal{V})^2\big) = \sum_{kq}\sum_{\alpha\alpha'}\sum_{\beta\beta'} G_0^{\alpha\alpha'}(k)\mathcal{V}^{\alpha'\beta}(\vec{k},\vec{k}+\vec{q})G_0^{\beta\beta'}(k+q)\mathcal{V}^{\beta'\alpha}(\vec{k}+\vec{q},\vec{k}). \tag{5.26}$$

We can start the calculation of this term by addressing the two bare Green functions first, but for that an expression for the matrix elements of $G_0(k) = \left(i\omega_n\mathbb{1} - h(\vec{k})\right)^{-1}$ is needed. Naively, one might think that they are just $(i\omega_n - \varepsilon_{\vec{k}}^{\eta})^{-1}$, where $\eta$ is the energy band index. However, this is only the case in a diagonal basis, which is not the case for the site-basis in which the current calculations are done. Hence, the inversion of the matrix is not as straightforward. Nonetheless, a short calculation shown in Appendix A.3 provides that all it entails is the addition of the eigenvectors of the non-interacting Hamiltonian, so that:

$$G_0^{\alpha\beta}(\vec{k}, i\omega_n) = \sum_{\eta} \frac{u_{\alpha\eta}(\vec{k})u^*_{\eta\beta}(\vec{k})}{i\omega_n - \varepsilon_{\vec{k}}^{\eta}} \ . \tag{5.27}$$

In many cases the $\mathcal{V}$ fields have no momemtum and Matsubara frequency dependence, so that their coefficient, which is the Matsubara sum involving the two bare propagators, becomes the bare susceptibility of the system. In the present case, it is a tensor in sublattice space:

$$\chi_0^{\beta\alpha'\beta'\alpha}(\vec{q}) = -\frac{1}{\beta}\sum_{n}\sum_{\vec{k}} G_0^{\alpha\alpha'}(\vec{k}; i\omega_n)G_0^{\beta\beta'}(\vec{k}+\vec{q}; i\omega_n) \ . \tag{5.28}$$

Substituting (5.27) and performing the Matsubara sum, one obtains:

$$\chi_0^{\beta\alpha'\beta'\alpha} = -\sum_{\eta\eta'} \frac{f(\varepsilon_{\vec{k}}^{\eta}) - f(\varepsilon_{\vec{k}+\vec{q}}^{\eta'})}{\varepsilon_{\vec{k}}^{\eta} - \varepsilon_{\vec{k}+\vec{q}}^{\eta'}} u_{\alpha\eta}(\vec{k})u^*_{\eta\alpha'}(\vec{k})u_{\beta\eta'}(\vec{k}+\vec{q})u^*_{\eta'\beta'}(\vec{k}+\vec{q}), \tag{5.29}$$

where $f(\varepsilon)$ is the Fermi-Dirac distribution function and $\varepsilon$ are the eigenvalues of the tight-binding Hamiltonian.

The analytical expression of (5.26) for an arbitrary $\vec{q}$ proves to be rather complicated, as shown in Appendix C.4. However, from the existing knowledge of the kagome lattice, we suspect that the main contributions of $\vec{q}$ will be related to the $M$-vectors. This can be confirmed by an analysis of the bare susceptibility (5.29), which can be calculated numerically both along the high-symmetry line and over the BZ (Fig. 5.2).

The sum over the momentum index is always performed by defining a $\vec{k}$-grid that covers the whole first BZ, which for all of the calculations (except for Fig. 5.2(b), done with a grid of $150 \times 150$) in the remaining of the thesis was chosen to be $250 \times 250$. In addition, the temperature is taken to be so that $\beta = 100$ and the tight-binding hopping is set to be one. This implies that there are temperature effects that will not be accounted for in this study. For more details on the numerical calculations, refer to Appendix C.6.

One may wonder, however, how to obtain the curves in Fig. 5.2 from (5.29), since the latter is a $(3 \times 3 \times 3 \times 3)$ tensor. Said tensor can be rewritten into $(9 \times 9)$ matrix in the sublattice basis $\{AA, AB, AC, BA, BB, BC, CA, CB, CC\}$. The diagonalization process will provide nine eigenvalues, and it is the leading eigenvalue at each $\vec{q}$ that is plotted in

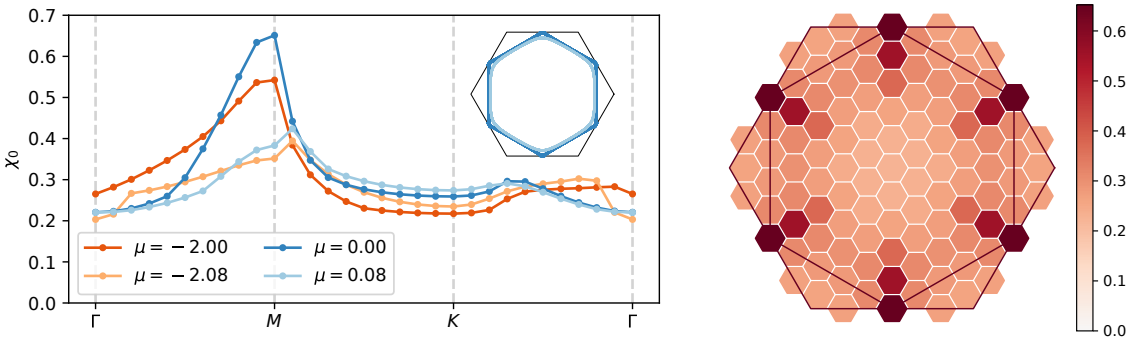


(a) (b)

Figure 5.2: Bare susceptibility plotted along the high-symmetry line (a), and over the first Brillouin zone for $\mu = 0$ (b). The inset in (a) shows the FS at both $\mu = 0$ and 0.08, which coincides with those at $\mu = -2$ and $-2.08$, respectively.

Fig. 5.2.

It is worth mentioning that the particular folding of the indices of the coefficients into this $(9 \times 9)$ matrix is important, i.e. how to arrange the indices in the reformulation $\chi^{\beta\alpha'\beta'\alpha} \to \chi^{\mu\nu}$ matters. For instance, if taking $\mu \equiv \alpha\alpha'$ and $\nu \equiv \beta\beta'$, diagonalizing $\chi_0$ provides both positive and negative eigenvalues. This does not make sense physically, since the susceptibility is required to be a positive magnitude, and hence, to have all positive eigenvalues. This was already taken into account when establishing the order of the indices in the definitions in (5.29), so that the adequate folding follows the intuitive fashion: $\mu \equiv \beta\alpha'$ and $\nu \equiv \beta'\alpha$.

In Fig. 5.2, one can observe a peak at the $M$-point at the vH points, which justifies the restriction of the momentum transferred $\vec{q}$ to be only one of the three M vectors $\vec{Q}_i$ with $i = 1, 2, 3$ for the rest of the calculations. Nonetheless, from 5.2(a) the electronic structure seems to be very sensitive to the precise chemical potential: a small deviation from the vH point causes both a drastic reduction of the peak, and the shift of the peak from the $M$-point. Therefore, even if this approximation is not ideal, it dramatically simplifies (5.26). More specifically, at these points the fields verify:

$$N^{\beta\alpha}_{\vec{Q}_i R} = N^{\beta\alpha}_{-\vec{Q}_i R} = N^{\alpha\beta}_{\vec{Q}_i R}, \qquad M^{\beta\alpha}_{\vec{Q}_i R} = M^{\beta\alpha}_{-\vec{Q}_i R} = e^{2i\vec{Q}_i\cdot\vec{a}_{\alpha\beta}} M^{\alpha\beta}_{\vec{Q}_i R},$$
$$N^{\beta\alpha}_{\vec{Q}_i I} = N^{\beta\alpha}_{-\vec{Q}_i I} = -N^{\alpha\beta}_{\vec{Q}_i I}, \qquad M^{\beta\alpha}_{\vec{Q}_i I} = M^{\beta\alpha}_{-\vec{Q}_i I} = -e^{2i\vec{Q}_i\cdot\vec{a}_{\alpha\beta}} M^{\alpha\beta}_{\vec{Q}_i I}.$$

After extensive rewriting (depicted in Appendix C.5), the second order term in the expansion, restricted to the M points, is

$$\mathrm{Tr}\big((G_0\mathcal{V})^2\big) = \beta\mathcal{N}\sum_i \sum_{\alpha\alpha'}\sum_{\beta\beta'} \Big[ C^{\beta\alpha'\beta'\alpha}_{NN}(\vec{Q}_i)\left(N^{\beta\alpha'}_{\vec{Q}_i R} N^{\beta'\alpha}_{\vec{Q}_i R} - N^{\beta\alpha'}_{\vec{Q}_i I} N^{\beta'\alpha}_{\vec{Q}_i I}\right) \tag{5.30}$$
$$+ C^{\beta\alpha'\beta'\alpha}_{MM}(\vec{Q}_i)\left(M^{\beta\alpha'}_{\vec{Q}_i R} M^{\beta'\alpha}_{\vec{Q}_i R} - M^{\beta\alpha'}_{\vec{Q}_i I} M^{\beta'\alpha}_{\vec{Q}_i I}\right) \tag{5.31}$$
$$+ C^{\beta\alpha'\beta'\alpha}_{NM}(\vec{Q}_i)\left(N^{\beta\alpha'}_{\vec{Q}_i R} M^{\beta'\alpha}_{\vec{Q}_i R} - N^{\beta\alpha'}_{\vec{Q}_i I} M^{\beta'\alpha}_{\vec{Q}_i I}\right)\Big], \tag{5.32}$$

with

$$C_{NN}^{\beta\alpha'\beta'\alpha}(\vec{Q}_i) =(1-\delta_{\alpha'\beta})(1-\delta_{\alpha\beta'})\frac{1}{\beta\mathcal{N}}\sum_k G_0^{\alpha\alpha'}(k)G_0^{\beta\beta'}(k+Q_i)\ , \tag{5.33a}$$

$$C_{MM}^{\beta\alpha'\beta'\alpha}(\vec{Q}_i) =(1-\delta_{\alpha'\beta})(1-\delta_{\alpha\beta'})\frac{1}{\beta\mathcal{N}}\sum_k G_0^{\alpha\alpha'}(k)G_0^{\beta\beta'}(k+Q_i)e^{-2i\vec{k}\cdot(\vec{a}_{\beta'\alpha}-\vec{a}_{\beta\alpha'})}\ , \tag{5.33b}$$

$$C_{NM}^{\beta\alpha'\beta'\alpha}(\vec{Q}_i) =2(1-\delta_{\alpha'\beta})(1-\delta_{\alpha\beta'})\frac{1}{\beta\mathcal{N}}\sum_k G_0^{\alpha\alpha'}(k)G_0^{\beta\beta'}(k+Q_i)e^{-2i\vec{k}\cdot\vec{a}_{\beta'\alpha}}\ . \tag{5.33c}$$

Nonetheless, it might be helpful to write the expression in terms of real fields instead, so that after defining $\tilde{N}_{\vec{Q}_iI}^{\alpha\beta} = iN_{\vec{Q}_iI}^{\alpha\beta}$ and $\tilde{M}_{\vec{Q}_iI}^{\alpha\beta} = iM_{\vec{Q}_iI}^{\alpha\beta}$,

$$\begin{aligned}\mathrm{Tr}\big((G_0\mathcal{V})^2\big) = \beta\mathcal{N}\sum_i\sum_{\alpha\alpha'}\sum_{\beta\beta'}\Big[&C_{NN}^{\beta\alpha'\beta'\alpha}(\vec{Q}_i)\left(N_{\vec{Q}_iR}^{\beta\alpha'}N_{\vec{Q}_iR}^{\beta'\alpha}+\tilde{N}_{\vec{Q}_iI}^{\beta\alpha'}\tilde{N}_{\vec{Q}_iI}^{\beta'\alpha}\right) &(5.34)\\ &+C_{MM}^{\beta\alpha'\beta'\alpha}(\vec{Q}_i)\left(M_{\vec{Q}_iR}^{\beta\alpha'}M_{\vec{Q}_iR}^{\beta'\alpha}+\tilde{M}_{\vec{Q}_iI}^{\beta\alpha'}\tilde{M}_{\vec{Q}_iI}^{\beta'\alpha}\right) &(5.35)\\ &+C_{NM}^{\beta\alpha'\beta'\alpha}(\vec{Q}_i)\left(N_{\vec{Q}_iR}^{\beta\alpha'}M_{\vec{Q}_iR}^{\beta'\alpha}+\tilde{N}_{\vec{Q}_iI}^{\beta\alpha'}\tilde{M}_{\vec{Q}_iI}^{\beta'\alpha}\right)\Big]\ . &(5.36)\end{aligned}$$

In the remaining discussions, when referring to the "imaginary" fields, it means the fields $\tilde{N}_{\vec{Q}_iI}$ and $\tilde{M}_{\vec{Q}_iI}$, which are real but come from the imaginary fields $N_{\vec{Q}_iI}$ and $M_{\vec{Q}_iI}$.

The coefficient (5.33a) can be identified as the bare susceptibility except for the existance of the delta functions, and the other two coefficients are weighted by exponential factors. The fact that the coefficients of $N_R$ and $\tilde{N}_I$, and of $M_R$ and $\tilde{M}_I$ are the same, respectively, means that these fields are degenerate at quadratic level. Hence, there is a symmetry that ensures that they are equal, and going to higher orders would be necessary to break the degeneracy.

Nonetheless, even at second order one can obtain ample information regarding the preferred ordering of the fields, a discussion that will be the focus of the next chapter.

# Chapter 6

# Landau theory for the free energy

As it was mentioned for the bare susceptibility, the coefficients of $\mathrm{Tr}\big((G_0\mathcal{V})^2\big)$ are $(3\times 3\times 3\times 3)$ tensors, which can be rewritten into $(9\times 9)$ matrices in the sublattice basis $\{AA, AB, AC, BA, BB, BC, CA, CB, CC\}$, as it can be seen in Fig. 6.1 for $\vec{q}=\vec{Q}_1$ at the upper vH point.

As they are, these matrices are not easily interpreted given the non diagonal elements, making their diagonalization the first natural step. The diagonalization process will provide a set of 9 eigenvalues and 9 eigenvectors. The latter will create a basis in which the fields can be expressed. Setting $v_{j,\vec{Q}_i}$ to be the eigenvectors of $C_{NN}(\vec{Q}_i)$, and $w_{j,\vec{Q}_i}$ those of $C_{MM}(\vec{Q}_i)$:

$$\begin{aligned} N^{\alpha\beta}_{\vec{Q}_iR} &= \sum_{j=1}^{9} a_{j,\vec{Q}_i} v^{\alpha\beta}_{j,\vec{Q}_i} \ , & \tilde{N}^{\alpha\beta}_{\vec{Q}_iI} &= \sum_{j=1}^{9} b_{j,\vec{Q}_i} v^{\alpha\beta}_{j,\vec{Q}_i} \ , \\ M^{\alpha\beta}_{\vec{Q}_iR} &= \sum_{j=1}^{9} c_{j,\vec{Q}_i} w^{\alpha\beta}_{j,\vec{Q}_i} \ , & \tilde{M}^{\alpha\beta}_{\vec{Q}_iI} &= \sum_{j=1}^{9} d_{j,\vec{Q}_i} w^{\alpha\beta}_{j,\vec{Q}_i} \ , \end{aligned} \tag{6.1}$$

where $a_{j,\vec{Q}_i}$, $b_{j,\vec{Q}_i}$, $c_{j,\vec{Q}_i}$ and $d_{j,\vec{Q}_i}$ are all real scalars, given that all of the fields are real. All sets of eigenvectors, in turn, can be viewed as $(3\times 3)$ matrices in the sublattice basis. For instance, both sets of eigenvectors $v_{j,\vec{Q}_i}$ and $w_{j,\vec{Q}_i}$ for $j=1,2,...,9$ are shown in Fig. 6.2 for the upper vH point.

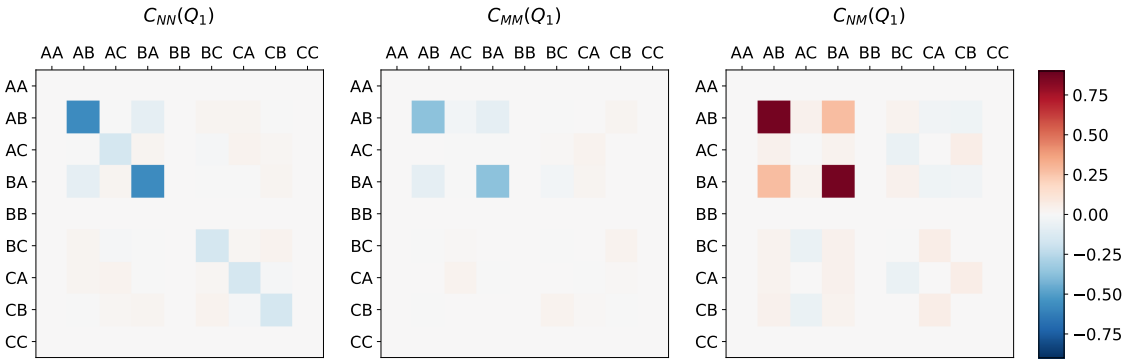


Figure 6.1: Graphical representation of the coefficients in (5.33) as $(9\times 9)$ matrices at the upper van Hove point ($\mu=0$).

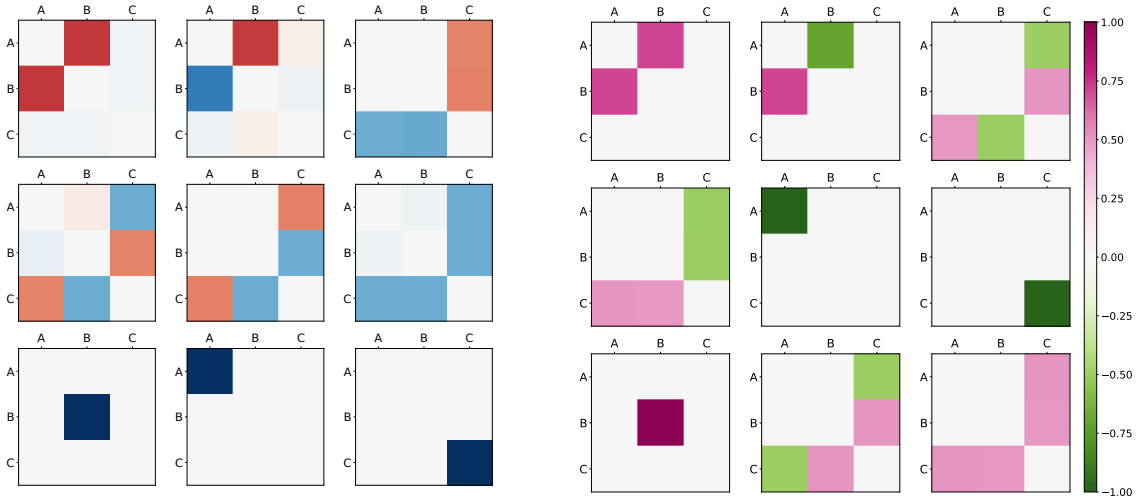


(a) (b)

Figure 6.2: Graphical representation of (a) $v_{j,\vec{Q}_1}$ and (b) $w_{j,\vec{Q}_1}$ for $j = 1, 2, ..., 9$ in order, from left to right and top to bottom, at the upper vH point. The ordering is done in reference to their associated eigenvalues, so that $j = 1$ correspond to the leading eigenvalue.

From (6.1) it becomes clear that the eigenvectors of the coefficients provide the sublattice structure to the fields. Indeed, if we look at the absolute value squared of these eigenvectors we will obtain the sublattice weights, in a similar fashion as we saw for the tight-binding model in Section 3.2. In Fig. 6.3(a)-(c) the graphical representation of $|v_{1,\vec{Q}_i}|^2$ in sublattice space at the upper vH point is displayed for each of the $M$-vectors.

A remarkable result can be extracted from this figure. To make it apparent, let us focus on Fig. 6.3(a), which represents $|v_{1,\vec{Q}_1}|^2$. The associated transferred momentum is $\vec{Q}_1$, which corresponds to the nesting vector that at the upper vH connects sites $A$ and $B$. And indeed, the main sublattice weights lie on $AB$ and $BA$. In contrast, one can look at the lower vH point, as depicted in Fig. 6.3(d). Now there is still only different site contributions, but now all of them have almost identical weight. Recall that the lower vH point is of mixed-type, so that for instance $\vec{Q}_1$ connects points with $AC$ and $BC$ distributions, and indeed, are the missing combinations, $AB$ and $BA$, the ones that have a slightly lower magnitude. A completely analogous discussion follows for Fig. 6.3(b)-(c), (e)-(f).

Consequently, even in the absence of interactions (if $V = 0$), the electrons already have a preference for bond ordering, which is purely a result of the sublattice structure of the system and nesting effects. [1]

However, without the addition of interactions, there will be no instability, and consequently, the system will not undergo a phase transition. Therefore, let us introduce these coefficients into the free energy to continue the discussion.

[1] One could argue that the preference for bond ordering is exclusively an aftermath of the delta functions present in (5.33), which prohibit same-site contributions in the coefficients. However, the calculation of the coefficients without said delta functions reveal that this statement remains true even in their absence.

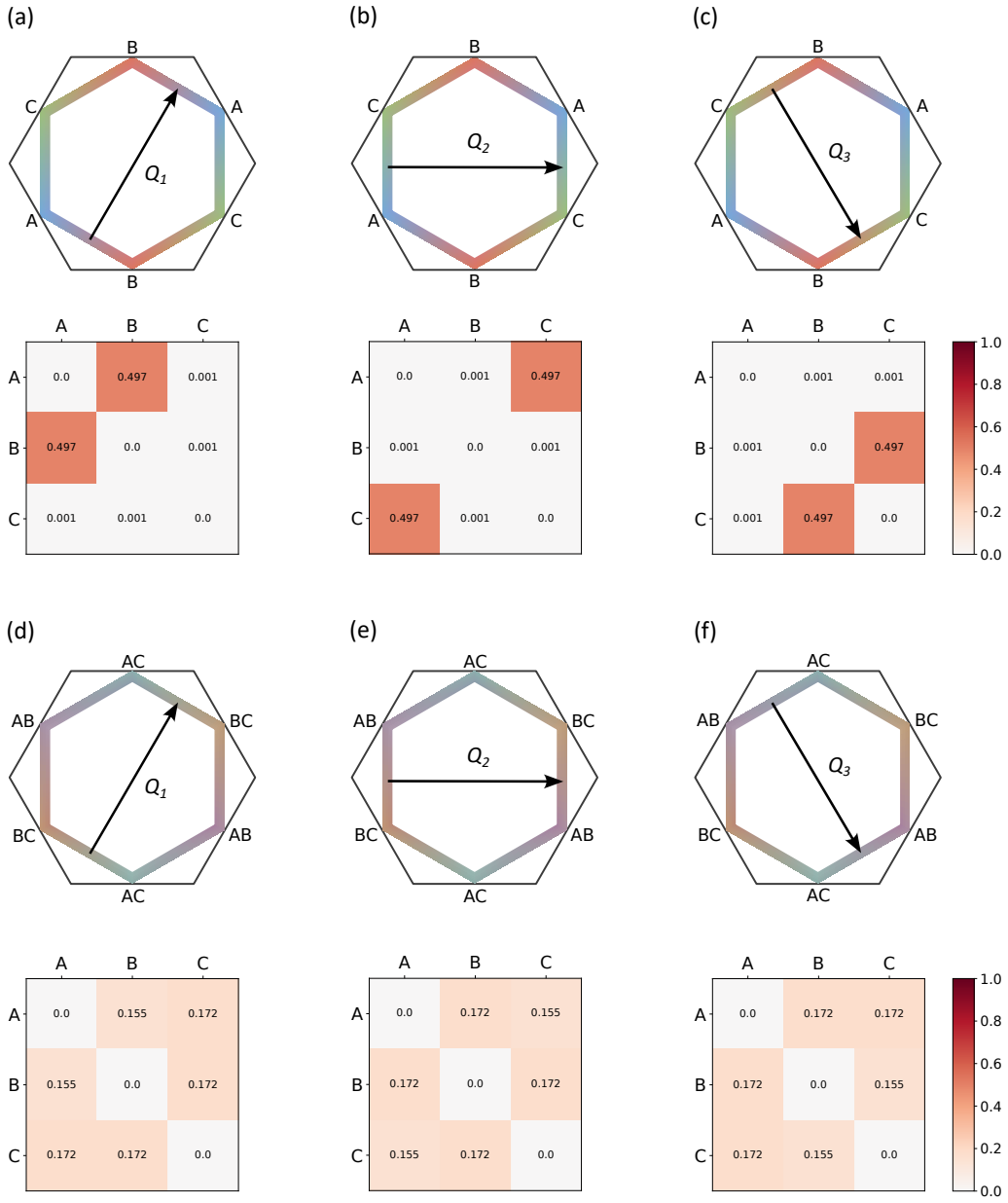


Figure 6.3: (a)-(c) Graphical representation of the Fermi surface and the sublattice distribution at the upper vH point with each of the M-vectors, and the sublattice structure $|v_{1,\vec{Q}_i}|^2$ of the corresponding field $N_{\vec{Q}_i}$. This can be compared to the equivalent calculations for the lower vH point (d)-(f). The plots corresponding to $|w_{1,\vec{Q}_i}|^2$ are identical.

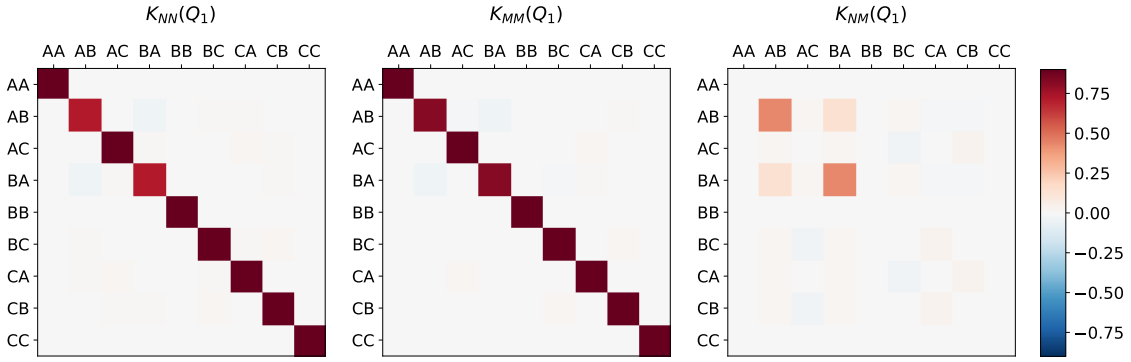


Figure 6.4: Graphical representation of the coefficients in (6.3) as $(9 \times 9)$ matrices at the upper van Hove point ($\mu = 0$) for $V = 0.5$.

## 6.1 Ginzburg-Landau free energy

Within the saddle point approximation, the partition function $\mathcal{Z} = e^{-\beta \mathcal{N} \mathcal{F}_E[N_R, N_I, M_R, M_I]} \approx e^{-S_E[N_R, N_I, M_R, M_I]}$, so the change in the effective free energy density of the electrons due to the mean-fields is

$$\begin{aligned}\Delta\mathcal{F}_E[N_R, N_I, M_R, M_I] = \frac{1}{\beta\mathcal{N}} \left[ \frac{1}{2} \operatorname{Tr}\big((G_0\mathcal{V})^2\big) - \frac{1}{3} \operatorname{Tr}\big((G_0\mathcal{V})^3\big) + \frac{1}{4} \operatorname{Tr}\big((G_0\mathcal{V})^4\big) - \ldots \right] \\ + \frac{1}{2V} \sum_{\vec{q}} \sum_{\alpha\beta} \left[ \big(N^{\alpha\beta}_{\vec{q}R}\big)^2 + \big(\tilde{N}^{\alpha\beta}_{\vec{q}I}\big)^2 + \big(M^{\alpha\beta}_{\vec{q}R}\big)^2 + \big(\tilde{M}^{\alpha\beta}_{\vec{q}I}\big)^2 \right].\end{aligned} \tag{6.2}$$

Applying the restriction of only having momentum transferred equally to the M-vectors, the second order term of this free energy density is

$$\begin{aligned}(\Delta\mathcal{F}_E)^{(2)}_V = \frac{1}{2} \sum_{\substack{\alpha\alpha' \\ \beta\beta'}} \sum_i \Big[ &\left( V^{-1}\delta_{\alpha\alpha'}\delta_{\beta\beta'} + C^{\beta\alpha'\beta'\alpha}_{NN}(\vec{Q}_i) \right) \left( N^{\beta\alpha'}_{\vec{Q}_iR} N^{\beta'\alpha}_{\vec{Q}_iR} + \tilde{N}^{\beta\alpha'}_{\vec{Q}_iI} \tilde{N}^{\beta'\alpha}_{\vec{Q}_iI} \right) \\ &+ \left( V^{-1}\delta_{\alpha\alpha'}\delta_{\beta\beta'} + C^{\beta\alpha'\beta'\alpha}_{MM}(\vec{Q}_i) \right) \left( M^{\beta\alpha'}_{\vec{Q}_iR} M^{\beta'\alpha}_{\vec{Q}_iR} + \tilde{M}^{\beta\alpha'}_{\vec{Q}_iI} \tilde{M}^{\beta'\alpha}_{\vec{Q}_iI} \right) \\ &+ C^{\beta\alpha'\beta'\alpha}_{NM}(\vec{Q}_i) \left( N^{\beta\alpha'}_{\vec{Q}_iR} M^{\beta'\alpha}_{\vec{Q}_iR} + \tilde{N}^{\beta\alpha'}_{\vec{Q}_iI} \tilde{M}^{\beta'\alpha}_{\vec{Q}_iI} \right) \Big].\end{aligned} \tag{6.3}$$

Now, we can define

$$\begin{aligned}K^{\beta\alpha'\beta'\alpha}_{NN}(\vec{Q}_i) &= \frac{1}{2} \left( V^{-1}\delta_{\alpha\alpha'}\delta_{\beta\beta'} + C^{\beta\alpha'\beta'\alpha}_{NN}(\vec{Q}_i) \right) , \\ K^{\beta\alpha'\beta'\alpha}_{MM}(\vec{Q}_i) &= \frac{1}{2} \left( V^{-1}\delta_{\alpha\alpha'}\delta_{\beta\beta'} + C^{\beta\alpha'\beta'\alpha}_{MM}(\vec{Q}_i) \right) , \\ K^{\beta\alpha'\beta'\alpha}_{NM}(\vec{Q}_i) &= \frac{1}{2} C^{\beta\alpha'\beta'\alpha}_{NM}(\vec{Q}_i) ,\end{aligned} \tag{6.4}$$

as the coefficients of the second order term of the free energy density. The interaction term $V^{-1}\delta_{\alpha\alpha'}\delta_{\beta\beta'}$, which couples bonds, will add elements in the diagonal of Fig. 6.1, so that for example for $V = 0.5$, this figure becomes Fig. 6.4.

Therefore, despite its complicated structure, what we have obtained is just a free energy analogous to those discussed in Chapter 4, but where the coefficients are now tensors instead of scalars. The approach taken in said chapter was to minimize the energy, and it was at the points that certain coefficients changed sign that marked that the instability

was taking place. The extension to the treatment of tensors would be to diagonalize the coefficients, and find when the eigenvalues change sign. However, there is a significant difference here: we have a term that couples the $N$ and $M$ fields. The fact that this term exists means that it is not sufficient with the diagonalization of $K_{NN}$ and $K_{MM}$. Furthermore, it implies that despite our efforts at the very beginning of this process to find the optimal definition of the bilinears in which to perform the HS transformation, the $N$ and $M$ fields are not the desired ones, in the sense that they will not tell us which are the fields that order at the phase transition. However, this issue can be address by diagonalizing the free energy in terms of the fields. Meaning, finding the combination of the $N$ and $M$ fields that do not couple in the free energy.

For this purpose, we can start by writing the fields in terms of the basis of eigenvectors of their associated coefficient as in the last section. Since the interaction matrix is diagonal, the eigenvectors are not affected, so that using the decomposition of the fields (6.1), equation (6.2) becomes

$$\begin{aligned}(\Delta\mathcal{F}_E)_V^{(2)} =& \sum_{i,j}\left[\sum_{\substack{\alpha\alpha'\\ \beta\beta'}} v_{j,\vec{Q}_i}^{\beta\alpha'} K_{NN}^{\beta\alpha'\beta'\alpha}(\vec{Q}_i) v_{j,\vec{Q}_i}^{\beta'\alpha}\right]\left[(a_{j,\vec{Q}_i})^2 + (b_{j,\vec{Q}_i})^2\right] \\ &+ \sum_{i,j}\left[\sum_{\substack{\alpha\alpha'\\ \beta\beta'}} w_{j,\vec{Q}_i}^{\beta\alpha'} K_{MM}^{\beta\alpha'\beta'\alpha}(\vec{Q}_i) w_{j,\vec{Q}_i}^{\beta'\alpha}\right]\left[(c_{j,\vec{Q}_i})^2 + (d_{j,\vec{Q}_i})^2\right] \\ &+ \sum_{i,j,j'}\left[\sum_{\substack{\alpha\alpha'\\ \beta\beta'}} v_{j,\vec{Q}_i}^{\beta\alpha'} K_{NM}^{\beta\alpha'\beta'\alpha}(\vec{Q}_i) w_{j',\vec{Q}_i}^{\beta'\alpha}\right]\left[a_{j,\vec{Q}_i} c_{j',\vec{Q}_i} + b_{j,\vec{Q}_i} d_{j',\vec{Q}_i}\right] \ .\end{aligned}$$

The factors in brackets can be seen as the contraction of the coefficients matrices by the vectors $v$, $w$. The first two are just the eigenvalues $\kappa_{NN,j}(\vec{Q}_i)$ and $\kappa_{MM,j}(\vec{Q}_i)$ of the corresponding matrices, since they are contracted by their own eigenvectors. Hence, $\kappa_{NN}(\vec{Q}_i)$ and $\kappa_{MM}(\vec{Q}_i)$ can be seen as diagonal matrices in $j, j'$-space additionally to being diagonal in "field"-space.

The third term couples both the $N$ and $M$ fields (represented by $a$ ($b$) and $c$ ($d$) for the $R$ ($I$) fields), and the different eigenvectors of each. For the sake of having symmetric? contractions, let us write this last term so that also the terms $c_{j,\vec{Q}_i} a_{j',\vec{Q}_i}$ and $d_{j,\vec{Q}_i} b_{j',\vec{Q}_i}$ appear. This is not as straightforward as it seems, since the order of the indices in $K_{NM}$ is very important: a different folding of the indices of the $(3\times3\times3\times3)$ will create a different $(9\times9)$ matrix.

By first swapping the roles of $j$ and $j'$, and later relabeling $\beta\leftrightarrow\beta'$, $\alpha\leftrightarrow\alpha'$, both of which one can do because there is a sum over all of those indices, we can define

$$\kappa_{NM,jj'}(\vec{Q}_i) = \frac{1}{2}\sum_{\substack{\alpha\alpha'\\ \beta\beta'}} v_{j',\vec{Q}_i}^{\beta\alpha'} K_{NM}^{\beta\alpha'\beta'\alpha}(\vec{Q}_i) w_{j,\vec{Q}_i}^{\beta'\alpha} \ , \tag{6.5a}$$

$$\kappa_{MN,jj'}(\vec{Q}_i) = \frac{1}{2}\sum_{\substack{\alpha\alpha'\\ \beta\beta'}} w_{j',\vec{Q}_i}^{\beta\alpha'} K_{NM}^{\beta'\alpha\beta\alpha'}(\vec{Q}_i) v_{j,\vec{Q}_i}^{\beta'\alpha} \ , \tag{6.5b}$$

so that the second order term of the free energy becomes

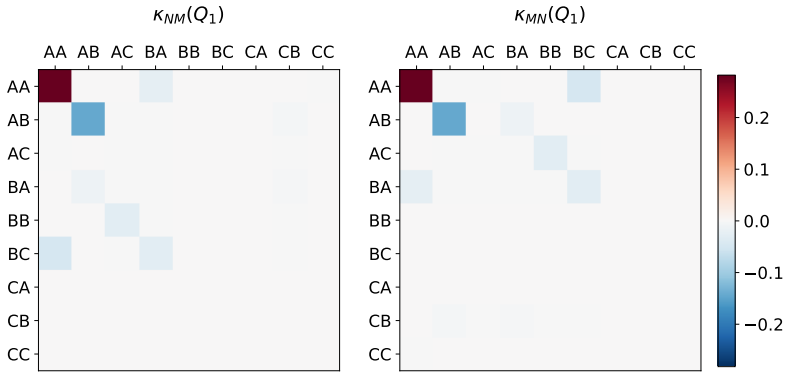


Figure 6.5: Representation of the non-diagonal $(9 \times 9)$ blocks $\kappa_{NM}(\vec{Q}_1)$ and $\kappa_{MN}(\vec{Q}_1)$ at the upper vH point.

$$
\begin{aligned}
(\Delta\mathcal{F}_E)_V^{(2)} = &\sum_{i,j} \kappa_{NN,j}(\vec{Q}_i)\left[(a_{j,\vec{Q}_i})^2 + (b_{j,\vec{Q}_i})^2\right] + \sum_{i,j} \kappa_{MM,j}(\vec{Q}_i)\left[(c_{j,\vec{Q}_i})^2 + (d_{j,\vec{Q}_i})^2\right] \\
&+ \sum_{i,j,j'} \kappa_{NM,jj'}(\vec{Q}_i)\left[a_{j,\vec{Q}_i} c_{j',\vec{Q}_i} + b_{j,\vec{Q}_i} d_{j',\vec{Q}_i}\right] \\
&+ \sum_{i,j,j'} \kappa_{MN,jj'}(\vec{Q}_i)\left[c_{j,\vec{Q}_i} a_{j',\vec{Q}_i} + d_{j,\vec{Q}_i} b_{j',\vec{Q}_i}\right] \ , \qquad (6.6)
\end{aligned}
$$

which can be written in matrix form in field-space in the following way:

$$
\begin{aligned}
(\Delta\mathcal{F}_E)_V^{(2)} = &\sum_i \left(a_{\vec{Q}_i}, c_{\vec{Q}_i}, b_{\vec{Q}_i}, d_{\vec{Q}_i}\right) \\
&\begin{pmatrix} \kappa_{NN}(\vec{Q}_i) & \kappa_{NM}(\vec{Q}_i) & 0 & 0 \\ \kappa_{MN}(\vec{Q}_i) & \kappa_{MM}(\vec{Q}_i) & 0 & 0 \\ 0 & 0 & \kappa_{NN}(\vec{Q}_i) & \kappa_{NM}(\vec{Q}_i) \\ 0 & 0 & \kappa_{MN}(\vec{Q}_i) & \kappa_{MM}(\vec{Q}_i) \end{pmatrix} \begin{pmatrix} a_{\vec{Q}_i} \\ c_{\vec{Q}_i} \\ b_{\vec{Q}_i} \\ d_{\vec{Q}_i} \end{pmatrix} \ . \qquad (6.7)
\end{aligned}
$$

Here, $a_{\vec{Q}_i}$ (and analogously for $b_{\vec{Q}_i}$, $c_{\vec{Q}_i}$ and $d_{\vec{Q}_i}$) is considered to be the 9 components vector $(a_{1,\vec{Q}_i}, a_{2,\vec{Q}_i}, ..., a_{9,\vec{Q}_i})$; and $\kappa_{NN}(\vec{Q}_i)$, $\kappa_{MM}(\vec{Q}_i)$, $\kappa_{NM}(\vec{Q}_i)$ and $\kappa_{MN}(\vec{Q}_i)$ to be $(9 \times 9)$ blocks in $j$-space. To recapitulate, each of the components of, for instance, the vector $a_{\vec{Q}_i}$ for $\mu = 0$ is the coefficient that accompanies each of the matrices in Fig. 6.2.

Given that the real and "imaginary" fields are not coupled, and they couple with each other with the same coefficients, the whole matrix is block diagonal, with the two non-zero blocks identical. Consequently, the diagonalization process is reduced to that of a single $(18 \times 18)$ matrix. Since $K_{NM}(\vec{Q}_i)$ and $K_{MN}(\vec{Q}_i)$, as well as $v_{j,\vec{Q}_i}$ and $w_{j,\vec{Q}_i}$, are independent of the interaction strength, the blocks $\kappa_{NM}(\vec{Q}_i)$ and $\kappa_{MN}(\vec{Q}_i)$ are constant with $V$ and can be seen in Fig. 6.5, highlighting that they are non-zero so indeed the fields couple.

The diagonalization of the $(18 \times 18)$ matrix will provide a set of eigenvalues, whose values will change depending on the interaction strength $V$. With increasing value of $V$, the eigenvalues will decrease in magnitude and some of them will eventually become negative, as one can appreciate from Fig. 6.6. It is at the point where the first eigen-

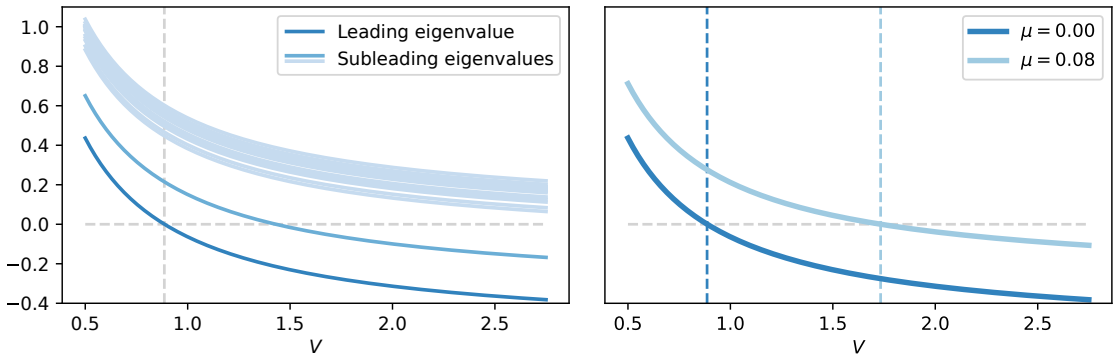


(a) (b)

Figure 6.6: (a) Eigenvalues of one of the $(18 \times 18)$ block-matrices in (6.7) with changing interaction strength for $\mu = 0$, and (b) Comparison of the minimum eigenvalue with changing $V$ for different chemical potentials. Vertical dashed lines signify the critical interaction strength $V_c$ in each case.

value reaches zero (let us call it $V_c$) that we can obtain the combination of fields that orders.

The last step it to look at what is the eigenvector associated to the eigenvalue that crosses zero at $V_c$. This 18 component eigenvector provides the field combination that orders at the instability. For example, for $\vec{Q}_1$ at $\mu = 0$, the 18 components $p_i$ with $i = 1, 2, ..., 18$ determine the weight that each of the matrices in Fig. 6.2 have, so that in general the combination of fields could be written like in Fig. 6.7. In this figure, distinct colors have been used to differentiate the matrices corresponding to the $N$ and $M$ fields, as it was represented in Fig. 6.2. In particular, the combination of fields arising from the obtain eigenvector that crosses zero is:

$$\Delta_{\vec{Q}_1} = 0.77 \; - 0.06 \; - 0.64 \; - 0.03 \; . \tag{6.8}$$

In conclusion, the field that orders $\Delta_{\vec{Q}_1}$ is mainly a combination of the $N^{AB}_{\vec{Q}_1}$, $N^{BA}_{\vec{Q}_1}$, $M^{AB}_{\vec{Q}_1}$ and $M^{BA}_{\vec{Q}_1}$.

However, two aspects are worth noting. First of all, the matrices that are used when making the combinations like the one showed in Fig. 6.7 change with the value of $\mu$. This means that from the beginning, it would not have been possible to perform the decoupling of the interaction in a particular set of bilinears. In turn, the field that orders at the phase transition is not a "universal" quantity of the system.

Secondly, it is important to address a result obtained in Chapter 4: contrary to the usual Ginzburg-Landau of the free energy, where only even powers of the order parameters appear, the OP of the rCDW phase had a trilinear term. The presence of this term meant that it was not the changing of the sign of the coefficient of the second order term that marked the phase transition, but that of the third order term. In this study we have only calculated the second order term and the third order term is not expected to be zero.

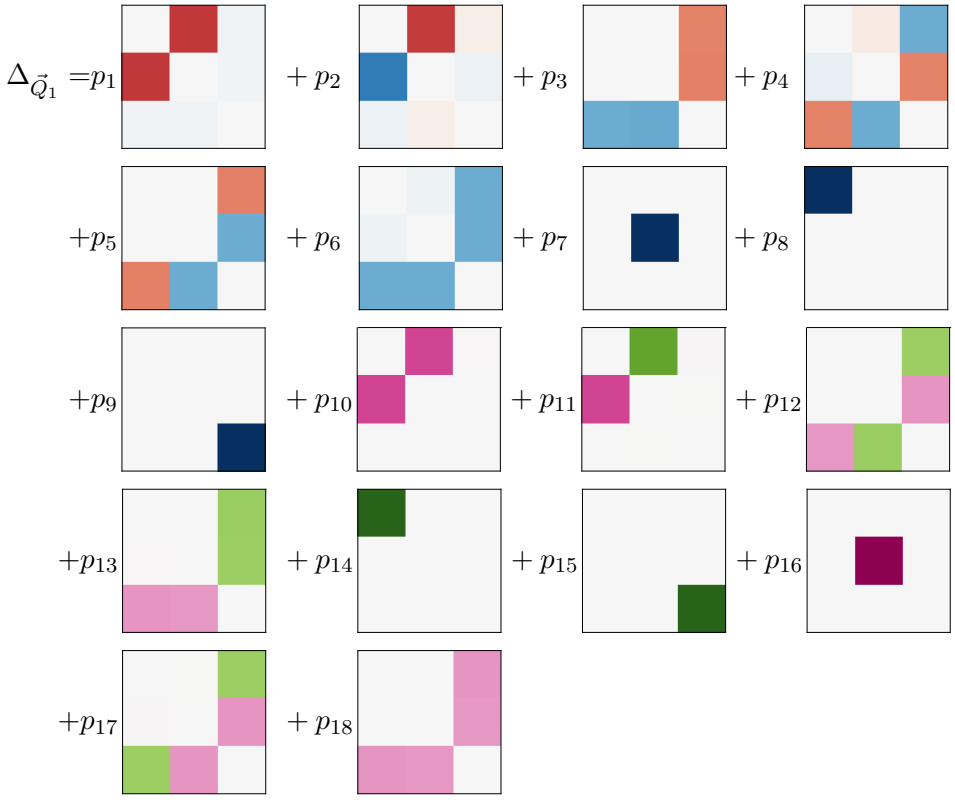


Figure 6.7: Representation of what the components of the eigenvector associated to the eigenvalue that crosses zero means. The matrices and the color scheme is that of Fig. 6.2.

Therefore, it is not the sign change of the coefficients presented here the ones give us the configuration of fields with minimum energy. However, what we have obtained is the field that will order. In other words, here we have obtained the expression of the order parameter (the analogous of, for example, (4.5) for the rCDW), but what we cannot obtain without the calculation of higher order terms is which combination of those OP is the one with minimum energy (which would be the analogous of not knowing which configuration ($3Q_+, 3Q_-, 1Q$, or any other) orders at the phase transition).

Finally, it is relevant to appreciate in Fig. 6.6(a) the large separation between the first two eigenvalues, and the rest, which show a strong preference for the ordering associated to these eigenvalues. Moreover, it is again surprising in Fig. 6.6(b) the strong dependence of the critical interaction strength to the van Hove physics: a slight departure from the vH singularity has a dramatic effect on the magnitude of $V_c$. Therefore, it can be of interest to evaluate its dependence around the saddle point, as well as how it compares with the case in which the system is at the lower vH point. This discussion, which is specially interesting since the FS around both vH points is identical, can be derived based on the information presented in Fig. 6.8.

To begin with, we can focus on the curve associated to the upper vH point. There is a very clear drop in the critical interaction strength at exactly the van Hove point, which does however not reach zero. The latter is probably caused by finite temperature effects, since in theory the system is at a point in which the bare susceptibility diverges, as it was

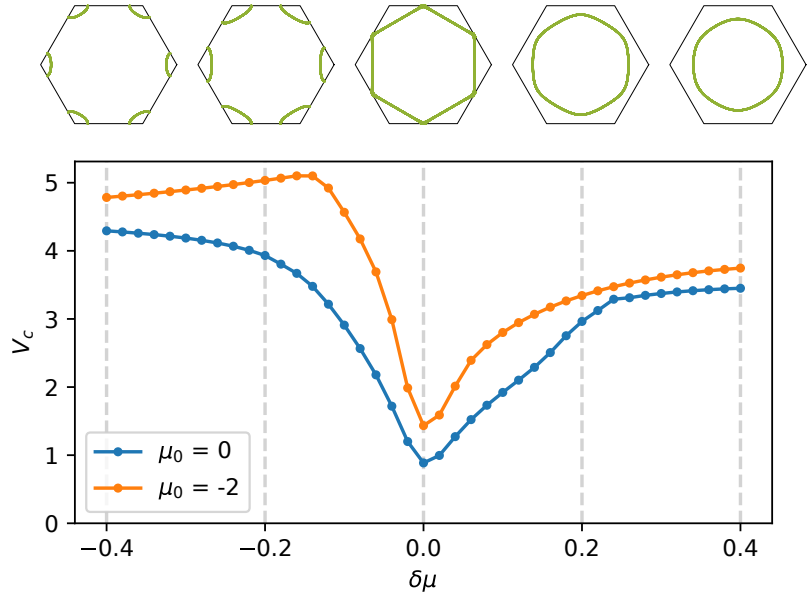


Figure 6.8: Interaction strength at which the instability happens as a function of the deviation from the van Hove singularities. This deviation $\delta\mu$ is defined as $\delta\mu = \mu - \mu_0$ for $\mu_0 = 0$ and $\delta\mu = \mu_0 - \mu$ for $\mu_0 = -2$. The values found for $V_c$ at $\mu = 0$ and $\mu = -2$ are 0.9 and 1.4, respectively. For reference, the Fermi surface at the chemical potential marked by vertical gray dashed lines are presented on top.

discussed in Chapter 4. As previously noted, the value of $V_c$ grows rapidly when moving away from the vH point, and in the figure one can also notice that the obtained values of $V_c$ are lower above than below the saddle point. Perhaps its origin could be in the different nesting in both Fermi surfaces. In order to address this, one can calculate the Linhard function (3.9) at two of these points, since this function is a measure of nesting. As seen in Fig. 6.9(a), the FS is more nested above the vH point, justifying at least partly the lower $V_c$. Additionally, a small kink can be seen close to $\mu = 0.2$ in Fig. 6.8 for $\mu = 0$. Its source is undetermined, but it does not seem to result from system size effects, since for a rather smaller grid of $\vec{k}$-points it is still present, as shown in Fig. 6.9(b).

At the lower vH point, a similar drop at the singularity is found, but at a higher value of $V_c$. Nonetheless, the curves are fairly distinct. Due to the identical Fermi surfaces, we could naively think that the differences between the two curves stem exclusively from the different sublattice structure of the fields. One has to be cautious, however, when addressing the results related to the lower vH point. At this point, as mentioned in Section 6.2(b), it is not suitable to disregard the on site interaction, as it has been done with this model, due to the different effect that sublattice interference causes at this point. Nonetheless, in both curves relatively flat regions are found when deviating enough from the saddle point, which is reasonable considering the small weight the FS has near the $M$-points.

At this point it is worth mentioning that while all of the discussion has been focused on $\vec{Q}_1$, the three $M$-vectors are symmetry equivalent, so that all of the presented results should stand for the remaining two. Nonetheless, in my numerical implementation there are small errors, possibly resulting from the numerical evaluation of the exponential factors, that accumulate and result in slight variations in the magnitudes of the eigenvalues, and consequently in $V_c$, between the three symmetry-equivalent $M$-points.

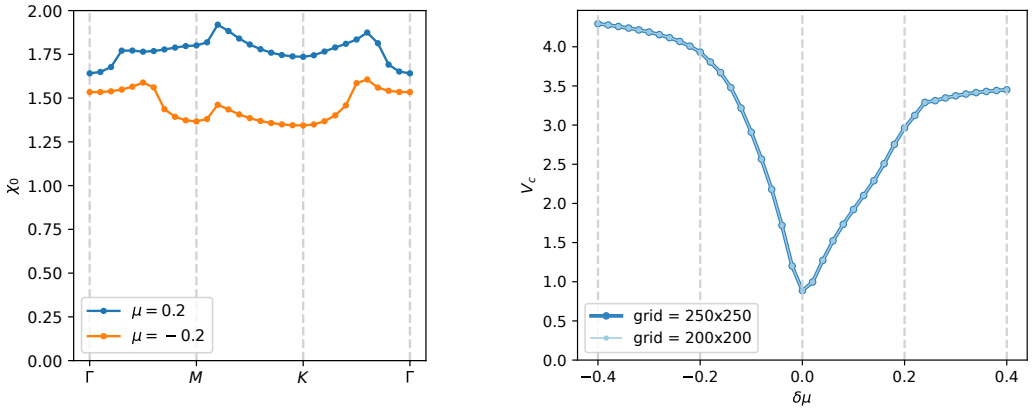


(a) (b)

Figure 6.9: (a) Linhard function at equal separation around the upper VH point. (b) Variation of $V_c$ with $\mu$ around the upper vH point for two different grid sizes.

# Chapter 7

# Conclusions and outlook

This thesis has been focused in the study of the charge density wave phase the the family of kagome metals $AV_3Sb_5$ are found to experience at around 90K from a microscopic point of view. Studies of this phase using patch models motivated the use of a more general model, with two main purposes: (1) to discover if the absence of an interaction that distinguish the interaction strengths of the real and imaginary order parameters of the CDW phase makes them degenerate; and (2) trying to uncover any features that might be overlooked by the strong simplifications assumed in patch models.

For that purpose, a nearest-neighbours Hubbard model was presented, where the kinetic part of the non-interacting Hamiltonian is taken to be the simplest tight-binding Hamiltonian with nearest-neighbours hopping. Since only the vanadium kagome layer was included in the model (motivated by the quasi-2D nature experimentally found in these materials), the present study is not restricted to the description of the $AV_3Sb_5$ materials.

A Hubbard-Stratonovich transformation was performed with the objective of obtaining the expression of the free energy. Within mean-field theory, the Ginzburg-Landau free energy up to second order was calculated, restricting the momentum transferred to only be the $M$-vectors. Despite the efforts directed at decoupling in a set of independent bilinears, the defined order parameters were found to couple in the expression of the free energy. Furthermore, the real and imaginary order parameters where indeed found to be degenerate at the second order level.

A diagonalization of the second order term of the free energy provided the expression of the order parameters that would order at the CDW phase transition. At the van Hove singularity, the OP is found to be a combination of the $N$ and $M$ fields, with similar but not equal weight, and with the sublattice structure that would be expected from the Fermi surface nesting discussion: the order modulated by $\vec{Q}_1$, $\vec{Q}_2$ and $\vec{Q}_3$ are mainly associated to bonds between $A-B$, $A-C$ and $B-C$ sites, respectively.

Exclusively from the second order term the minimum energy configuration cannot be obtain due to the presence of a trilinear term in the free energy. Hence, the calculation of higher order terms in the free energy would be necessary. Additionally, this would allow to see if the degeneracy between the real and imaginary order parameters is lifted.

However, the dependence of the expressions of the order parameters with the exact value of the chemical potential represent the fact that there is not a “universal” set of

bilinears that can be defined from the expression of the Hamiltonian. As a result, this approach seems to be too general for the study for the study that was proposed, since despite the heavy approximations very complex expressions were obtained.

Nonetheless, (not presented in this report) calculations of the free energy coefficients were performed for a different decoupling, which had sinusoidal prefactors on the fermionic operators instead of exponential, provided much simpler coefficients in the free energy that allowed the calculation of the coefficients for a general $\vec{q}$, and not exclusively restricted to the $M$-points. In turn, the classification of the fields into real and imaginary was not possible and they were all complex. It could still be useful to do the diagonalization of the free energy, since simpler expression might arise, and with the advantage of being expression with less approximations.

# Appendix A

## A.1 van Hove singularities and the DOS

Let us show that in two dimensions having an energy dispersion with a saddle point means that the density of states (DOS) has a logarithmic divergence.

If we focus on the Kagome lattice, and the saddle point at for example the $M_1$ point, the Taylor expansion of the tight-binding energy dispersion at the upper van Hove point is $\varepsilon(\vec{q}) = aq_x^2 - bq_y^2$. The expression for the density of states will then be

$$g(\varepsilon) = \int_{|\vec{q}|<\Lambda} \frac{dq^2}{(2\pi)^2} \delta(\varepsilon - \varepsilon(\vec{q})) \tag{A.1}$$

Performing the integral becomes significantly easier if one does the change of variables $q_x = q\cosh(\theta)/\sqrt{a}$ and $q_y = q\sinh(\theta)/\sqrt{b}$. Then, $\varepsilon(\vec{q}) = q^2$ and the area element becomes $d^2q = \left|\frac{\partial(q_x,q_y)}{\partial(q,\theta)}\right| dqd\theta = \frac{1}{\sqrt{ab}}|q|dqd\theta$. Substituting in the DOS,

$$g(\varepsilon) = \frac{1}{\sqrt{ab}} \frac{1}{(2\pi)^2} \int d\theta \int |q| dq \delta(\varepsilon - q^2) = \frac{1}{\sqrt{ab}} \frac{1}{(2\pi)^2} \int d\theta \tag{A.2}$$

where the integral over $q$ has been performed by using that $\int dx f(x)\delta(g(x)) = \sum_{x_i} \frac{f(x_i)}{|g'(x_i)|}$, where $x_i$ are the roots of $g(x)$. Now all is left is to consider the integration limits of $\theta$. Since $|\vec{q}| = q\sqrt{\frac{1}{a}(\cosh^2(\theta) + \frac{a}{b}\sinh^2(\theta))} < \Lambda$, considering that the integration over $q$ has been performed over the surface such that $\varepsilon(\vec{q}) = q^2 = \varepsilon$ and assuming perfect nesting ($a/b = 3$) without loss of generality, one gets that $|\theta| < \frac{1}{2}\cosh^{-1}\left(\frac{a\Lambda^2+\varepsilon}{2\varepsilon}\right)$. Finally,

$$g(\varepsilon) = \frac{1}{(2\pi)^2} \frac{\sqrt{3}}{a} \cosh^{-1}\left(\frac{a\Lambda^2 + \varepsilon}{2\varepsilon}\right) \tag{A.3}$$

$$\approx \frac{1}{(2\pi)^2} \frac{\sqrt{3}}{2a} \left(\frac{\varepsilon}{a\Lambda^2 + \varepsilon} + \log\left(\frac{a\Lambda^2}{\varepsilon}\right)\right) \tag{A.4}$$

The second line has been obtained by Taylor expading around $\varepsilon = 0$. In this last equation is now trasparent that the DOS diverges logarithmically at the saddle-point $\varepsilon = 0$.

## A.2 Energy dispersion around the saddle points

Since it has been shown the many interesting effects that happen at the $M$-point when the Fermi energy sits at the upper vH point, let us see what are the expressions that the

energy dispersion take at each of the three $M$-points. In order to do this, one can set the momentum to only move apart from $\vec{Q}_i$ a small amount $\vec{q}$. Substituting in (3.8),

$$\varepsilon^+(\vec{Q}_i+\vec{q}) = t\left(-1+\sqrt{3+2\cos\left(2(\vec{q}+\vec{Q}_i)\cdot\vec{a}_{AB}\right)+2\cos\left(2(\vec{q}+\vec{Q}_i)\cdot\vec{a}_{AC}\right)+2\cos\left(2(\vec{q}+\vec{Q}_i)\cdot\vec{a}_{BC}\right)}\right) \tag{A.5}$$

Considering the product of $\vec{Q}_i$ and $\vec{a}_{\mu\nu}$, one gets that, in particular for $\vec{Q}_1$

$$\varepsilon^+(\vec{Q}_1+\vec{q}) = t\left(-1+\sqrt{3+2\cos\left(2\vec{q}\cdot\vec{a}_{AB}\right)+2\cos\left(2\vec{q}\cdot\vec{a}_{AC}+\pi\right)+2\cos\left(2\vec{q}\cdot\vec{a}_{BC}+\pi\right)}\right) \tag{A.6}$$

Using that $\cos(x+\pi) = -\cos(\pi)$ and Taylor expanding $\cos(\pi) \approx 1-\frac{x^2}{2}$, one can also use the expressions of the

$$\begin{aligned}
\varepsilon^+(\vec{Q}_1+\vec{q}) =& t\left(-1+\sqrt{1-\left(2\vec{q}\cdot\vec{a}_{AB}\right)^2+\left(2\vec{q}\cdot\vec{a}_{AC}\right)^2+\left(2\vec{q}\cdot\vec{a}_{BC}\right)^2}\right)\\
=& t\left(-1+\sqrt{1-\frac{1}{4}\left(q_x+\sqrt{3}q_y\right)^2+q_x^2+\frac{1}{4}\left(q_x-\sqrt{3}q_y\right)^2}\right)\\
=& t\left(-1+\sqrt{1+q_x^2-\sqrt{3}q_xq_y}\right)
\end{aligned}$$

Taking that $\sqrt{1+x} \approx 1+\frac{x}{2}$,

$$\varepsilon^+(\vec{Q}_1+\vec{q}) = \frac{t}{2}\left(q_x^2-\sqrt{3}q_xq_y\right) \tag{A.7}$$

Doing an analogous calculation,

$$\varepsilon^+(\vec{Q}_2+\vec{q}) \approx \frac{t}{4}\left(-q_x^2+3q_y^2\right) \tag{A.8}$$

$$\varepsilon^+(\vec{Q}_3+\vec{q}) \approx \frac{t}{2}\left(q_x^2+\sqrt{3}q_xq_y\right) \tag{A.9}$$

One can compare these expressions with those stated in [5]. In order to compare them, one has to do the appropriate change of coordinates: reflection across the y axis, followed by a 30° clockwise rotation. Then, doing the substitution $q_x \to \frac{1}{2}(-\sqrt{3}q_x+q_y)$ and $q_y \to \frac{1}{2}(q_x+\sqrt{3}q_y)$ in equation (2) of [5] and assuming perfect nesting ($a/b=3$):

$$\begin{aligned}
\varepsilon_1(\vec{q}) &= aq_x^2-bq_y^2 &\to\quad & 2b(q_x^2-\sqrt{3}q_xq_y)\\
\varepsilon_2(\vec{q}) &= \frac{a-3b}{4}q_x^2+\frac{\sqrt{3}(a+b)}{2}q_xq_y+\frac{3a-b}{4}q_y^2 &\to\quad & b\left(-q_x^2+3q_y^2\right)\\
\varepsilon_3(\vec{q}) &= \frac{a-3b}{4}q_x^2+\frac{\sqrt{3}(a+b)}{2}q_xq_y+\frac{3a-b}{4}q_y^2 &\to\quad & 2b\left(q_x^2+\sqrt{3}q_xq_y\right),
\end{aligned}$$

which correspond to my expressions for $b = t/4$.

## A.3 Bare Green function

The time-ordered one-particle Green function is defined as $G_0^{\lambda\lambda'}(\vec{k},\vec{k}';t-t') = -i\left\langle Tc_{\vec{k}\lambda}(t)c^\dagger_{\vec{k}'\lambda'}(t')\right\rangle$, where the expectation value is taken in the ground state, $T$ represents the time ordering and $\lambda$ denotes the other degrees of freedom. In the case of translationally invariant systems in which $\lambda$ is a good quantum number, $G_0^{\lambda\lambda'}(\vec{k},\vec{k}';t-t') = \delta_{\lambda\lambda'}\delta_{\vec{k}\vec{k}'}G_0^{\lambda}(\vec{k},t-t')$ and one finds that in frequency space $G_0^{\lambda}(\vec{k},\omega) = (\omega-\varepsilon^{\lambda}_{\vec{k}})^{-1}$. In the imaginary-time formalism for finite temperature systems, the Greens function becomes $G_0^{\lambda}(\vec{k},\tau-\tau') = -\left\langle T_\tau c_{\vec{k}\lambda}(\tau)c^\dagger_{\vec{k}'\lambda'}(\tau')\right\rangle$ and $G_0^{\lambda}(\vec{k},i\omega_n) = (i\omega_n-\varepsilon^{\lambda}_{\vec{k}})^{-1}$, where $\tau$ is the imaginary time and $\omega_n$ are the fermionic Matsubara frequencies.

In the case that we have present, the non-interacting Hamiltonian in momentum space is diagonal in the energy-band basis, but not in the site basis. In the former case, the previous equations can therefore be used taking $\lambda=\eta$ the energy band index, with $\eta=0,\pm1$. But since I will be working in the site-basis, it is necessary to obtain a new expression for the bare Green function, which that can be obtained in terms of $G_0^{\eta}(\vec{k},i\omega_n)$.

Denoting $d_{\vec{k}\eta}$ ($d^\dagger_{\vec{k}\eta}$) the annihilation (creation) fermionic operators in the energy-band space and $u_\eta(\vec{k}) = (u_{\eta A}(\vec{k}), u_{\eta B}(\vec{k}), u_{\eta C}(\vec{k}))^T$ the eigenvectors of $H_0$, the basis change of the operators is

$$c_{\vec{k}\alpha} = \sum_\eta u_{\alpha\eta}d_{\vec{k}\eta} \qquad c^\dagger_{\vec{k}\alpha} = \sum_\eta u^*_{\eta\alpha}d^\dagger_{\vec{k}\eta} \tag{A.10}$$

and the Green function

$$\begin{aligned}
G_0^{\alpha\beta}(\vec{k},\vec{k}';\tau-\tau') &= -\left\langle T_\tau c_{\vec{k}\alpha}(\tau)c^\dagger_{\vec{k}'\beta}(\tau')\right\rangle = -\sum_{\eta\eta'}u_{\alpha\eta}(\vec{k})u^*_{\eta'\beta}(\vec{k}')\left\langle T_\tau d_{\vec{k}\eta}(\tau)d^\dagger_{\vec{k}'\eta'}(\tau')\right\rangle \\
&= \sum_{\eta\eta'}u_{\alpha\eta}(\vec{k})u^*_{\eta'\beta}(\vec{k}')G_0^{\eta\eta'}(\vec{k},\vec{k}';\tau-\tau') = \sum_\eta u_{\alpha\eta}(\vec{k})u^*_{\eta\beta}(\vec{k})G_0^{\eta}(\vec{k},\tau-\tau')\delta_{\vec{k}\vec{k}'} \\
&= G_0^{\alpha\beta}(\vec{k},\tau-\tau')
\end{aligned}$$

$$G_0^{\alpha\beta}(\vec{k},i\omega_n) = \int_0^\beta d\tau e^{i\omega_n(\tau-\tau')}G_0^{\alpha\beta}(\vec{k},\tau-\tau') \tag{A.11}$$

$$= \sum_\eta u_{\alpha\eta}(\vec{k})u^*_{\eta\beta}(\vec{k})\int_0^\beta d\tau e^{i\omega_n(\tau-\tau')}G_0^{\eta}(\vec{k},\tau-\tau') \tag{A.12}$$

$$= \sum_\eta u_{\alpha\eta}(\vec{k})u^*_{\eta\beta}(\vec{k})G_0^{\eta}(\vec{k},i\omega_n) = \sum_\eta \frac{u_{\alpha\eta}(\vec{k})u^*_{\eta\beta}(\vec{k})}{i\omega_n-\varepsilon^\eta_{\vec{k}}} \tag{A.13}$$

## A.4 Peierls instability

Let us show how for one-dimensional systems, an electonic instability can cause an spontaneous lattice instability. Below the critical temperature, there is no cost in energy to excite a phonon, so the phonon system becomes unstable and a phase transition occurs towards a structure that breaks translational symmetry.

Let us consider a simple tight-binding model for a 1D chain with $\mathcal{N}$ sites where the chemical potential is set to be zero: $H_0 = \sum_{k\sigma}\xi_k c^\dagger_{k\sigma}c_{k\sigma}$, where $\xi_k = -2t\cos(ak)$, $t$ is the

nearest-neighbour hopping amplitude and $a$ the lattice constant, that we can set to one. The first BZ is just $k \in [-\pi, \pi]$.

In the low temperature regime ($T \ll t$) the retarded electronic polarization bubble is

$$\chi_0^R(q, i\nu_n) = -\int \frac{dk}{2\pi} \sum_\sigma \frac{1}{\beta} \sum_{i\omega_n} G(k, i\omega_n) G(k+q, i\omega_n + i\nu_n) \tag{A.14}$$

$$= -\frac{1}{\pi} \int dk \frac{1}{\beta} \sum_{i\omega_n} \frac{1}{i\omega_n - \xi_k} \frac{1}{i\omega_n + i\nu_n - \xi_k - \xi_{k+q}} \ . \tag{A.15}$$

Solving the Matsubara sum,

$$\chi_0^R(q, i\nu_n) = -\frac{1}{\pi} \int dk \frac{f(\xi_k) - f(\xi_{k+q})}{i\nu_n + \xi_k - \xi_{k+q}} \ , \tag{A.16}$$

with $f$ being the Fermin function. We can identify the Linhard response function.

Since $k_F$ is the momentum such that the energy is the Fermi level, $\xi_{k_F} = -2t\cos(ak_F) = 0$ and $2k_F = \pi/a$. Now, we can notice that since $\xi_{k+2k_F} = -2t\cos(ak + \pi) = 2t\cos(ak) = -\xi_k$, $q = 2k_F$ is the nesting vector. Evaluating the polarization bubble at this point,

$$\chi_0^R(2k_F, i\nu_n) = \frac{1}{\pi} \int dk \frac{1 - 2f(\xi_k)}{i\nu_n + 2\xi_k} \ . \tag{A.17}$$

Performing analytic continuation and using that $1 - 2f(\xi_k) = \tanh\left(\frac{\beta\xi_k}{2}\right)$

$$\chi_0^R(2k_F, \omega) = \frac{1}{\pi} \int dk \frac{\tanh\left(\frac{\beta\xi_k}{2}\right)}{\omega + 2\xi_k} \ , \tag{A.18}$$

and in the static? limit, when $\omega \to 0$

$$\chi_0^R(2k_F, 0) = \frac{1}{\pi} \int_{-\pi/a}^{\pi/a} dk \frac{\tanh\left(\frac{\beta\xi_k}{2}\right)}{2\xi_k} = \frac{1}{\pi} \int_{-\pi/a}^{0} dk \frac{\tanh\left(\frac{\beta\xi_k}{2}\right)}{2\xi_k} + \frac{1}{\pi} \int_{0}^{\pi/a} dk \frac{\tanh\left(\frac{\beta\xi_k}{2}\right)}{2\xi_k} \ , \tag{A.19}$$

and since $\xi_k = \xi_{-k}$

$$\chi_0^R(2k_F, 0) = -\frac{1}{\pi} \int_{\pi/a}^{0} dk \frac{\tanh\left(\frac{\beta\xi_k}{2}\right)}{2\xi_k} + \frac{1}{\pi} \int_{0}^{\pi/a} dk \frac{\tanh\left(\frac{\beta\xi_k}{2}\right)}{2\xi_k} = \frac{1}{\pi} \int_{0}^{\pi/a} dk \frac{\tanh\left(\frac{\beta\xi_k}{2}\right)}{\xi_k} \ . \tag{A.20}$$

Doing the change of variables $x = \beta\xi_k/2$:

$$\chi_0^R(2k_F, 0) = \frac{\beta t}{2\pi a t} \int_0^{\beta t} dx \frac{\tanh(x)}{x\sqrt{(\beta t)^2 - x^2}} \ . \tag{A.21}$$

which for $\beta t \gg 1$ can be approximated to

$$\chi_0^R(2k_F, 0) \approx \frac{1}{2\pi a t} \ln\left(\frac{4\beta t e^\gamma}{\pi}\right) \ , \tag{A.22}$$

where $\gamma$ is the Euler's constant. Here we can see that the electronic polarization diverges as $T$ goes to zero.

Now we can turn our attention to the vibrations of the underlying lattice, which can be described by the retarded free phonon propagator, which after analytic continuation is

$$\mathcal{D}_0^R(q,\omega) = \frac{2\Omega_q}{(\omega + i0^+)^2 - \Omega_q^2} \ , \tag{A.23}$$

where under the Debye model the acustic phonon dispersion relation is given by $\Omega_q = v_D|q|$. The renormalized phonon Green function for $q \approx 2k_F$, $\omega \approx 0$ and $T \ll t$, can be obtained by solving the Dyson equation

$$\mathcal{D}^R(q,\omega) = \mathcal{D}_0^R(q,\omega) + \mathcal{D}_0^R(q,\omega)\frac{g_p^2}{V}\chi_0^R(q,\omega)\mathcal{D}^R(q,\omega) \ , \tag{A.24}$$

with $g_p = i\left(\lambda\frac{\Omega_q V}{d(0)}\right)^{1/2}$ being the electron-phonon interaction vertex and $d(0) = \frac{1}{2\pi at}$ the density of states at the Fermi level. Neglecting the momentum and frequency dependence of the polarization bubble and approximating it by (A.22):

$$\mathcal{D}^R(q,\omega)\left(1 + \frac{2\Omega_q}{(\omega + i0^+)^2 - \Omega_q^2}\lambda\Omega_q \ln\left(\frac{4\beta t e^\gamma}{\pi}\right)\right) = \frac{2\Omega_q}{(\omega + i0^+)^2 - \Omega_q^2} \ , \tag{A.25}$$

so that

$$\mathcal{D}^R(q,\omega) = \frac{2\Omega_q}{(\omega + i0^+)^2 - \Omega_q^2\left(1 - 2\lambda\ln\left(\frac{4\beta t e^\gamma}{\pi}\right)\right)} \ . \tag{A.26}$$

By comparing with (A.23), we obtain that the renormalized phonon dispersion relation for $q \approx 2k_F$ is

$$\tilde{\Omega}_q^2 = \Omega_q^2\left(1 - 2\lambda\ln\left(\frac{4\beta t e^\gamma}{\pi}\right)\right) \tag{A.27}$$

This dispersion relation vanishes when decreasing the temperature below a certain value $T_C$

$$0 = 1 - 2\lambda\ln\left(\frac{4te^\gamma}{\pi T_C}\right) \quad \Rightarrow \quad T_C = \frac{4te^\gamma}{\pi}e^{2\lambda} \ . \tag{A.28}$$

Rewriting $\tilde{\Omega}_q$ in terms of $T_C$:

$$\tilde{\Omega}_q^2 = \Omega_q^2\left(1 - 2\lambda\ln\left(\frac{T_C}{T}e^{1/2\lambda}\right)\right) = 2\lambda\Omega_q^2\ln\left(\frac{T}{T_C}\right) \ . \tag{A.29}$$

Near the phase transition, $\ln\left(\frac{T}{T_C}\right) = \ln\left(1 + \frac{T-T_C}{T_C}\right) \approx \frac{T-T_C}{T_C}$, so that

$$\tilde{\Omega}_q \approx \Omega_q\sqrt{\frac{2\lambda}{T_C}}|T - T_C|^{1/2} \ . \tag{A.30}$$

Thus, $\tilde{\Omega}_q$ vanishes as a power law when approaching the phase transition. For $T$ below the critical temperature, $\tilde{\Omega}_q$ becomes imaginary, which is physically meaningless, and it is said that there is a soft phonon mode. It costs no energy to excite a phonon, so the phonon system becomes unstable towards a spontaneous deformation with a different lattice spacing.

# Appendix B

The interaction can be decoupled by means of a Hubbard-Stratonovich transformation in both channels. The partition function can be written in the path-integral formalism as follows:

$$\mathcal{Z} = \int \mathcal{D}[\bar{c}, c] e^{-S[\bar{c},c]} = \int \mathcal{D}[\bar{c}, c] e^{-\int_0^\beta d\tau \left[\sum_{\alpha\vec{q}} \bar{c}_{\alpha\vec{q}}(\partial_\tau + \varepsilon_\alpha(\vec{q}))c_{\alpha\vec{q}} + H_{int}\right]}, \tag{B.1}$$

where $\mathcal{D}[\bar{c}, c] \equiv \prod_\lambda d\bar{c}_\lambda dc_\lambda$ is the shorthand notation for the measure of the fermionic operators, and inside the path integral the fermionic operators $c^\dagger, c$ have been replaced by the associated anticommuting Grassman numbers $\bar{c}, c$.

The first step is to introduce the white noise variables $A_{rC,\alpha}$ and $A_{iC,\alpha}$, with Gaussian path integrals

$$\mathcal{Z}_{A_{rC(iC)}} = \int \mathcal{D}[A_{rC(iC)}] e^{-S[A_{rC(iC)}]} = \int \mathcal{D}[A_{rC(iC)}] e^{-\int_0^\beta d\tau \sum_\alpha G^{-1}_{rC(iC)} A_{rC(iC),\alpha} A_{rC(iC),\alpha}} \tag{B.2}$$

Since the correlation functions of these white-noise fields are just a constant, multiplying the original partition function by $\mathcal{Z}_{A_{rC}} \mathcal{Z}_{A_{iC}}$ will just imply a shift in the free energy $\mathcal{F} = -T \ln(\mathcal{Z}) = -T \ln\left(\mathcal{Z} \mathcal{Z}_{A_{rC}} \mathcal{Z}_{A_{iC}} \frac{1}{\mathcal{Z}_{A_{rC}} \mathcal{Z}_{A_{iC}}}\right) = -T \ln(\mathcal{Z} \mathcal{Z}_{A_{rC}} \mathcal{Z}_{A_{iC}}) + T \ln(\mathcal{Z}_{A_{rC}} \mathcal{Z}_{A_{iC}})$, so it can be done without any consequence. In turn, entangling the two functional integrals will allow for the definition of an effective action that decouples the interactions. In order to see this, let us first notice that the product of the two integrals describes two independent systems.

$$\mathcal{Z} \times \mathcal{Z}_{A_{rC}} \times \mathcal{Z}_{A_{iC}} = \int \mathcal{D}[\bar{c}, c] \int \mathcal{D}[A_{rC}] \int \mathcal{D}[A_{iC}] e^{-\int_0^\beta d\tau \sum_\alpha \left[\sum_{\vec{q}} \bar{c}_{\alpha\vec{q}}(\partial_\tau + \varepsilon_\alpha(\vec{q}))c_{\alpha\vec{q}} + H'_{int}\right]} \tag{B.3}$$

with

$$H'_{int} = -\frac{\mathcal{N}}{2} \sum_\alpha G_{rC} \rho_{rC,\alpha} \rho_{rC,\alpha} - \sum_\alpha G^{-1}_{rC} A_{rC,\alpha} A_{rC,\alpha} \tag{B.4}$$

$$-\frac{\mathcal{N}}{2} \sum_\alpha G_{iC} \rho_{iC,\alpha} \rho_{iC,\alpha} - \sum_\alpha G^{-1}_{iC} A_{iC,\alpha} A_{iC,\alpha} \tag{B.5}$$

Written in this way, the integral over the white-noise fields are inside that of the original fermionic operators. Therefore, for each of the white-noise fields configurations one can consider the $\bar{c}, c$ fields (and therefore the $\rho_{rC}, \rho_{iC}$ fields) as constants. Consequently,

a variable shift of the form $A_{rC,\alpha} = N_\alpha - G_{rC}\rho_{rC,\alpha}$ and $A_{iC,\alpha} = \phi_\alpha + G_{iC}\rho_{iC,\alpha}$ is allowed, since the measure remains unchanged, allowing the writing of $\mathcal{D}[A_{rC}] = \mathcal{D}[N]$ and $\mathcal{D}[A_{iC}] = \mathcal{D}[\phi]$.

The newly introduced variables $N_\alpha$ and $\phi_\alpha$, which are a combination of the white-noise fields $A_{rC(iC)}$ and the physical fields $\rho_{rC(iC)}$, are often referred as the *Weiss fields*. When the bilinears $\rho_{rC(iC)}$ are to enter a broken-symmetry phase, the ....

Then, the transformed interaction becomes

$$H'_{int} = \frac{\mathcal{N}}{2G_{rC}}\sum_\alpha N_\alpha^2 + \frac{\mathcal{N}}{2G_{iC}}\sum_\alpha \phi_\alpha^2 - \mathcal{N}\sum_\alpha N_\alpha\rho_{rC,\alpha} - \mathcal{N}\sum_\alpha \phi_\alpha\rho_{iC,\alpha}, \tag{B.6}$$

in which the the new variables $N_\alpha, \phi_\alpha$ couple linearly to the bilinears.

At this point, one can substitute back the expression of the bilinears in terms of the annihilation and creation operators, so that the action can be written as

$$S[\bar{c}, c, N, \phi] = \int_0^\beta d\tau \left[ \sum_{\beta\gamma q} \bar{c}_{\beta\vec{q}} \left( (\partial_\tau + \varepsilon_\beta(\vec{q}))\delta_{\beta\gamma} - \frac{1}{2}\sum_\alpha N_\alpha|\epsilon_{\alpha\beta\gamma}| - \frac{1}{2i}\sum_\alpha \phi_\alpha\epsilon_{\alpha\beta\gamma} \right) c_{\gamma\vec{q}} \right. \tag{B.7}$$

$$\left. + \frac{\mathcal{N}}{2G_{rC}}\sum_\alpha N_\alpha^2 + \frac{\mathcal{N}}{2G_{iC}}\sum_\alpha \phi_\alpha^2 \right] = \tag{B.8}$$

$$= \int_0^\beta d\tau \left[ \sum_{\vec{q}} \bar{c}_{\vec{q}} \left(\partial_\tau + \mathcal{H}[N, \phi]\right) c_{\vec{q}} + \frac{\mathcal{N}}{2G_{rC}}\sum_\alpha N_\alpha^2 + \frac{\mathcal{N}}{2G_{iC}}\sum_\alpha \phi_\alpha^2 \right] \tag{B.9}$$

$\mathcal{H}$ is the matrix representation of the effective Hamiltonian.

Substituting back in B.3, and inverting the order of integration,

$$\mathcal{Z} = \int \mathcal{D}[N] e^{-\frac{\mathcal{N}}{2G_{rC}}\int_0^\beta d\tau \sum_\alpha N_\alpha^2} \int \mathcal{D}[\phi] e^{-\frac{\mathcal{N}}{2G_{iC}}\int_0^\beta d\tau \sum_\alpha \phi_\alpha^2} \int \mathcal{D}[\bar{c}, c] e^{-\int_0^\beta d\tau \sum_{\vec{q}} \bar{c}_{\vec{q}}(\partial_\tau + \mathcal{H})c_{\vec{q}}} \tag{B.10}$$

The last of the integrals represents the path integral of the electrons moving in the fluctuating fields $N_\alpha$ and $\phi_\alpha$. These fluctuations are the ones that mediate the interactions between the electrons in this new picture. Furthermore, it is a gaussian path integral, so it can be evaluated, doing what is commonly referred to as "integrating out the electrons", yielding

$$\mathcal{Z} = \det(\partial_\tau + \mathcal{H}) \int \mathcal{D}[N] e^{-\frac{\mathcal{N}}{2G_{rC}}\int_0^\beta d\tau \sum_\alpha N_\alpha^2} \int \mathcal{D}[\phi] e^{-\frac{\mathcal{N}}{2G_{iC}}\int_0^\beta d\tau \sum_\alpha \phi_\alpha^2}. \tag{B.11}$$

Using the identity $\det(A) = e^{\log(\det(A))} = e^{\mathrm{Tr}(\log(A))}$ and writing the partition function in terms of an effective action, one obtains

$$\mathcal{Z} = \int \mathcal{D}[N] \int \mathcal{D}[\phi] e^{-S_E[N,\phi]} \tag{B.12}$$

with

$$S_E[N,\phi] = -\operatorname{Tr}\left(\log\left(\partial_\tau + \mathcal{H}[N,\phi]\right)\right) + \frac{\mathcal{N}}{2G_{rC}}\int_0^\beta d\tau \sum_\alpha N_\alpha^2 + \frac{\mathcal{N}}{2G_{iC}}\int_0^\beta d\tau \sum_\alpha \phi_\alpha^2 \quad \text{(B.13)}$$

Furthermore, it can be written in terms of the fermionic Matsubara frequencies $i\omega_n$ and within the mean field approach it is sensible to assume static configurations ($N_\alpha(\tau) = N_\alpha$ and $\phi_\alpha(\tau) = \phi_\alpha$), so that the effective action is

$$S_E[N,\phi] = -\operatorname{Tr}\left(\log\left(-i\omega_n + \mathcal{H}[N,\phi]\right)\right) + \frac{\mathcal{N}\beta}{2}\sum_\alpha\left(\frac{1}{G_{rC}}N_\alpha^2 + \frac{1}{G_{iC}}\phi_\alpha^2\right) \quad \text{(B.14)}$$

$$= -\operatorname{Tr}\big(\log\big(-\mathcal{G}^{-1}\big)\big) + \frac{\mathcal{N}\beta}{2}\sum_\alpha\left(\frac{1}{G_{rC}}N_\alpha^2 + \frac{1}{G_{iC}}\phi_\alpha^2\right) \quad \text{(B.15)}$$

Finally, within the saddle point approximation $\mathcal{Z} \approx e^{-S_E[N,\phi]} = e^{-\beta\mathcal{F}_E[N,\phi]}$, so the effective free energy is

$$\mathcal{F}_E[N,\phi] = -\frac{1}{\beta}\operatorname{Tr}\big(\log\big(-\mathcal{G}^{-1}\big)\big) + \frac{\mathcal{N}}{2G_{rC}}\sum_\alpha N_\alpha^2 + \frac{\mathcal{N}}{2G_{iC}}\sum_\alpha \phi_\alpha^2 \quad \text{(B.16)}$$

with [1]

$$\mathcal{G}^{-1} = \begin{pmatrix} i\omega_n - \varepsilon_1(\vec{q}) & \frac{N_3 - i\phi_3}{2} & \frac{N_2 + i\phi_2}{2} \\ \frac{N_3 + i\phi_3}{2} & i\omega_n - \varepsilon_2(\vec{q}) & \frac{N_1 - i\phi_1}{2} \\ \frac{N_2 - i\phi_2}{2} & \frac{N_1 + i\phi_1}{2} & i\omega_n - \varepsilon_3(\vec{q}) \end{pmatrix} \quad \text{(B.17)}$$

### B.0.1 Mean field solutions

At this point one can look for the mean field solutions by solving the saddle-point equations:

$$\frac{\partial S_E[N,\phi]}{\partial N_\alpha} = 0 \quad , \quad \frac{\partial S_E[N,\phi]}{\partial \phi_\alpha} = 0 \quad \text{(B.18)}$$

Starting from the first of the equations, since $\frac{\partial e^{-S_E[N,\phi]}}{\partial N_\alpha} = -e^{-S_E[N,\phi]}\frac{\partial S_E[N,\phi]}{\partial N_\alpha}$,

$$\begin{aligned}
\frac{\partial S_E[N,\phi]}{\partial N_\alpha} =& -e^{S_E[N,\phi]}\frac{\partial e^{-S_E[N,\phi]}}{\partial N_\alpha} = -e^{S_E[N,\phi]}\frac{\partial}{\partial N_\alpha}\left(\int \mathcal{D}[\bar{c},c]e^{-S[\bar{c},c,N,\phi]}\right) \\
=& e^{S_E[N,\phi]}\int \mathcal{D}[\bar{c},c]e^{-S[\bar{c},c,N,\phi]}\frac{\partial S[\bar{c},c,N,\phi]}{\partial N_\alpha} \\
=& e^{S_E[N,\phi]}\int \mathcal{D}[\bar{c},c]e^{-S[\bar{c},c,N,\phi]}\left(-\frac{1}{2}|\epsilon_{\alpha\beta\gamma}|\sum_{\vec{q}}\bar{c}_{\beta\vec{q}}c_{\gamma\vec{q}} + \frac{\mathcal{N}}{G_{rC}}N_\alpha\right) \\
=& -\frac{1}{2}|\epsilon_{\alpha\beta\gamma}|e^{S_E[N,\phi]}\int \mathcal{D}[\bar{c},c]e^{-S[\bar{c},c,N,\phi]}\sum_{\vec{q}}\bar{c}_{\beta\vec{q}}c_{\gamma\vec{q}} + \frac{\mathcal{N}}{G_{rC}}e^{S_E[N,\phi]}\underbrace{\int \mathcal{D}[\bar{c},c]e^{-S[\bar{c},c,N,\phi]}}_{e^{-S_E[N,\phi]}}N_\alpha \\
=& -\frac{1}{2}|\epsilon_{\alpha\beta\gamma}|\sum_{\vec{q}}\left\langle\bar{c}_{\beta\vec{q}}c_{\gamma\vec{q}}\right\rangle + \frac{\mathcal{N}}{G_{rC}}N_\alpha = 0
\end{aligned}$$

[1] Here, and in the following, I am using the notation in [?] and [?] for the signs of the Green function, which are the opposite of those of [5].

$$N_\alpha = G_{rC}\frac{|\epsilon_{\alpha\beta\gamma}|}{2\mathcal{N}}\sum_{\vec{q}}\langle \bar{c}_{\beta\vec{q}}c_{\gamma\vec{q}}\rangle \tag{B.19}$$

With a completely analogous calculation, one obtains that

$$\phi_\alpha = G_{iC}\frac{\epsilon_{\alpha\beta\gamma}}{2i\mathcal{N}}\sum_{\vec{q}}\langle \bar{c}_{\beta\vec{q}}c_{\gamma\vec{q}}\rangle \tag{B.20}$$

### B.0.2 Free energy expansion

The inverse of the full Green function in (B.17) can be rewritten into two parts: the diagonal part corresponds to the inverse of the bare Green function $\mathcal{G}_0$, and the non-diagonal one is the scattering potential $\mathcal{V}$. Therefore, $\mathrm{Tr}\big(\log\big(-\mathcal{G}^{-1}\big)\big) = \mathrm{Tr}\big(\log\big(-\mathcal{G}_0^{-1}-\mathcal{V}\big)\big) = \mathrm{Tr}\big(\log\big(-\mathcal{G}_0^{-1}\big)\big) + \mathrm{Tr}(\log(1+\mathcal{G}_0\mathcal{V}))$. The first of these terms, normalised by $\frac{1}{\beta}$, corresponds to the free energy of the non-interacting system. The second term represents the change in the free energy due to the $N$ and $\phi$ fields. This last term can be interpreted as the repeated scattering off the exchange field, and can be viewed as the infinite sum of Feynman diagrams

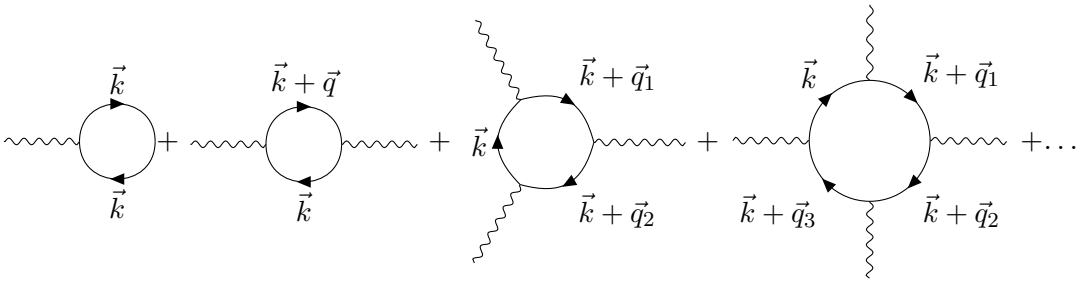


And therefore, the $\mathrm{Tr}\big(\log\big(\mathcal{G}^{-1}\big)\big)$ that appears in (**??**) can be expanded in the following way:

$$\begin{gathered}\mathrm{Tr}\big(\log\big(\mathcal{G}^{-1}\big)\big) = \mathrm{Tr}\big(\log\big(\mathcal{G}_0^{-1}+\mathcal{V}\big)\big) = \mathrm{Tr}\big(\log\big(\mathcal{G}_0^{-1}(\mathbb{I}+\mathcal{G}_0\mathcal{V})\big)\big) = \\ = \mathrm{Tr}\big(\log\big(\mathcal{G}_0^{-1}\big)\big) + \mathrm{Tr}(\log(\mathbb{I}+\mathcal{G}_0\mathcal{V})) \approx \\ \approx \mathrm{Tr}\big(\log\big(\mathcal{G}_0^{-1}\big)\big) + \mathrm{Tr}(\mathcal{G}_0\mathcal{V}) - \frac{1}{2}\mathrm{Tr}\big((\mathcal{G}_0\mathcal{V})^2\big) + \frac{1}{3}\mathrm{Tr}\big((\mathcal{G}_0\mathcal{V})^3\big) - \frac{1}{4}\mathrm{Tr}\big((\mathcal{G}_0\mathcal{V})^4\big) + ...\end{gathered}$$

The term $\mathrm{Tr}\big(\log\big(\mathcal{G}_0^{-1}\big)\big)$ is included in the free energy of the non-interacting system, so the free energy density of the CDW phase up to forth order is

$$f_{CDW} = \frac{1}{2G_{rCDW}}\sum_\alpha N_\alpha^2 + \frac{1}{2G_{iCDW}}\sum_\alpha \phi_\alpha^2 - \mathrm{Tr}(\mathcal{G}_0\mathcal{V}) + \frac{1}{2}\mathrm{Tr}\big((\mathcal{G}_0\mathcal{V})^2\big) - \frac{1}{3}\mathrm{Tr}\big((\mathcal{G}_0\mathcal{V})^3\big) + \frac{1}{4}\mathrm{Tr}\big((\mathcal{G}_0\mathcal{V})^4\big) \tag{B.21}$$

Let us now evaluate each of the terms, and write them in terms of the complex order parameter.

The first two terms can be easily rewritten by using that $N_\alpha = |\Delta_\alpha|\cos(\theta_\alpha)$ and $\phi_\alpha = |\Delta_\alpha| sin(\theta_\alpha)$.

$$\frac{1}{2G_{rCDW}}\sum_\alpha N_\alpha^2+\frac{1}{2G_{iCDW}}\sum_\alpha \phi_\alpha^2=\sum_\alpha|\Delta_\alpha|^2\left(\frac{1}{2G_{rCDW}}\cos^2(\theta_\alpha)+\frac{1}{2G_{iCDW}}sin^2(\theta_\alpha)\right)=$$
$$=\frac{1}{2}\sum_\alpha|\Delta_\alpha|^2\left(\frac{1}{2G_{rCDW}}+\frac{1}{2G_{rCDW}}\cos(2\theta_\alpha)+\frac{1}{2G_{iCDW}}-\frac{1}{2G_{iCDW}}\cos(2\theta_\alpha)\right)=$$
$$=\frac{1}{2}\left(\frac{1}{2G_{rCDW}}+\frac{1}{2G_{iCDW}}\right)\sum_\alpha|\Delta_\alpha|^2+\frac{1}{2}\left(\frac{1}{2G_{rCDW}}-\frac{1}{2G_{iCDW}}\right)\sum_\alpha|\Delta_\alpha|^2\cos(2\theta_\alpha) \tag{B.22}$$

Now, since $\mathcal{G}_0^{-1}$ is diagonal,

$$\mathcal{G}_0=\begin{pmatrix}\frac{1}{-i\omega_n+\varepsilon_1(\vec{q})} & 0 & 0\\ 0 & \frac{1}{-i\omega_n+\varepsilon_2(\vec{q})} & 0\\ 0 & 0 & \frac{1}{-i\omega_n+\varepsilon_3(\vec{q})}\end{pmatrix} \tag{B.23}$$

so we can easily obtain the traces of the matrix products with the help of Mathematica:

$$\mathrm{Tr}(\mathcal{G}_0\mathcal{V})=0 \tag{B.24}$$

$$\mathrm{Tr}\big((\mathcal{G}_0\mathcal{V})^2\big)=\frac{1}{2}\sum_{q\in BZ}\frac{1}{\beta}\sum_n\left(\frac{|\Delta_1|^2}{(-i\omega_n+\varepsilon_2(\vec{q}))(-i\omega_n+\varepsilon_3(\vec{q}))}+\right.$$
$$\left.+\frac{|\Delta_2|^2}{(-i\omega_n+\varepsilon_1(\vec{q}))(-i\omega_n+\varepsilon_3(\vec{q}))}+\frac{|\Delta_3|^2}{(-i\omega_n+\varepsilon_1(\vec{q}))(-i\omega_n+\varepsilon_2(\vec{q}))}\right)=$$
$$=\frac{1}{4}\sum_{q\in BZ}\frac{1}{\beta}\sum_n\sum_\alpha\frac{|\Delta_\alpha|^2|\epsilon_{\alpha\beta\gamma}|}{(-i\omega_n+\varepsilon_\beta(\vec{q}))(-i\omega_n+\varepsilon_\gamma(\vec{q}))} \tag{B.25}$$

$$\mathrm{Tr}\big((\mathcal{G}_0\mathcal{V})^3\big)=-\frac{3}{4}\sum_{q\in BZ}\frac{1}{\beta}\sum_n\frac{|\Delta_1||\Delta_2||\Delta_3|\cos(\theta_1+\theta_2+\theta_3)}{(-i\omega_n+\varepsilon_1(\vec{q}))(-i\omega_n+\varepsilon_2(\vec{q}))(-i\omega_n+\varepsilon_3(\vec{q}))} \tag{B.26}$$

$$\mathrm{Tr}\big((\mathcal{G}_0\mathcal{V})^4\big)=\frac{1}{16}\sum_{q\in BZ}\frac{1}{\beta}\sum_n\sum_\alpha\frac{|\Delta_\alpha|^4|\epsilon_{\alpha\beta\gamma}|}{(-i\omega_n+\varepsilon_\beta(\vec{q}))^2(-i\omega_n+\varepsilon_\gamma(\vec{q}))^2}+$$
$$+\frac{1}{8}\sum_{q\in BZ}\frac{1}{\beta}\sum_n\sum_{\alpha\beta}\frac{|\Delta_\alpha|^2|\Delta_\beta|^2|\epsilon_{\alpha\beta\gamma}|}{(-i\omega_n+\varepsilon_\alpha(\vec{q}))(-i\omega_n+\varepsilon_\beta(\vec{q}))(-i\omega_n+\varepsilon_\gamma(\vec{q}))^2} \tag{B.27}$$

Let us look at each of these expressions in more detail. The first step is to evaluate the Matsubara sum. For that, we will follow the usual procedure. Let $f$ be the Fermi function and $g(i\omega_n)$ the function of which we want to evaluate the sum, which has poles $z$ of order $n$, and $i\omega_n$ are bosonic Matsubara frequencies (because they are the difference of fermionic frequencies):

$$S=\frac{1}{\beta}\sum_n g(i\omega_n)=\oint\frac{dz}{2\pi i}f(z)g(z)e^{z\tau}=\sum_z Res[f(z)g(z),z] \tag{B.28}$$

$$Res[f(z)g(z),z]=\frac{1}{(n-1)!}\lim_{z\to c}\frac{\mathrm{d}^{n-1}}{\mathrm{d}z^{n-1}}((z-c)^n f(z)g(z)) \tag{B.29}$$

The Matsubara sum in $\mathrm{Tr}\big((\mathcal{G}_0\mathcal{V})^2\big)$ is

$$S_1 = \frac{1}{\beta}\sum_n \frac{1}{(-i\omega_n + \varepsilon_\beta(\vec{q}))(-i\omega_n + \varepsilon_\gamma(\vec{q}))} = \frac{1}{\beta}\sum_n \frac{1}{(i\omega_n - \varepsilon_\beta(\vec{q}))(i\omega_n - \varepsilon_\gamma(\vec{q}))} \tag{B.30}$$

It has two single poles: $z = \varepsilon_\beta$ with residue $\frac{1}{\varepsilon_\beta - \varepsilon_\gamma}$ and $z = \varepsilon_\gamma$ with residue $\frac{1}{\varepsilon_\gamma - \varepsilon_\beta}$, so

$$S_1 = \frac{f(\varepsilon_\beta)}{\varepsilon_\beta - \varepsilon_\gamma} + \frac{f(\varepsilon_\gamma)}{\varepsilon_\gamma - \varepsilon_\beta} = \frac{f(\varepsilon_\beta) - f(\varepsilon_\gamma)}{\varepsilon_\beta - \varepsilon_\gamma} = \frac{f(\varepsilon_\gamma) - f(\varepsilon_\beta)}{\varepsilon_\gamma - \varepsilon_\beta} \tag{B.31}$$

$$\begin{aligned}
\mathrm{Tr}\big((\mathcal{G}_0\mathcal{V})^2\big) &= \frac{1}{4}\sum_\alpha |\Delta_\alpha|^2 |\epsilon_{\alpha\beta\gamma}| \sum_{q\in BZ} \frac{f(\varepsilon_\beta(\vec{q})) - f(\varepsilon_\gamma(\vec{q}))}{\varepsilon_\beta(\vec{q}) - \varepsilon_\gamma(\vec{q})} = \\
&= \frac{1}{2}\Bigg( |\Delta_1|^2 \sum_{q\in BZ} \frac{f(\varepsilon_2(\vec{q})) - f(\varepsilon_3(\vec{q}))}{\varepsilon_2(\vec{q}) - \varepsilon_3(\vec{q})} + |\Delta_2|^2 \sum_{q\in BZ} \frac{f(\varepsilon_1(\vec{q})) - f(\varepsilon_3(\vec{q}))}{\varepsilon_1(\vec{q}) - \varepsilon_3(\vec{q})} + \\
&\qquad + |\Delta_3|^2 \sum_{q\in BZ} \frac{f(\varepsilon_2(\vec{q})) - f(\varepsilon_1(\vec{q}))}{\varepsilon_2(\vec{q}) - \varepsilon_1(\vec{q})} \Bigg)
\end{aligned} \tag{B.32}$$

Further rewritting can be done if one notices that, since the sum over $q$ involves the whole Brillouin Zone, rotating $q$ by $\pm\pi/3$ will only rotate the energies into each other. When rotating $-\pi/3$:

$$\begin{pmatrix} q'_x \\ q'_y \end{pmatrix} = \begin{pmatrix} \cos(\alpha) & -\sin(\alpha) \\ \sin(\alpha) & \cos(\alpha) \end{pmatrix} \begin{pmatrix} q_x \\ q_y \end{pmatrix} = \begin{pmatrix} \frac{1}{2} & \frac{\sqrt{3}}{2} \\ -\frac{\sqrt{3}}{2} & \frac{1}{2} \end{pmatrix} \begin{pmatrix} q_x \\ q_y \end{pmatrix} = \begin{pmatrix} \frac{1}{2}q_x + \frac{\sqrt{3}}{2}q_y \\ -\frac{\sqrt{3}}{2}q_x + \frac{1}{2}q_y \end{pmatrix} \tag{B.33}$$

$$\begin{aligned}
\varepsilon_1(q') =& a(q'_x)^2 - b(q'_y)^2 = \frac{a-3b}{4}q_x^2 + \frac{\sqrt{3}(a+b)}{2}q_x q_y + \frac{3a-b}{4}q_y^2 = \varepsilon_2(\vec{q}) \\
\varepsilon_2(q') =& \frac{a-3b}{4}(q'_x)^2 + \frac{\sqrt{3}(a+b)}{2}q'_x q'_y + \frac{3a-b}{4}(q'_y)^2 = \\
=& \frac{a-3b}{4}q_x^2 - \frac{\sqrt{3}(a+b)}{2}q_x q_y + \frac{3a-b}{4}q_y^2 = \varepsilon_3(\vec{q}) \\
\varepsilon_3(q') =& \frac{a-3b}{4}(q'_x)^2 - \frac{\sqrt{3}(a+b)}{2}q'_x q'_y + \frac{3a-b}{4}(q'_y)^2 = aq_x^2 - bq_y^2 = \varepsilon_1(\vec{q})
\end{aligned}$$

Therefore, under the sum of $q$ over the BZ, we can do the substitution $\varepsilon_1 \to \varepsilon_3$, $\varepsilon_3 \to \varepsilon_2$ and $\varepsilon_2 \to \varepsilon_1$ without changing the result.

Applying this result, one can see that

$$\begin{aligned}
\sum_{q\in BZ} \frac{f(\varepsilon_1(\vec{q})) - f(\varepsilon_3(\vec{q}))}{\varepsilon_1(\vec{q}) - \varepsilon_3(\vec{q})} &= \sum_{q\in BZ} \frac{f(\varepsilon_3(\vec{q})) - f(\varepsilon_2(\vec{q}))}{\varepsilon_3(\vec{q}) - \varepsilon_2(\vec{q})} = \sum_{q\in BZ} \frac{f(\varepsilon_2(\vec{q})) - f(\varepsilon_3(\vec{q}))}{\varepsilon_2(\vec{q}) - \varepsilon_3(\vec{q})} \\
\sum_{q\in BZ} \frac{f(\varepsilon_2(\vec{q})) - f(\varepsilon_1(\vec{q}))}{\varepsilon_2(\vec{q}) - \varepsilon_1(\vec{q})} &= \sum_{q\in BZ} \frac{f(\varepsilon_1(\vec{q})) - f(\varepsilon_3(\vec{q}))}{\varepsilon_1(\vec{q}) - \varepsilon_3(\vec{q})} = \sum_{q\in BZ} \frac{f(\varepsilon_2(\vec{q})) - f(\varepsilon_3(\vec{q}))}{\varepsilon_2(\vec{q}) - \varepsilon_3(\vec{q})}
\end{aligned}$$

And therefore

$$\begin{aligned}\mathrm{Tr}\big((\mathcal{G}_0\mathcal{V})^2\big) =& \frac{1}{2}\sum_{q\in BZ}\frac{f(\varepsilon_2(\vec{q}))-f(\varepsilon_3(\vec{q}))}{\varepsilon_2(\vec{q})-\varepsilon_3(\vec{q})}\left(|\Delta_1|^2+|\Delta_2|^2+|\Delta_3|^2\right)= \\ =& \frac{1}{2}\sum_{q\in BZ}\frac{f(\varepsilon_2(\vec{q}))-f(\varepsilon_3(\vec{q}))}{\varepsilon_2(\vec{q})-\varepsilon_3(\vec{q})}\sum_{\alpha}|\Delta_\alpha|^2\end{aligned} \tag{B.34}$$

In $\mathrm{Tr}\big((\mathcal{G}_0\mathcal{V})^3\big)$ the Matsubara sum that appears is

$$\begin{aligned}S_2 =& \frac{1}{\beta}\sum_n \frac{1}{(-i\omega_n+\varepsilon_1(\vec{q}))(-i\omega_n+\varepsilon_2(\vec{q}))(-i\omega_n+\varepsilon_3(\vec{q}))}= \\ =& -\frac{1}{\beta}\sum_n \frac{1}{(i\omega_n-\varepsilon_1(\vec{q}))(i\omega_n-\varepsilon_2(\vec{q}))(i\omega_n-\varepsilon_3(\vec{q}))}\end{aligned} \tag{B.35}$$

It has three single order poles $z=\varepsilon_1,\varepsilon_2,\varepsilon_3$, so equivalent to $S_1$:

$$S_2 = -\left(\frac{f(\varepsilon_1)}{(\varepsilon_1-\varepsilon_2)(\varepsilon_1-\varepsilon_3)}+\frac{f(\varepsilon_2)}{(\varepsilon_2-\varepsilon_1)(\varepsilon_2-\varepsilon_3)}+\frac{f(\varepsilon_3)}{(\varepsilon_3-\varepsilon_1)(\varepsilon_3-\varepsilon_2)}\right) \tag{B.36}$$

And therefore

$$\begin{aligned}\mathrm{Tr}\big((\mathcal{G}_0\mathcal{V})^3\big) =& \frac{3}{4}\left(\frac{f(\varepsilon_1)}{(\varepsilon_1-\varepsilon_2)(\varepsilon_1-\varepsilon_3)}+\frac{f(\varepsilon_2)}{(\varepsilon_2-\varepsilon_1)(\varepsilon_2-\varepsilon_3)}+\frac{f(\varepsilon_3)}{(\varepsilon_3-\varepsilon_1)(\varepsilon_3-\varepsilon_2)}\right) \\ & \sum_{q\in BZ}|\Delta_1||\Delta_2||\Delta_3|\cos(\theta_1+\theta_2+\theta_3)= \\ =& \frac{9}{4}\frac{f(\varepsilon_1)}{(\varepsilon_1-\varepsilon_2)(\varepsilon_1-\varepsilon_3)}\sum_{q\in BZ}|\Delta_1||\Delta_2||\Delta_3|\cos(\theta_1+\theta_2+\theta_3)\end{aligned} \tag{B.37}$$

In $\mathrm{Tr}\big((\mathcal{G}_0\mathcal{V})^4\big)$ there appears two Matsubara sums. The first one is

$$S_3 = \frac{1}{\beta}\sum_n \frac{1}{(-i\omega_n+\varepsilon_\beta(\vec{q}))^2(-i\omega_n+\varepsilon_\gamma(\vec{q}))^2} = \frac{1}{\beta}\sum_n \frac{1}{(i\omega_n-\varepsilon_\beta(\vec{q}))^2(i\omega_n-\varepsilon_\gamma(\vec{q}))^2} \tag{B.38}$$

It has two second order poles $z=\varepsilon_\beta$ and $z=\varepsilon_\gamma$.

$$Res[f(z)g(z), z=\varepsilon_\beta] = \lim_{z\to\varepsilon_\beta}\frac{\mathrm{d}}{\mathrm{d}z}\left(\frac{f(z)}{(z-\varepsilon_\gamma)^2}\right) = \frac{f'(\varepsilon_\beta)}{(\varepsilon_\beta-\varepsilon_\gamma)^2}-\frac{2f(\varepsilon_\beta)}{(\varepsilon_\beta-\varepsilon_\gamma)^3} \tag{B.39}$$

$$Res[f(z)g(z), z=\varepsilon_\gamma] = \frac{f'(\varepsilon_\gamma)}{(\varepsilon_\gamma-\varepsilon_\beta)^2}-\frac{2f(\varepsilon_\gamma)}{(\varepsilon_\gamma-\varepsilon_\beta)^3} \tag{B.40}$$

$$S_3 = \frac{f'(\varepsilon_\beta)+f'(\varepsilon_\gamma)}{(\varepsilon_\beta-\varepsilon_\gamma)^2}-2\frac{f(\varepsilon_\beta)-f(\varepsilon_\gamma)}{(\varepsilon_\beta-\varepsilon_\gamma)^3} \tag{B.41}$$

When taking the sum over $q$ of this sum, we can see that

$$\sum_{q\in BZ}\left(\frac{f'(\varepsilon_3)+f'(\varepsilon_1)}{(\varepsilon_3-\varepsilon_1)^2}-2\frac{f(\varepsilon_3)-f(\varepsilon_1)}{(\varepsilon_3-\varepsilon_1)^3}\right)=\sum_{q\in BZ}\left(\frac{f'(\varepsilon_2)+f'(\varepsilon_3)}{(\varepsilon_2-\varepsilon_3)^2}-2\frac{f(\varepsilon_2)-f(\varepsilon_3)}{(\varepsilon_2-\varepsilon_3)^3}\right)$$

$$\sum_{q\in BZ}\left(\frac{f'(\varepsilon_1)+f'(\varepsilon_2)}{(\varepsilon_1-\varepsilon_2)^2}-2\frac{f(\varepsilon_1)-f(\varepsilon_2)}{(\varepsilon_1-\varepsilon_2)^3}\right)=\sum_{q\in BZ}\left(\frac{f'(\varepsilon_3)+f'(\varepsilon_1)}{(\varepsilon_3-\varepsilon_1)^2}-2\frac{f(\varepsilon_3)-f(\varepsilon_1)}{(\varepsilon_3-\varepsilon_1)^3}\right)=$$

$$=\sum_{q\in BZ}\left(\frac{f'(\varepsilon_2)+f'(\varepsilon_3)}{(\varepsilon_2-\varepsilon_3)^2}-2\frac{f(\varepsilon_2)-f(\varepsilon_3)}{(\varepsilon_2-\varepsilon_3)^3}\right)$$

The second Matsubara sum is

$$S_4=\frac{1}{\beta}\sum_n\frac{1}{(-i\omega_n+\varepsilon_\alpha(\vec{q}))(-i\omega_n+\varepsilon_\beta(\vec{q}))(-i\omega_n+\varepsilon_\gamma(\vec{q}))^2}=$$
$$=\frac{1}{\beta}\sum_n\frac{1}{(i\omega_n-\varepsilon_\alpha(\vec{q}))(i\omega_n-\varepsilon_\beta(\vec{q}))(i\omega_n-\varepsilon_\gamma(\vec{q}))^2} \tag{B.42}$$

This one has three poles, two single poles $z=\varepsilon_\alpha,\varepsilon_\beta$ and one second order pole $z=\varepsilon_\gamma$.

$$Res[f(z)g(z),z=\varepsilon_\alpha]=\lim_{z\to\varepsilon_\alpha}\frac{f(z)}{(z-\varepsilon_\beta)(z-\varepsilon_\gamma)^2}=\frac{f(\varepsilon_\alpha)}{(\varepsilon_\alpha-\varepsilon_\beta)(\varepsilon_\alpha-\varepsilon_\gamma)^2} \tag{B.43}$$

$$Res[f(z)g(z),z=\varepsilon_\beta]=\frac{f(\varepsilon_\beta)}{(\varepsilon_\beta-\varepsilon_\alpha)(\varepsilon_\beta-\varepsilon_\gamma)^2} \tag{B.44}$$

$$Res[f(z)g(z),z=\varepsilon_\gamma]=\lim_{z\to\varepsilon_\gamma}\frac{\mathrm{d}}{\mathrm{d}z}\left(\frac{f(z)}{(z-\varepsilon_\alpha)(z-\varepsilon_\beta)}\right)=$$
$$=\frac{f'(\varepsilon_\gamma)}{(\varepsilon_\gamma-\varepsilon_\alpha)(\varepsilon_\gamma-\varepsilon_\beta)}-\frac{f(\varepsilon_\gamma)}{(\varepsilon_\gamma-\varepsilon_\alpha)^2(\varepsilon_\gamma-\varepsilon_\beta)}-\frac{f(\varepsilon_\gamma)}{(\varepsilon_\gamma-\varepsilon_\alpha)(\varepsilon_\gamma-\varepsilon_\beta)^2} \tag{B.45}$$

$$S_4=\frac{f(\varepsilon_\alpha)}{(\varepsilon_\alpha-\varepsilon_\beta)(\varepsilon_\alpha-\varepsilon_\gamma)^2}+\frac{f(\varepsilon_\beta)}{(\varepsilon_\beta-\varepsilon_\alpha)(\varepsilon_\beta-\varepsilon_\gamma)^2}+\frac{f'(\varepsilon_\gamma)}{(\varepsilon_\gamma-\varepsilon_\alpha)(\varepsilon_\gamma-\varepsilon_\beta)}+$$
$$-\frac{f(\varepsilon_\gamma)}{(\varepsilon_\gamma-\varepsilon_\alpha)^2(\varepsilon_\gamma-\varepsilon_\beta)}-\frac{f(\varepsilon_\gamma)}{(\varepsilon_\gamma-\varepsilon_\alpha)(\varepsilon_\gamma-\varepsilon_\beta)^2} \tag{B.46}$$

Taking $\alpha=1,\beta=2,\gamma=3$ and the sum of $q$ over the BZ of $S_4$:

$$\sum_{q\in BZ}\frac{f(\varepsilon_1)}{(\varepsilon_1-\varepsilon_2)(\varepsilon_1-\varepsilon_3)^2}+\sum_{q\in BZ}\frac{f(\varepsilon_2)}{(\varepsilon_2-\varepsilon_1)(\varepsilon_2-\varepsilon_3)^2}+\sum_{q\in BZ}\frac{f'(\varepsilon_3)}{(\varepsilon_3-\varepsilon_1)(\varepsilon_3-\varepsilon_2)}+$$
$$-\sum_{q\in BZ}\frac{f(\varepsilon_3)}{(\varepsilon_3-\varepsilon_1)^2(\varepsilon_3-\varepsilon_2)}-\sum_{q\in BZ}\frac{f(\varepsilon_3)}{(\varepsilon_3-\varepsilon_1)(\varepsilon_3-\varepsilon_2)^2}=$$
$$=\cancel{\sum_{q\in BZ}\frac{f(\varepsilon_3)}{(\varepsilon_3-\varepsilon_1)(\varepsilon_3-\varepsilon_2)^2}}+\cancel{\sum_{q\in BZ}\frac{f(\varepsilon_2)}{(\varepsilon_2-\varepsilon_1)(\varepsilon_2-\varepsilon_3)^2}}+\sum_{q\in BZ}\frac{f'(\varepsilon_3)}{(\varepsilon_3-\varepsilon_1)(\varepsilon_3-\varepsilon_2)}+$$
$$-\cancel{\sum_{q\in BZ}\frac{f(\varepsilon_2)}{(\varepsilon_2-\varepsilon_3)^2(\varepsilon_2-\varepsilon_1)}}-\cancel{\sum_{q\in BZ}\frac{f(\varepsilon_3)}{(\varepsilon_3-\varepsilon_1)(\varepsilon_3-\varepsilon_2)^2}}=\sum_{q\in BZ}\frac{f'(\varepsilon_3)}{(\varepsilon_3-\varepsilon_1)(\varepsilon_3-\varepsilon_2)}$$

Analogously, for $\alpha = 2, \beta = 3, \gamma = 1$ and for $\alpha = 1, \beta = 3, \gamma = 2$, one gets

$$\sum_{q\in BZ} \frac{f'(\varepsilon_3)}{(\varepsilon_3 - \varepsilon_1)(\varepsilon_3 - \varepsilon_2)} \tag{B.47}$$

Substituting these sums in (B.27):

$$\begin{aligned}
\mathrm{Tr}\big((\mathcal{G}_0\mathcal{V})^4\big) &= \frac{1}{16}\sum_{q\in BZ}\frac{1}{\beta}\sum_n\sum_\alpha \frac{|\Delta_\alpha|^4|\epsilon_{\alpha\beta\gamma}|}{(-i\omega_n+\varepsilon_\beta(\vec{q}))^2(-i\omega_n+\varepsilon_\gamma(\vec{q}))^2}+\\
&+\frac{1}{8}\sum_{q\in BZ}\frac{1}{\beta}\sum_n\sum_{\alpha\beta} \frac{|\Delta_\alpha|^2|\Delta_\beta|^2|\epsilon_{\alpha\beta\gamma}|}{(-i\omega_n+\varepsilon_\alpha(\vec{q}))(-i\omega_n+\varepsilon_\beta(\vec{q}))(-i\omega_n+\varepsilon_\gamma(\vec{q}))^2}\\
&= \frac{1}{8}\sum_{q\in BZ}\left(\frac{f'(\varepsilon_2)+f'(\varepsilon_3)}{(\varepsilon_2-\varepsilon_3)^2} - 2\frac{f(\varepsilon_2)-f(\varepsilon_3)}{(\varepsilon_2-\varepsilon_3)^3}\right)\sum_\alpha|\Delta_\alpha|^4+\\
&+\frac{1}{4}\sum_{q\in BZ}\frac{f'(\varepsilon_3)}{(\varepsilon_3-\varepsilon_1)(\varepsilon_3-\varepsilon_2)}\sum_{\alpha\beta}|\Delta_\alpha|^2|\Delta_\beta|^2 =\\
&= \frac{1}{4}\sum_{q\in BZ}\left(\frac{f'(\varepsilon_2)+f'(\varepsilon_3)}{2(\varepsilon_2-\varepsilon_3)^2} - \frac{f(\varepsilon_2)-f(\varepsilon_3)}{(\varepsilon_2-\varepsilon_3)^3}\right)\sum_\alpha|\Delta_\alpha|^4+\\
&+\frac{1}{12}\sum_{q\in BZ}\left(\frac{f'(\varepsilon_1)}{(\varepsilon_1-\varepsilon_2)(\varepsilon_1-\varepsilon_3)}+\frac{f'(\varepsilon_2)}{(\varepsilon_2-\varepsilon_3)(\varepsilon_2-\varepsilon_1)}+\frac{f'(\varepsilon_3)}{(\varepsilon_3-\varepsilon_1)(\varepsilon_3-\varepsilon_2)}\right)\sum_{\alpha\beta}|\Delta_\alpha|^2|\Delta_\beta|^2
\end{aligned} \tag{B.48}$$

Putting it all together, we get that the free energy for the CDW complex parameter is:

$$\begin{aligned}
f_{CDW} &= \frac{1}{2}\left(\frac{1}{2G_{rCDW}}+\frac{1}{2G_{iCDW}}\right)\sum_\alpha|\Delta_\alpha|^2+\frac{1}{2}\left(\frac{1}{2G_{rCDW}}-\frac{1}{2G_{iCDW}}\right)\sum_\alpha|\Delta_\alpha|^2\cos(2\theta_\alpha)+\\
&+\frac{1}{4}\sum_{q\in BZ}\frac{f(\varepsilon_2(\vec{q}))-f(\varepsilon_3(\vec{q}))}{\varepsilon_2(\vec{q})-\varepsilon_3(\vec{q})}\sum_\alpha|\Delta_\alpha|^2+\\
&-\frac{3}{4}\sum_{q\in BZ}\frac{f(\varepsilon_1)}{(\varepsilon_1-\varepsilon_2)(\varepsilon_1-\varepsilon_3)}|\Delta_1||\Delta_2||\Delta_3|\cos(\theta_1+\theta_2+\theta_3)+\\
&+\frac{1}{16}\sum_{q\in BZ}\left(\frac{f'(\varepsilon_2)+f'(\varepsilon_3)}{2(\varepsilon_2-\varepsilon_3)^2}-\frac{f(\varepsilon_2)-f(\varepsilon_3)}{(\varepsilon_2-\varepsilon_3)^3}\right)\sum_\alpha|\Delta_\alpha|^4+\\
&+\frac{1}{48}\sum_{q\in BZ}\left(\frac{f'(\varepsilon_1)}{(\varepsilon_1-\varepsilon_2)(\varepsilon_1-\varepsilon_3)}+\frac{f'(\varepsilon_2)}{(\varepsilon_2-\varepsilon_3)(\varepsilon_2-\varepsilon_1)}+\frac{f'(\varepsilon_3)}{(\varepsilon_3-\varepsilon_1)(\varepsilon_3-\varepsilon_2)}\right)\sum_{\alpha\beta}|\Delta_\alpha|^2|\Delta_\beta|^2 =\\
&= \frac{1}{2}\left(\frac{1}{2G_{rCDW}}+\frac{1}{2G_{iCDW}}\right)\sum_\alpha|\Delta_\alpha|^2+\frac{1}{2}\left(\frac{1}{2G_{rCDW}}-\frac{1}{2G_{iCDW}}\right)\sum_\alpha|\Delta_\alpha|^2\cos(2\theta_\alpha)+\\
&+K_1\sum_\alpha|\Delta_\alpha|^2+K_2|\Delta_1||\Delta_2||\Delta_3|\cos(\theta_1+\theta_2+\theta_3)+K_4\sum_\alpha|\Delta_\alpha|^4+K_3\sum_{\alpha\beta}|\Delta_\alpha|^2|\Delta_\beta|^2
\end{aligned}$$

$$\boxed{\begin{aligned} f_{CDW} =& \frac{r_N + r_\phi}{2} \sum_\alpha |\Delta_\alpha|^2 + \frac{r_N - r_\phi}{2} \sum_\alpha |\Delta_\alpha|^2 \cos(2\theta_\alpha) + K_2 |\Delta_1||\Delta_2||\Delta_3| \cos(\theta_1 + \theta_2 + \theta_3) + \\ &+ K_4 \left( \sum_\alpha |\Delta_\alpha|^2| \right)^2 + (K_3 - 2K_4) \sum_{\alpha\beta} |\Delta_\alpha|^2 |\Delta_\beta|^2 \end{aligned}} \tag{B.49}$$

$$r_N = \frac{1}{2G_{rCDW}} + K_1 \qquad r_\phi = \frac{1}{2G_{iCDW}} + K_1 \tag{B.50}$$

$$K_1 = \frac{1}{4} \sum_{q \in BZ} \frac{f(\varepsilon_2(\vec{q})) - f(\varepsilon_3(\vec{q}))}{\varepsilon_2(\vec{q}) - \varepsilon_3(\vec{q})} \tag{B.51}$$

$$K_2 = -\frac{3}{4} \sum_{q \in BZ} \frac{f(\varepsilon_1)}{(\varepsilon_1 - \varepsilon_2)(\varepsilon_1 - \varepsilon_3)} = \tag{B.52}$$

$$= -\frac{1}{4} \left( \frac{f(\varepsilon_1)}{(\varepsilon_1 - \varepsilon_2)(\varepsilon_1 - \varepsilon_3)} + \frac{f(\varepsilon_2)}{(\varepsilon_2 - \varepsilon_1)(\varepsilon_2 - \varepsilon_3)} + \frac{f(\varepsilon_3)}{(\varepsilon_3 - \varepsilon_1)(\varepsilon_3 - \varepsilon_2)} \right) \tag{B.53}$$

$$K_3 = \frac{1}{16} \sum_{q \in BZ} \frac{f'(\varepsilon_1)}{(\varepsilon_1 - \varepsilon_2)(\varepsilon_1 - \varepsilon_3)} = \tag{B.54}$$

$$= \frac{1}{48} \sum_{q \in BZ} \left( \frac{f'(\varepsilon_1)}{(\varepsilon_1 - \varepsilon_2)(\varepsilon_1 - \varepsilon_3)} + \frac{f'(\varepsilon_2)}{(\varepsilon_2 - \varepsilon_3)(\varepsilon_2 - \varepsilon_1)} + \frac{f'(\varepsilon_3)}{(\varepsilon_3 - \varepsilon_1)(\varepsilon_3 - \varepsilon_2)} \right) \tag{B.55}$$

$$K_4 = -\frac{1}{16} \sum_{q \in BZ} \left( \frac{f(\varepsilon_2) - f(\varepsilon_3)}{(\varepsilon_2 - \varepsilon_3)^3} - \frac{f'(\varepsilon_2) + f'(\varepsilon_3)}{2(\varepsilon_2 - \varepsilon_3)^2} \right) \tag{B.56}$$

Therefore, we obtain equation (9) with the coefficients given in (D1)-(D4)

# Appendix C

## C.1 Hubbard-Stratonovich transformation to decouple the interactions.

Starting from the Hamiltonian in (**??**):

$$\begin{aligned} H'' =& -\frac{V}{2\mathcal{N}}\sum_{\alpha\beta}\sum_{\vec{q}\vec{k}\vec{k}'}(1-\delta_{\alpha\beta})\left(1+e^{-2i(\vec{k}'-\vec{k})\cdot\vec{a}_{\alpha\beta}}\right)c^{\dagger}_{\vec{k}'\beta}c_{\vec{k}'+\vec{q}\alpha}c^{\dagger}_{\vec{k}+\vec{q}\alpha}c_{\vec{k}\beta} \\ =& -\frac{V}{2\mathcal{N}}\sum_{\alpha\beta}\sum_{\vec{q}\vec{k}\vec{k}'}(1-\delta_{\alpha\beta})\left[c^{\dagger}_{\vec{k}'\beta}c_{\vec{k}'+\vec{q}\alpha}c^{\dagger}_{\vec{k}+\vec{q}\alpha}c_{\vec{k}\beta}+e^{-2i\vec{k}'\cdot\vec{a}_{\alpha\beta}}c^{\dagger}_{\vec{k}'\beta}c_{\vec{k}'+\vec{q}\alpha}e^{-2i\vec{k}\cdot\vec{a}_{\beta\alpha}}c^{\dagger}_{\vec{k}+\vec{q}\alpha}c_{\vec{k}\beta}\right] . \end{aligned}$$

At first we can define the fields:

$$n^{\alpha\beta}_{\vec{q}}=\frac{1}{\mathcal{N}}(1-\delta_{\alpha\beta})\sum_{\vec{k}}c^{\dagger}_{\vec{k}+\vec{q}\alpha}c_{\vec{k}\beta}\ , \qquad (n^{\alpha\beta}_{\vec{q}})^{\dagger}=\frac{1}{\mathcal{N}}(1-\delta_{\alpha\beta})\sum_{\vec{k}}c^{\dagger}_{\vec{k}\beta}c_{\vec{k}+\vec{q}\alpha}\ ,$$

$$m^{\alpha\beta}_{\vec{q}}=\frac{1}{\mathcal{N}}(1-\delta_{\alpha\beta})\sum_{\vec{k}}e^{-2i\vec{k}\cdot\vec{a}_{\alpha\beta}}c^{\dagger}_{\vec{k}+\vec{q}\alpha}c_{\vec{k}\beta}\ , \qquad (m^{\alpha\beta}_{\vec{q}})^{\dagger}=\frac{1}{\mathcal{N}}(1-\delta_{\alpha\beta})\sum_{\vec{k}}e^{-2i\vec{k}\cdot\vec{a}_{\beta\alpha}}c^{\dagger}_{\vec{k}\beta}c_{\vec{k}+\vec{q}\alpha}\ ,$$

so that the Hamiltonian is

$$H''=-\frac{V\mathcal{N}}{2}\sum_{\alpha\beta}\sum_{\vec{q}}(1-\delta_{\alpha\beta})\left[(n^{\alpha\beta}_{\vec{q}})^{\dagger}n^{\alpha\beta}_{\vec{q}}+(m^{\alpha\beta}_{\vec{q}})^{\dagger}m^{\alpha\beta}_{\vec{q}}\right] .$$

But we can also divide these fields in their real and imaginary parts as given by (5.13):

$$n^{\alpha\beta}_{\vec{q}}=n^{\alpha\beta}_{\vec{q}R}+n^{\alpha\beta}_{\vec{q}I} \quad \Rightarrow \quad (n^{\alpha\beta}_{\vec{q}})^{\dagger}=(n^{\alpha\beta}_{\vec{q}R})^{\dagger}+(n^{\alpha\beta}_{\vec{q}I})^{\dagger}=n^{\alpha\beta}_{\vec{q}R}-n^{\alpha\beta}_{\vec{q}I}\ ,$$

where we can recall that:

$$\begin{aligned} n^{\alpha\beta}_{\vec{q}R}&=\frac{1}{2\mathcal{N}}(1-\delta_{\alpha\beta})\sum_{\vec{k}}\left(c^{\dagger}_{\vec{k}+\vec{q}\alpha}c_{\vec{k}\beta}+c^{\dagger}_{\vec{k}\beta}c_{\vec{k}+\vec{q}\alpha}\right)=(n^{\alpha\beta}_{\vec{q}R})^{\dagger}\ , \\ n^{\alpha\beta}_{\vec{q}I}&=\frac{1}{2\mathcal{N}}(1-\delta_{\alpha\beta})\sum_{\vec{k}}\left(c^{\dagger}_{\vec{k}+\vec{q}\alpha}c_{\vec{k}\beta}-c^{\dagger}_{\vec{k}\beta}c_{\vec{k}+\vec{q}\alpha}\right)=-(n^{\alpha\beta}_{\vec{q}I})^{\dagger}\ , \end{aligned}$$

so that the associated term in the Hamiltonian is:

$$\begin{aligned} (n^{\alpha\beta}_{\vec{q}})^{\dagger}n^{\alpha\beta}_{\vec{q}}&=\left(n^{\alpha\beta}_{\vec{q}R}+n^{\alpha\beta}_{\vec{q}I}\right)\left(n^{\alpha\beta}_{\vec{q}R}-n^{\alpha\beta}_{\vec{q}I}\right)=(n^{\alpha\beta}_{\vec{q}R})^2-n^{\alpha\beta}_{\vec{q}R}n^{\alpha\beta}_{\vec{q}I}+n^{\alpha\beta}_{\vec{q}I}n^{\alpha\beta}_{\vec{q}R}-(n^{\alpha\beta}_{\vec{q}I})^2 \\ &=(n^{\alpha\beta}_{\vec{q}R})^2-(n^{\alpha\beta}_{\vec{q}I})^2\ . \end{aligned}$$

Analogous for the other bilinear,

$$m_{\vec{q}}^{\alpha\beta} = m_{\vec{q}R}^{\alpha\beta} + m_{\vec{q}I}^{\alpha\beta} \quad \Rightarrow \quad (m_{\vec{q}}^{\alpha\beta})^\dagger = (m_{\vec{q}R}^{\alpha\beta})^\dagger + (m_{\vec{q}I}^{\alpha\beta})^\dagger = m_{\vec{q}R}^{\alpha\beta} - m_{\vec{q}I}^{\alpha\beta} \ ,$$

where we can recall that:

$$m_{\vec{q}R}^{\alpha\beta} = \frac{1}{2\mathcal{N}}(1-\delta_{\alpha\beta})\sum_{\vec{k}}\left(e^{-2i\vec{k}\cdot\vec{a}_{\alpha\beta}}c_{\vec{k}+\vec{q}\alpha}^\dagger c_{\vec{k}\beta} + e^{-2i\vec{k}\cdot\vec{a}_{\beta\alpha}}c_{\vec{k}\beta}^\dagger c_{\vec{k}+\vec{q}\alpha}\right) = (m_{\vec{q}R}^{\alpha\beta})^\dagger \ ,$$

$$m_{\vec{q}I}^{\alpha\beta} = \frac{1}{2\mathcal{N}}(1-\delta_{\alpha\beta})\sum_{\vec{k}}\left(e^{-2i\vec{k}\cdot\vec{a}_{\alpha\beta}}c_{\vec{k}+\vec{q}\alpha}^\dagger c_{\vec{k}\beta} - e^{-2i\vec{k}\cdot\vec{a}_{\beta\alpha}}c_{\vec{k}\beta}^\dagger c_{\vec{k}+\vec{q}\alpha}\right) = -(m_{\vec{q}I}^{\alpha\beta})^\dagger \ ,$$

so that the associated term in the Hamiltonian is:

$$\begin{aligned}(m_{\vec{q}}^{\alpha\beta})^\dagger m_{\vec{q}}^{\alpha\beta} &= \left(m_{\vec{q}R}^{\alpha\beta} + m_{\vec{q}I}^{\alpha\beta}\right)\left(m_{\vec{q}R}^{\alpha\beta} - m_{\vec{q}I}^{\alpha\beta}\right) = (m_{\vec{q}R}^{\alpha\beta})^2 - m_{\vec{q}R}^{\alpha\beta}m_{\vec{q}I}^{\alpha\beta} + m_{\vec{q}I}^{\alpha\beta}m_{\vec{q}R}^{\alpha\beta} - (m_{\vec{q}I}^{\alpha\beta})^2 \\ &= (m_{\vec{q}R}^{\alpha\beta})^2 - (m_{\vec{q}I}^{\alpha\beta})^2 \ .\end{aligned}$$

Now, the Hamiltonian can be rewritten as

$$H'' = -\frac{V\mathcal{N}}{2}\sum_{\alpha\beta}\sum_{\vec{q}}\left[(n_{\vec{q}R}^{\alpha\beta})^2 - (n_{\vec{q}I}^{\alpha\beta})^2 + (m_{\vec{q}R}^{\alpha\beta})^2 - (m_{\vec{q}I}^{\alpha\beta})^2\right]$$

but for the doing the HS transformation I will use the Hamiltonian in the form:

$$H'' = -\frac{V\mathcal{N}}{2}\sum_{\alpha\beta}\sum_{\vec{q}}\left[(n_{\vec{q}R}^{\alpha\beta})^\dagger n_{\vec{q}R}^{\alpha\beta} + (n_{\vec{q}I}^{\alpha\beta})^\dagger n_{\vec{q}I}^{\alpha\beta} + (m_{\vec{q}R}^{\alpha\beta})^\dagger m_{\vec{q}R}^{\alpha\beta} + (m_{\vec{q}I}^{\alpha\beta})^\dagger m_{\vec{q}I}^{\alpha\beta}\right]$$

so that in the transformation I will not use the fact that they are real or imaginary, and all of the bilinears will be decoupled as the usual repulsive interactions.

One can introduce four white-noise fields $\gamma_i$ with the gaussian actions

$$S_{\gamma_1} = -\frac{\mathcal{N}}{2V}\int_0^\beta d\tau \sum_{\vec{q}\alpha\beta}\bar{\gamma}_{\vec{q}i}^{\alpha\beta}\gamma_{\vec{q}i}^{\alpha\beta} \qquad \text{with} \qquad i = 1,2,3,4. \tag{C.1}$$

Then, in the action one can do the substitution

$$\begin{aligned}H'' \to \tilde{H}'' = \frac{\mathcal{N}}{2}\sum_{\vec{q}\mu}\Bigg( &- V\bar{n}_{\vec{q}R}^{\alpha\beta}n_{\vec{q}R}^{\alpha\beta} + V^{-1}\bar{\gamma}_{\vec{q}1}^{\alpha\beta}\gamma_{\vec{q}1}^{\alpha\beta} - V\bar{n}_{\vec{q}I}^{\alpha\beta}n_{\vec{q}I}^{\alpha\beta} + V^{-1}\bar{\gamma}_{\vec{q}2}^{\alpha\beta}\gamma_{\vec{q}2}^{\alpha\beta} &\text{(C.2)}\\ &- V\bar{m}_{\vec{q}R}^{\alpha\beta}m_{\vec{q}R}^{\alpha\beta} + V^{-1}\bar{\gamma}_{\vec{q}3}^{\alpha\beta}\gamma_{\vec{q}3}^{\alpha\beta} - V\bar{m}_{\vec{q}I}^{\alpha\beta}m_{\vec{q}I}^{\alpha\beta} + V^{-1}\bar{\gamma}_{\vec{q}4}^{\alpha\beta}\gamma_{\vec{q}4}^{\alpha\beta}\Bigg) &\text{(C.3)}\end{aligned}$$

Doing the variable shifts,

$$\gamma_{\vec{q}1}^{\alpha\beta} = N_{\vec{q}R}^{\alpha\beta} - Vn_{\vec{q}R}^{\alpha\beta} \ , \quad \gamma_{\vec{q}2}^{\alpha\beta} = N_{\vec{q}I}^{\alpha\beta} - Vn_{\vec{q}I}^{\alpha\beta} \ , \quad \gamma_{\vec{q}3}^{\alpha\beta} = M_{\vec{q}R}^{\alpha\beta} - Vm_{\vec{q}R}^{\alpha\beta} \ , \quad \gamma_{\vec{q}4}^{\alpha\beta} = M_{\vec{q}I}^{\alpha\beta} - Vm_{\vec{q}I}^{\alpha\beta} \ ,$$

we get that, for instance, the term corresponding to $\gamma_1$ is:

$$\begin{aligned}V^{-1}\sum_{\alpha\beta}\bar{\gamma}_{\vec{q}1}^{\alpha\beta}\gamma_{\vec{q}1}^{\alpha\beta} =& V^{-1}\sum_{\alpha\beta}\left(\bar{N}_{\vec{q}R}^{\alpha\beta} - V\bar{n}_{\vec{q}R}^{\alpha\beta}\right)\left(N_{\vec{q}R}^{\alpha\beta} - Vn_{\vec{q}R}^{\alpha\beta}\right) \\ =& \sum_{\alpha\beta}\left(V^{-1}\bar{N}_{\vec{q}R}^{\alpha\beta}N_{\vec{q}R}^{\alpha\beta} - \bar{N}_{\vec{q}R}^{\alpha\beta}n_{\vec{q}R}^{\alpha\beta} - \bar{n}_{\vec{q}R}^{\alpha\beta}N_{\vec{q}R}^{\alpha\beta} + V\bar{n}_{\vec{q}R}^{\alpha\beta}n_{\vec{q}R}^{\alpha\beta}\right) \ .\end{aligned}$$

We can see that the last term will cancel the corresponding bilinear term in (C.3). Analogous for the rest of the fields, (C.3) becomes:

$$\begin{aligned}\tilde{H}'' =& -\frac{\mathcal{N}}{2}\sum_{\vec{q}\alpha\beta}\Big(\bar{N}^{\alpha\beta}_{\vec{q}R}n^{\alpha\beta}_{\vec{q}R}+\bar{n}^{\alpha\beta}_{\vec{q}R}N^{\alpha\beta}_{\vec{q}R}+\bar{N}^{\alpha\beta}_{\vec{q}I}n^{\alpha\beta}_{\vec{q}I}+\bar{n}^{\alpha\beta}_{\vec{q}I}N^{\alpha\beta}_{\vec{q}I}+\bar{M}^{\alpha\beta}_{\vec{q}R}m^{\alpha\beta}_{\vec{q}R}+\bar{m}^{\alpha\beta}_{\vec{q}R}M^{\alpha\beta}_{\vec{q}R}\\ &+\bar{M}^{\alpha\beta}_{\vec{q}I}m^{\alpha\beta}_{\vec{q}I}+\bar{m}^{\alpha\beta}_{\vec{q}I}M^{\alpha\beta}_{\vec{q}I}\Big)+\frac{\mathcal{N}}{2V}\sum_{\vec{q}\alpha\beta}\Big(\bar{N}^{\alpha\beta}_{\vec{q}R}N^{\alpha\beta}_{\vec{q}R}+\bar{N}^{\alpha\beta}_{\vec{q}I}N^{\alpha\beta}_{\vec{q}I}+\bar{M}^{\alpha\beta}_{\vec{q}R}M^{\alpha\beta}_{\vec{q}R}+\bar{M}^{\alpha\beta}_{\vec{q}I}M^{\alpha\beta}_{\vec{q}I}\Big)\ .\end{aligned}$$

Now we can use whether they are real or imaginary to simplify some of the terms:

$$\begin{aligned}\tilde{H}'' =& -\frac{\mathcal{N}}{2}\sum_{\vec{q}\mu}\Big(N^{\alpha\beta}_{\vec{q}R}n^{\alpha\beta}_{\vec{q}R}+n^{\alpha\beta}_{\vec{q}R}N^{\alpha\beta}_{\vec{q}R}-N^{\alpha\beta}_{\vec{q}I}n^{\alpha\beta}_{\vec{q}I}-n^{\alpha\beta}_{\vec{q}I}N^{\alpha\beta}_{\vec{q}I}+M^{\alpha\beta}_{\vec{q}R}m^{\alpha\beta}_{\vec{q}R}+m^{\alpha\beta}_{\vec{q}R}M^{\alpha\beta}_{\vec{q}R}\\ &-M^{\alpha\beta}_{\vec{q}I}m^{\alpha\beta}_{\vec{q}I}-m^{\alpha\beta}_{\vec{q}I}M^{\alpha\beta}_{\vec{q}I}\Big)+\frac{\mathcal{N}}{2V}\sum_{\vec{q}\mu}\Big(N^{\alpha\beta}_{\vec{q}R}N^{\alpha\beta}_{\vec{q}R}-N^{\alpha\beta}_{\vec{q}I}N^{\alpha\beta}_{\vec{q}I}+M^{\alpha\beta}_{\vec{q}R}M^{\alpha\beta}_{\vec{q}R}-M^{\alpha\beta}_{\vec{q}I}M^{\alpha\beta}_{\vec{q}I}\Big)\\ =& -\mathcal{N}\sum_{\vec{q}\mu}\Big(N^{\alpha\beta}_{\vec{q}R}n^{\alpha\beta}_{\vec{q}R}-N^{\alpha\beta}_{\vec{q}I}n^{\alpha\beta}_{\vec{q}I}+M^{\alpha\beta}_{\vec{q}R}m^{\alpha\beta}_{\vec{q}R}-M^{\alpha\beta}_{\vec{q}I}m^{\alpha\beta}_{\vec{q}I}\Big)\\ &+\frac{\mathcal{N}}{2V}\sum_{\vec{q}\mu}\Big(\big(N^{\alpha\beta}_{\vec{q}R}\big)^2-\big(N^{\alpha\beta}_{\vec{q}I}\big)^2+\big(M^{\alpha\beta}_{\vec{q}R}\big)^2-\big(M^{\alpha\beta}_{\vec{q}I}\big)^2\Big)\ .\end{aligned}\tag{C.4}$$

Introducing this expression of $H''$ in the action, we get:

$$\begin{aligned}S=\int_0^\beta d\tau\Bigg[&\sum_{\vec{k}\alpha}\bar{c}_{\vec{k}\alpha}\partial_\tau c_{\vec{k}\alpha}+\sum_{\vec{k}\alpha\beta}\bar{c}_{\vec{k}\alpha}h_{\alpha\beta}(\vec{k})c_{\vec{k}\beta}-\mathcal{N}\sum_{\vec{q}\alpha\beta}\Big(N^{\alpha\beta}_{\vec{q}R}n^{\alpha\beta}_{\vec{q}R}-N^{\alpha\beta}_{\vec{q}I}n^{\alpha\beta}_{\vec{q}I}+M^{\alpha\beta}_{\vec{q}R}m^{\alpha\beta}_{\vec{q}R}\\ &-M^{\alpha\beta}_{\vec{q}I}m^{\alpha\beta}_{\vec{q}I}\Big)+\frac{\mathcal{N}}{2V}\sum_{\vec{q}\alpha\beta}\Big(\big(N^{\alpha\beta}_{\vec{q}R}\big)^2-\big(N^{\alpha\beta}_{\vec{q}I}\big)^2+\big(M^{\alpha\beta}_{\vec{q}R}\big)^2-\big(M^{\alpha\beta}_{\vec{q}I}\big)^2\Big)\Bigg]\ .\end{aligned}$$

Substituting back the expression of the bilinears in terms of the fermionic operators:

$$\begin{aligned}S=\int_0^\beta d\tau\Bigg[&\sum_{\vec{k}\alpha}\bar{c}_{\vec{k}\alpha}\partial_\tau c_{\vec{k}\alpha}+\sum_{\vec{k}\alpha\beta}\bar{c}_{\vec{k}\alpha}h_{\alpha\beta}(\vec{k})c_{\vec{k}\beta}-\frac{1}{2}(1-\delta_{\alpha\beta})\sum_{\alpha\beta}\sum_{\vec{k}\vec{q}}\Bigg(N^{\alpha\beta}_{\vec{q}R}\Big(\bar{c}_{\vec{k}+\vec{q}\alpha}c_{\vec{k}\beta}+\bar{c}_{\vec{k}\beta}c_{\vec{k}+\vec{q}\alpha}\Big)\\ &-N^{\alpha\beta}_{\vec{q}I}\Big(\bar{c}_{\vec{k}+\vec{q}\alpha}c_{\vec{k}\beta}-\bar{c}_{\vec{k}\beta}c_{\vec{k}+\vec{q}\alpha}\Big)+M^{\alpha\beta}_{\vec{q}R}\Big(e^{-2i\vec{k}\cdot\vec{a}_{\alpha\beta}}\bar{c}_{\vec{k}+\vec{q}\alpha}c_{\vec{k}\beta}+e^{-2i\vec{k}\cdot\vec{a}_{\beta\alpha}}\bar{c}_{\vec{k}\beta}c_{\vec{k}+\vec{q}\alpha}\Big)\\ &-M^{\alpha\beta}_{\vec{q}I}\Big(e^{-2i\vec{k}\cdot\vec{a}_{\alpha\beta}}\bar{c}_{\vec{k}+\vec{q}\alpha}c_{\vec{k}\beta}-e^{-2i\vec{k}\cdot\vec{a}_{\beta\alpha}}\bar{c}_{\vec{k}\beta}c_{\vec{k}+\vec{q}\alpha}\Big)\Bigg)\\ &+\frac{\mathcal{N}}{2V}\sum_{\vec{q}\alpha\beta}\Big(\big(N^{\alpha\beta}_{\vec{q}R}\big)^2-\big(N^{\alpha\beta}_{\vec{q}I}\big)^2+\big(M^{\alpha\beta}_{\vec{q}R}\big)^2-\big(M^{\alpha\beta}_{\vec{q}I}\big)^2\Big)\Bigg]\\ =\int_0^\beta d\tau\Bigg[&\sum_{\vec{k}\alpha}\bar{c}_{\vec{k}\alpha}\partial_\tau c_{\vec{k}\alpha}+\sum_{\vec{k}\alpha\beta}\bar{c}_{\vec{k}\alpha}h_{\alpha\beta}(\vec{k})c_{\vec{k}\beta}-\frac{1}{2}(1-\delta_{\alpha\beta})\sum_{\alpha\beta}\sum_{\vec{k}\vec{q}}\Bigg(N^{\alpha\beta}_{\vec{q}R}\bar{c}_{\vec{k}+\vec{q}\alpha}c_{\vec{k}\beta}\\ &+N^{\alpha\beta}_{\vec{q}R}\bar{c}_{\vec{k}\beta}c_{\vec{k}+\vec{q}\alpha}-N^{\alpha\beta}_{\vec{q}I}\bar{c}_{\vec{k}+\vec{q}\alpha}c_{\vec{k}\beta}+N^{\alpha\beta}_{\vec{q}I}\bar{c}_{\vec{k}\beta}c_{\vec{k}+\vec{q}\alpha}+M^{\alpha\beta}_{\vec{q}R}e^{-2i\vec{k}\cdot\vec{a}_{\alpha\beta}}\bar{c}_{\vec{k}+\vec{q}\alpha}c_{\vec{k}\beta}\\ &+M^{\alpha\beta}_{\vec{q}R}e^{-2i\vec{k}\cdot\vec{a}_{\beta\alpha}}\bar{c}_{\vec{k}\beta}c_{\vec{k}+\vec{q}\alpha}-M^{\alpha\beta}_{\vec{q}I}e^{-2i\vec{k}\cdot\vec{a}_{\alpha\beta}}\bar{c}_{\vec{k}+\vec{q}\alpha}c_{\vec{k}\beta}+M^{\alpha\beta}_{\vec{q}I}e^{-2i\vec{k}\cdot\vec{a}_{\beta\alpha}}\bar{c}_{\vec{k}\beta}c_{\vec{k}+\vec{q}\alpha}\Bigg)\\ &+\frac{\mathcal{N}}{2V}\sum_{\vec{q}\alpha\beta}\Big(\big(N^{\alpha\beta}_{\vec{q}R}\big)^2-\big(N^{\alpha\beta}_{\vec{q}I}\big)^2+\big(M^{\alpha\beta}_{\vec{q}R}\big)^2-\big(M^{\alpha\beta}_{\vec{q}I}\big)^2\Big)\Bigg]\ .\end{aligned}$$

We would like to have all of the terms that include the fermionic operators in terms of the same $\bar{c}_{\vec{k}\alpha}$ , $c_{\vec{k}'\beta}$ so that we can write them all as $\bar{c}_{\vec{k}\alpha}(\quad)c_{\vec{k}'\beta}$. Therefore, we can first asjust the sublattice indices, which we can do by relabeling given that we are summing over all of them. Therefore,

$$\begin{aligned}
S = \int_0^\beta d\tau \sum_{\alpha\beta} \Bigg[ & \sum_{\vec{k}} \bar{c}_{\vec{k}\alpha} \partial_\tau \delta_{\alpha\beta} c_{\vec{k}\beta} + \sum_{\vec{k}} \bar{c}_{\vec{k}\alpha} h_{\alpha\beta}(\vec{k}) c_{\vec{k}\beta} - \frac{1}{2}(1-\delta_{\alpha\beta}) \sum_{\vec{k}\vec{q}} \Bigg( N^{\alpha\beta}_{\vec{q}R} \bar{c}_{\vec{k}+\vec{q}\alpha} c_{\vec{k}\beta} \\
& + N^{\beta\alpha}_{\vec{q}R} \bar{c}_{\vec{k}\alpha} c_{\vec{k}+\vec{q}\beta} - N^{\alpha\beta}_{\vec{q}I} \bar{c}_{\vec{k}+\vec{q}\alpha} c_{\vec{k}\beta} + N^{\beta\alpha}_{\vec{q}I} \bar{c}_{\vec{k}\alpha} c_{\vec{k}+\vec{q}\beta} + M^{\alpha\beta}_{\vec{q}R} e^{-2i\vec{k}\cdot\vec{a}_{\alpha\beta}} \bar{c}_{\vec{k}+\vec{q}\alpha} c_{\vec{k}\beta} \\
& + M^{\beta\alpha}_{\vec{q}R} e^{-2i\vec{k}\cdot\vec{a}_{\alpha\beta}} \bar{c}_{\vec{k}\alpha} c_{\vec{k}+\vec{q}\beta} - M^{\alpha\beta}_{\vec{q}I} e^{-2i\vec{k}\cdot\vec{a}_{\alpha\beta}} \bar{c}_{\vec{k}+\vec{q}\alpha} c_{\vec{k}\beta} + M^{\beta\alpha}_{\vec{q}I} e^{-2i\vec{k}\cdot\vec{a}_{\alpha\beta}} \bar{c}_{\vec{k}\alpha} c_{\vec{k}+\vec{q}\beta} \Bigg) \\
& + \frac{\mathcal{N}}{2V} \sum_{\vec{q}} \left( \left(N^{\alpha\beta}_{\vec{q}R}\right)^2 - \left(N^{\alpha\beta}_{\vec{q}I}\right)^2 + \left(M^{\alpha\beta}_{\vec{q}R}\right)^2 - \left(M^{\alpha\beta}_{\vec{q}I}\right)^2 \right) \Bigg] .
\end{aligned}$$

Now we can adjust the momentum indices in the same way:

$$\begin{aligned}
S = \int_0^\beta d\tau \sum_{\alpha\beta} \Bigg[ & \sum_{\vec{k}\vec{k}'} \bar{c}_{\vec{k}\alpha} \partial_\tau \delta_{\alpha\beta} \delta_{\vec{k}\vec{k}'} c_{\vec{k}'\beta} + \sum_{\vec{k}\vec{k}'} \bar{c}_{\vec{k}\alpha} h_{\alpha\beta}(\vec{k}) \delta_{\vec{k}\vec{k}'} c_{\vec{k}'\beta} - \frac{1}{2}(1-\delta_{\alpha\beta}) \sum_{\vec{k}\vec{k}'} \Bigg( N^{\alpha\beta}_{\vec{k}-\vec{k}'R} \bar{c}_{\vec{k}\alpha} c_{\vec{k}'\beta} \\
& + N^{\beta\alpha}_{\vec{k}'-\vec{k}R} \bar{c}_{\vec{k}\alpha} c_{\vec{k}'\beta} - N^{\alpha\beta}_{\vec{k}-\vec{k}'I} \bar{c}_{\vec{k}\alpha} c_{\vec{k}'\beta} + N^{\beta\alpha}_{\vec{k}'-\vec{k}I} \bar{c}_{\vec{k}\alpha} c_{\vec{k}'\beta} + M^{\alpha\beta}_{\vec{k}-\vec{k}'R} e^{-2i\vec{k}'\cdot\vec{a}_{\alpha\beta}} \bar{c}_{\vec{k}\alpha} c_{\vec{k}'\beta} \\
& + M^{\beta\alpha}_{\vec{k}'-\vec{k}R} e^{-2i\vec{k}\cdot\vec{a}_{\alpha\beta}} \bar{c}_{\vec{k}\alpha} c_{\vec{k}'\beta} - M^{\alpha\beta}_{\vec{k}-\vec{k}'I} e^{-2i\vec{k}'\cdot\vec{a}_{\alpha\beta}} \bar{c}_{\vec{k}\alpha} c_{\vec{k}'\beta} + M^{\beta\alpha}_{\vec{k}'-\vec{k}I} e^{-2i\vec{k}\cdot\vec{a}_{\alpha\beta}} \bar{c}_{\vec{k}\alpha} c_{\vec{k}'\beta} \Bigg) \\
& + \frac{\mathcal{N}}{2V} \sum_{\vec{q}} \left( \left(N^{\alpha\beta}_{\vec{q}R}\right)^2 - \left(N^{\alpha\beta}_{\vec{q}I}\right)^2 + \left(M^{\alpha\beta}_{\vec{q}R}\right)^2 - \left(M^{\alpha\beta}_{\vec{q}I}\right)^2 \right) \Bigg] \\
= \int_0^\beta d\tau \sum_{\alpha\beta} \Bigg[ & \sum_{\vec{k}\vec{k}'} \bar{c}_{\vec{k}\alpha} \Bigg( \partial_\tau \delta_{\alpha\beta} \delta_{\vec{k}\vec{k}'} + h_{\alpha\beta}(\vec{k}) \delta_{\vec{k}\vec{k}'} - \frac{1}{2}(1-\delta_{\alpha\beta}) \Big( N^{\alpha\beta}_{\vec{k}-\vec{k}'R} + N^{\beta\alpha}_{\vec{k}'-\vec{k}R} - N^{\alpha\beta}_{\vec{k}-\vec{k}'I} \\
& + N^{\beta\alpha}_{\vec{k}'-\vec{k}I} + M^{\alpha\beta}_{\vec{k}-\vec{k}'R} e^{-2i\vec{k}'\cdot\vec{a}_{\alpha\beta}} + M^{\beta\alpha}_{\vec{k}'-\vec{k}R} e^{-2i\vec{k}\cdot\vec{a}_{\alpha\beta}} - M^{\alpha\beta}_{\vec{k}-\vec{k}'I} e^{-2i\vec{k}'\cdot\vec{a}_{\alpha\beta}} \\
& + M^{\beta\alpha}_{\vec{k}'-\vec{k}I} e^{-2i\vec{k}\cdot\vec{a}_{\alpha\beta}} \Big) \Bigg) c_{\vec{k}'\beta} + \frac{\mathcal{N}}{2V} \sum_{\vec{q}} \left( \left(N^{\alpha\beta}_{\vec{q}R}\right)^2 - \left(N^{\alpha\beta}_{\vec{q}I}\right)^2 + \left(M^{\alpha\beta}_{\vec{q}R}\right)^2 - \left(M^{\alpha\beta}_{\vec{q}I}\right)^2 \right) \Bigg] .
\end{aligned}$$

Finally, defining the effective Hamiltonian

$$\begin{aligned}
\mathcal{H}_{\alpha\beta}(\vec{k},\vec{k}')[N_R, N_I, M_R, M_I] = & h_{\alpha\beta}(\vec{k}) \delta_{\vec{k}\vec{k}'} - \frac{1}{2}(1-\delta_{\alpha\beta}) \Big[ N^{\alpha\beta}_{\vec{k}-\vec{k}'R} + N^{\beta\alpha}_{\vec{k}'-\vec{k}R} - N^{\alpha\beta}_{\vec{k}-\vec{k}'I} \\
& + N^{\beta\alpha}_{\vec{k}'-\vec{k}I} + \left( M^{\alpha\beta}_{\vec{k}-\vec{k}'R} - M^{\alpha\beta}_{\vec{k}-\vec{k}'I} \right) e^{-2i\vec{k}'\cdot\vec{a}_{\alpha\beta}} \\
& + \left( M^{\beta\alpha}_{\vec{k}'-\vec{k}R} + M^{\beta\alpha}_{\vec{k}'-\vec{k}I} \right) e^{-2i\vec{k}\cdot\vec{a}_{\alpha\beta}} \Big] ,
\end{aligned} \tag{C.5}$$

we get that the action is

$$\begin{aligned}
S = \int_0^\beta d\tau \sum_{\alpha\beta} \Bigg[ & \sum_{\vec{k}\vec{k}'} \bar{c}_{\vec{k}\alpha} \Big( \partial_\tau \delta_{\vec{k}\vec{k}'} \delta_{\alpha\beta} + \mathcal{H}_{\alpha\beta}(\vec{k},\vec{k}')[N_R, N_I, M_R, M_I] \Big) c_{\vec{k}'\beta} \\
& + \frac{\mathcal{N}}{2V} \sum_{\vec{q}} \left( \left(N^{\alpha\beta}_{\vec{q}R}\right)^2 - \left(N^{\alpha\beta}_{\vec{q}I}\right)^2 + \left(M^{\alpha\beta}_{\vec{q}R}\right)^2 - \left(M^{\alpha\beta}_{\vec{q}I}\right)^2 \right) \Bigg] .
\end{aligned} \tag{C.6}$$

At this point, we can substitute in the expression for the partition function and integrate out the fermions

$$\begin{aligned}\mathcal{Z} &\equiv \int \mathcal{D}[N_R, N_I, M_R, M_I] \int \mathcal{D}[c, \bar{c}] e^{-S[c,\bar{c},N_R,N_I,M_R,M_I]} \\ &= \int \mathcal{D}[N_R, N_I, M_R, M_I] e^{-S_E[N_R,N_I,M_R,M_I]}, \end{aligned} \tag{C.7}$$

where

$$\begin{aligned} e^{-S_E[N,\bar{N},M,\bar{M}]} &= \int \mathcal{D}[c, \bar{c}] e^{-S[c,\bar{c},N_R,N_I,M_R,M_I]} \\ &= \left[ \int \mathcal{D}[c, \bar{c}] e^{-\int_0^\beta d\tau \bar{c}(\partial_\tau \mathbb{1} + \mathcal{H}[N_R,N_I,M_R,M_I])c} \right] e^{-\frac{\mathcal{N}}{2V}\int_0^\beta d\tau \sum_{\vec{q}} \sum_{\alpha\beta} \left( (N^{\alpha\beta}_{\vec{q}R})^2 - (N^{\alpha\beta}_{\vec{q}I})^2 + (M^{\alpha\beta}_{\vec{q}R})^2 - (M^{\alpha\beta}_{\vec{q}I})^2 \right)} \\ &= \det\left(\partial_\tau \mathbb{1} + \mathcal{H}[N_R, N_I, M_R, M_I]\right) e^{-\frac{\mathcal{N}}{2V}\int_0^\beta d\tau \sum_{\vec{q}} \sum_{\alpha\beta} \left( (N^{\alpha\beta}_{\vec{q}R})^2 - (N^{\alpha\beta}_{\vec{q}I})^2 + (M^{\alpha\beta}_{\vec{q}R})^2 - (M^{\alpha\beta}_{\vec{q}I})^2 \right)} . \end{aligned}$$

In the last equality the Gaussian integral has been carried out. Furthermore, using the property $\det(A) = e^{\log(\det(A))} = e^{\mathrm{Tr}(\log(A))}$,

$$\begin{aligned} S_E[N, \bar{N}, M, \bar{M}] = &- \mathrm{Tr}\left(\log\left(\partial_\tau \mathbb{1} + \mathcal{H}[N_R, N_I, M_R, M_I]\right)\right) \\ &+ \frac{\mathcal{N}}{2V} \int_0^\beta d\tau \sum_{\vec{q}} \sum_{\alpha\beta} \left( (N^{\alpha\beta}_{\vec{q}R})^2 - (N^{\alpha\beta}_{\vec{q}I})^2 + (M^{\alpha\beta}_{\vec{q}R})^2 - (M^{\alpha\beta}_{\vec{q}I})^2 \right) \end{aligned} \tag{C.8}$$

## C.2 Saddle-point equations and mean-field solutions.

Let us solve the saddle point equation:

$$\left. \frac{\delta S_E[N_R, N_I, M_R, M_I]}{\delta N_R} \right|_{N_R = N_R^{(0)}} = 0 .$$

$$\frac{\delta e^{-S_E[N_R,N_I,M_R,M_I]}}{\delta N^{\alpha\beta}_{\vec{q}R}} = -e^{-S_E[N_R,N_I,M_R,M_I]} \frac{\delta S_E[N_R, N_I, M_R, M_I]}{\delta N^{\alpha\beta}_{\vec{q}R}} ,$$

so that

$$\begin{aligned}
\frac{\delta S_E[N_R,N_I,M_R,M_I]}{\delta N^{\alpha\beta}_{\vec{q}R}} =& -e^{+S_E[N_R,N_I,M_R,M_I]}\frac{\delta e^{-S_E[N_R,N_I,M_R,M_I]}}{\delta N^{\alpha\beta}_{\vec{q}R}}\\
=& -e^{S_E[N_R,N_I,M_R,M_I]}\frac{\partial}{N^{\alpha\beta}_{\vec{q}R}}\left(\int\mathcal{D}[c,\bar{c}]e^{-S[c,\bar{c},N_R,N_I,M_R,M_I]}\right)\\
=& e^{S_E[N_R,N_I,M_R,M_I]}\int\mathcal{D}[c,\bar{c}]e^{-S[c,\bar{c},N_R,N_I,M_R,M_I]}\frac{\delta S[c,\bar{c},N_R,N_I,M_R,M_I]}{\delta N^{\alpha\beta}_{\vec{q}R}}\\
=& e^{S_E[N_R,N_I,M_R,M_I]}\int\mathcal{D}[c,\bar{c}]e^{-S[c,\bar{c},N_R,N_I,M_R,M_I]}\left(-\mathcal{N}n^{\alpha\beta}_{\vec{q}R}+\frac{\mathcal{N}}{V}N^{\alpha\beta}_{\vec{q}R}\right)\\
=& -\mathcal{N}e^{S_E[N_R,N_I,M_R,M_I]}\underbrace{\int\mathcal{D}[c,\bar{c}]e^{-S[c,\bar{c},N_R,N_I,M_R,M_I]}n^{\alpha\beta}_{\vec{q}R}}_{\left\langle n^{\alpha\beta}_{\vec{q}R}\right\rangle}\\
&+\frac{\mathcal{N}}{V}N^{\alpha\beta}_{\vec{q}R}e^{S_E[N_R,N_I,M_R,M_I]}\underbrace{\int\mathcal{D}[c,\bar{c}]e^{-S[c,\bar{c},N_R,N_I,M_R,M_I]}}_{e^{-S_E[N_R,N_I,M_R,M_I]}}\\
\Rightarrow\quad \left.\frac{\delta S_E[N_R,N_I,M_R,M_I]}{\delta N_R}\right|_{N_R=N_R^{(0)}} =& -\mathcal{N}\left\langle n^{\alpha\beta}_{\vec{q}R}\right\rangle+\frac{\mathcal{N}}{V}N^{\alpha\beta(0)}_{\vec{q}R}=0\\
\Rightarrow\quad \boxed{N^{\alpha\beta(0)}_{\vec{q}R}=V\left\langle n^{\alpha\beta}_{\vec{q}R}\right\rangle=\left(N^{\alpha\beta(0)}_{\vec{q}R}\right)^\dagger}&
\end{aligned}$$

## C.3 Properties of the Mean fields

This property comes from the fact that, since we are summing over all momenta in the BZ, we can shift $\vec{k}$ by $\vec{k}+\vec{q}$:

$$N^{\beta\alpha(0)}_{-\vec{q}R}=\frac{V}{2\mathcal{N}}\sum_{\vec{k}}\left\langle c^\dagger_{\vec{k}-\vec{q}\beta}c_{\vec{k}\alpha}+c^\dagger_{\vec{k}\alpha}c_{\vec{k}-\vec{q}\beta}\right\rangle\overset{\vec{k}\to\vec{k}+\vec{q}}{=}\frac{V}{2\mathcal{N}}\sum_{\vec{k}}\left\langle c^\dagger_{\vec{k}\beta}c_{\vec{k}+\vec{q}\alpha}+c^\dagger_{\vec{k}+\vec{q}\alpha}c_{\vec{k}\beta}\right\rangle=N^{\alpha\beta(0)}_{\vec{q}R},$$

$$N^{\beta\alpha(0)}_{-\vec{q}I}=\frac{V}{2\mathcal{N}}\sum_{\vec{k}}\left\langle c^\dagger_{\vec{k}-\vec{q}\beta}c_{\vec{k}\alpha}-c^\dagger_{\vec{k}\alpha}c_{\vec{k}-\vec{q}\beta}\right\rangle\overset{\vec{k}\to\vec{k}+\vec{q}}{=}\frac{V}{2\mathcal{N}}\sum_{\vec{k}}\left\langle c^\dagger_{\vec{k}\beta}c_{\vec{k}+\vec{q}\alpha}-c^\dagger_{\vec{k}+\vec{q}\alpha}c_{\vec{k}\beta}\right\rangle=-N^{\alpha\beta(0)}_{\vec{q}I}.$$

However, in general

$$\begin{aligned}
M^{\beta\alpha(0)}_{-\vec{q}R}=&\frac{V}{2\mathcal{N}}\sum_{\vec{k}}\left\langle e^{-2i\vec{k}\cdot\vec{a}_{\beta\alpha}}c^\dagger_{\vec{k}-\vec{q}\beta}c_{\vec{k}\alpha}+e^{-2i\vec{k}\cdot\vec{a}_{\alpha\beta}}c^\dagger_{\vec{k}\alpha}c_{\vec{k}-\vec{q}\beta}\right\rangle\\
\overset{\vec{k}\to\vec{k}+\vec{q}}{=}&\frac{V}{2\mathcal{N}}\sum_{\vec{k}}\left\langle e^{-2i(\vec{k}+\vec{q})\cdot\vec{a}_{\beta\alpha}}c^\dagger_{\vec{k}\beta}c_{\vec{k}+\vec{q}\alpha}+e^{-2i(\vec{k}+\vec{q})\cdot\vec{a}_{\alpha\beta}}c^\dagger_{\vec{k}+\vec{q}\alpha}c_{\vec{k}\beta}\right\rangle\not\propto M^{\alpha\beta(0)}_{\vec{q}R}\\
M^{\beta\alpha(0)}_{-\vec{q}I}=&\frac{V}{2\mathcal{N}}\sum_{\vec{k}}\left\langle e^{-2i\vec{k}\cdot\vec{a}_{\beta\alpha}}c^\dagger_{\vec{k}-\vec{q}\beta}c_{\vec{k}\alpha}-e^{-2i\vec{k}\cdot\vec{a}_{\alpha\beta}}c^\dagger_{\vec{k}\alpha}c_{\vec{k}-\vec{q}\beta}\right\rangle\\
\overset{\vec{k}\to\vec{k}+\vec{q}}{=}&\frac{V}{2\mathcal{N}}\sum_{\vec{k}}\left\langle e^{-2i(\vec{k}+\vec{q})\cdot\vec{a}_{\beta\alpha}}c^\dagger_{\vec{k}\beta}c_{\vec{k}+\vec{q}\alpha}-e^{-2i(\vec{k}+\vec{q})\cdot\vec{a}_{\alpha\beta}}c^\dagger_{\vec{k}+\vec{q}\alpha}c_{\vec{k}\beta}\right\rangle\not\propto M^{\alpha\beta(0)}_{\vec{q}I}
\end{aligned}$$

### C.3.1 At the M point

Making use of the following relations between the $\vec{Q}_i$ and the $\vec{a}_{\mu\nu}$ we can further analyse the $M$ fields:

$$\vec{Q}_1\cdot\vec{a}_{AB}=\frac{1}{4}\vec{g}_1\cdot\vec{t}_2=0 \qquad \vec{Q}_1\cdot\vec{a}_{AC}=\frac{1}{4}\vec{g}_1\cdot\vec{t}_1=\frac{\pi}{2} \qquad \vec{Q}_1\cdot\vec{a}_{BC}=\frac{1}{4}\vec{g}_1\cdot(\vec{t}_1-\vec{t}_2)=\frac{\pi}{2}$$
$$\vec{Q}_2\cdot\vec{a}_{AB}=\frac{1}{4}\vec{g}_2\cdot\vec{t}_2=\frac{\pi}{2} \qquad \vec{Q}_2\cdot\vec{a}_{AC}=\frac{1}{4}\vec{g}_2\cdot\vec{t}_1=0 \qquad \vec{Q}_2\cdot\vec{a}_{BC}=\frac{1}{4}\vec{g}_2\cdot(\vec{t}_1-\vec{t}_2)=-\frac{\pi}{2}$$
$$\vec{Q}_3\cdot\vec{a}_{AB}=\frac{1}{4}(\vec{g}_1+\vec{g}_2)\cdot\vec{t}_2=\frac{\pi}{2} \qquad \vec{Q}_3\cdot\vec{a}_{AC}=\frac{1}{4}(\vec{g}_1+\vec{g}_2)\cdot\vec{t}_1=\frac{\pi}{2}$$
$$\vec{Q}_3\cdot\vec{a}_{BC}=\frac{1}{4}(\vec{g}_1+\vec{g}_2)\cdot(\vec{t}_1-\vec{t}_2)=0$$

and the fact that $e^{\pm\pi}=-1$ .

Therefore, $e^{2i\vec{Q}_i\cdot\vec{a}_{\alpha\beta}}=e^{-2i\vec{Q}_i\cdot\vec{a}_{\alpha\beta}}$ so we can write that at the M point

$$\begin{aligned}
M^{\beta\alpha}_{-\vec{Q}_iR} &= \frac{V}{2\mathcal{N}}\sum_{\vec{k}}\left\langle e^{-2i(\vec{k}+\vec{Q}_i)\cdot\vec{a}_{\beta\alpha}}c^\dagger_{\vec{k}\beta}c_{\vec{k}+\vec{Q}_i\alpha}+e^{-2i(\vec{k}+\vec{Q}_i)\cdot\vec{a}_{\alpha\beta}}c^\dagger_{\vec{k}+\vec{Q}_i\alpha}c_{\vec{k}\beta}\right\rangle \\
&= \frac{V}{2\mathcal{N}}e^{2i\vec{Q}_i\cdot\vec{a}_{\alpha\beta}}\sum_{\vec{k}}\left\langle e^{-2i\vec{k}\cdot\vec{a}_{\beta\alpha}}c^\dagger_{\vec{k}\beta}c_{\vec{k}+\vec{Q}_i\alpha}+e^{-2i\vec{k}\cdot\vec{a}_{\alpha\beta}}c^\dagger_{\vec{k}+\vec{Q}_i\alpha}c_{\vec{k}\beta}\right\rangle \\
&= e^{2i\vec{Q}_i\cdot\vec{a}_{\alpha\beta}}(M^{\alpha\beta}_{\vec{Q}_iR})^\dagger = e^{2i\vec{Q}_i\cdot\vec{a}_{\alpha\beta}}M^{\alpha\beta}_{\vec{Q}_iR} \\
M^{\beta\alpha}_{-\vec{Q}_iI} &= \frac{V}{2\mathcal{N}}\sum_{\vec{k}}\left\langle e^{-2i(\vec{k}+\vec{Q}_i)\cdot\vec{a}_{\beta\alpha}}c^\dagger_{\vec{k}\beta}c_{\vec{k}+\vec{Q}_i\alpha}-e^{-2i(\vec{k}+\vec{Q}_i)\cdot\vec{a}_{\alpha\beta}}c^\dagger_{\vec{k}+\vec{Q}_i\alpha}c_{\vec{k}\beta}\right\rangle \\
&= \frac{V}{2\mathcal{N}}e^{2i\vec{Q}_i\cdot\vec{a}_{\alpha\beta}}\sum_{\vec{k}}\left\langle e^{-2i\vec{k}\cdot\vec{a}_{\beta\alpha}}c^\dagger_{\vec{k}\beta}c_{\vec{k}+\vec{Q}_i\alpha}-e^{-2i\vec{k}\cdot\vec{a}_{\alpha\beta}}c^\dagger_{\vec{k}+\vec{Q}_i\alpha}c_{\vec{k}\beta}\right\rangle \\
&= e^{2i\vec{Q}_i\cdot\vec{a}_{\alpha\beta}}(M^{\alpha\beta}_{\vec{Q}_iI})^\dagger = -e^{2i\vec{Q}_i\cdot\vec{a}_{\alpha\beta}}M^{\alpha\beta}_{\vec{Q}_iI}
\end{aligned}$$

$$\boxed{M^{\beta\alpha}_{-\vec{Q}_iR}=e^{2i\vec{Q}_i\cdot\vec{a}_{\alpha\beta}}(M^{\alpha\beta}_{\vec{Q}_iR})^\dagger=e^{2i\vec{Q}_i\cdot\vec{a}_{\alpha\beta}}M^{\alpha\beta}_{\vec{Q}_iR}} \qquad \boxed{M^{\beta\alpha}_{-\vec{Q}_iI}=e^{2i\vec{Q}_i\cdot\vec{a}_{\alpha\beta}}(M^{\alpha\beta}_{\vec{q}I})^\dagger=-e^{2i\vec{Q}_i\cdot\vec{a}_{\alpha\beta}}M^{\alpha\beta}_{\vec{Q}_iI}}$$

But also, at the M point, since $\vec{Q}_i\equiv-\vec{Q}_i$

$$\boxed{N^{\beta\alpha}_{\vec{Q}_iR}=N^{\alpha\beta}_{\vec{Q}_iR}} \qquad \boxed{N^{\beta\alpha}_{\vec{Q}_iI}=-N^{\alpha\beta}_{\vec{Q}_iI}} \qquad \boxed{M^{\beta\alpha}_{\vec{Q}_iR}=e^{2i\vec{Q}_i\cdot\vec{a}_{\alpha\beta}}M^{\alpha\beta}_{\vec{Q}_iR}} \qquad \boxed{M^{\beta\alpha}_{\vec{Q}_iI}=-e^{2i\vec{Q}_i\cdot\vec{a}_{\alpha\beta}}M^{\alpha\beta}_{\vec{Q}_iI}}$$

Since we know that the only three independent components are $\alpha\beta=AB,AC,BC$, we find that

$$M^{AB}_{\vec{Q}_1R}=M^{BA}_{\vec{Q}_1R} \qquad M^{AC}_{\vec{Q}_1R}=-M^{CA}_{\vec{Q}_1R} \qquad M^{BC}_{\vec{Q}_1R}=-M^{CB}_{\vec{Q}_1R} \tag{C.9}$$
$$M^{AB}_{\vec{Q}_2R}=-M^{BA}_{\vec{Q}_2R} \qquad M^{AC}_{\vec{Q}_2R}=M^{CA}_{\vec{Q}_2R} \qquad M^{BC}_{\vec{Q}_2R}=-M^{CB}_{\vec{Q}_2R} \tag{C.10}$$
$$M^{AB}_{\vec{Q}_3R}=-M^{BA}_{\vec{Q}_3R} \qquad M^{AC}_{\vec{Q}_3R}=-M^{CA}_{\vec{Q}_3R} \qquad M^{BC}_{\vec{Q}_3R}=M^{CB}_{\vec{Q}_3R} \tag{C.11}$$

$$M^{AB}_{\vec{Q}_1I}=-M^{BA}_{\vec{Q}_1I} \qquad M^{AC}_{\vec{Q}_1I}=M^{CA}_{\vec{Q}_1I} \qquad M^{BC}_{\vec{Q}_1I}=M^{CB}_{\vec{Q}_1I} \tag{C.12}$$
$$M^{AB}_{\vec{Q}_2I}=M^{BA}_{\vec{Q}_2I} \qquad M^{AC}_{\vec{Q}_2I}=-M^{CA}_{\vec{Q}_2I} \qquad M^{BC}_{\vec{Q}_2I}=M^{CB}_{\vec{Q}_2I} \tag{C.13}$$
$$M^{AB}_{\vec{Q}_3I}=M^{BA}_{\vec{Q}_3I} \qquad M^{AC}_{\vec{Q}_3I}=M^{CA}_{\vec{Q}_3I} \qquad M^{BC}_{\vec{Q}_3I}=-M^{CB}_{\vec{Q}_3I} \tag{C.14}$$

Therefore, while $N_R$ are always symmetric in sublattice space and $N_I$ antisymmetric, for $M_R, M_I$ it depends on the components. However, if sublattice interference is exact, $M_R$ is symmetric and $M_I$ antisymmetric.

## C.4 TrLog2 for arbitrary $\vec{q}$

$$
\begin{aligned}
\mathrm{Tr}\big((G_0V)^2\big) =& \sum_{\vec{k}\vec{q}}\sum_{\alpha\alpha'}\sum_{\beta\beta'} G_0^{\alpha\alpha'}(\vec{k})\mathcal{V}^{\alpha'\beta}(\vec{k},\vec{k}+\vec{q})G_0^{\beta\beta'}(\vec{k}+\vec{q})\mathcal{V}^{\beta'\alpha}(\vec{k}+\vec{q},\vec{k}) \\
=& \frac{1}{4}\sum_{\vec{k}\vec{q}}\sum_{\alpha\alpha'}\sum_{\beta\beta'}(1-\delta_{\alpha'\beta})(1-\delta_{\alpha\beta'})G_0^{\alpha\alpha'}(\vec{k})G_0^{\beta\beta'}(\vec{k}+\vec{q}) \\
& \Big[2\left(N_{\vec{q}R}^{\beta\alpha'}+N_{\vec{q}I}^{\beta\alpha'}\right)+e^{-2i(\vec{k}+\vec{q})\cdot\vec{a}_{\alpha'\beta}}\left(M_{-\vec{q}R}^{\alpha'\beta}-M_{-\vec{q}I}^{\alpha'\beta}\right)+e^{-2i\vec{k}\cdot\vec{a}_{\alpha'\beta}}\left(M_{\vec{q}R}^{\beta\alpha'}+M_{\vec{q}I}^{\beta\alpha'}\right)\Big] \\
& \Big[2\left(N_{\vec{q}R}^{\beta'\alpha}-N_{\vec{q}I}^{\beta'\alpha}\right)+e^{-2i\vec{k}\cdot\vec{a}_{\beta'\alpha}}\left(M_{\vec{q}R}^{\beta'\alpha}-M_{\vec{q}I}^{\beta'\alpha}\right)+e^{-2i(\vec{k}+\vec{q})\cdot\vec{a}_{\beta'\alpha}}\left(M_{-\vec{q}R}^{\alpha\beta'}+M_{-\vec{q}I}^{\alpha\beta'}\right)\Big] \\
=& \frac{1}{4}\sum_{\vec{k}\vec{q}}\sum_{\alpha\alpha'}\sum_{\beta\beta'}(1-\delta_{\alpha'\beta})(1-\delta_{\alpha\beta'})G_0^{\alpha\alpha'}(\vec{k})G_0^{\beta\beta'}(\vec{k}+\vec{q}) \\
& \Big[4\left(N_{\vec{q}R}^{\beta\alpha'}N_{\vec{q}R}^{\beta'\alpha}+N_{\vec{q}I}^{\beta\alpha'}N_{\vec{q}R}^{\beta'\alpha}-N_{\vec{q}R}^{\beta\alpha'}N_{\vec{q}I}^{\beta'\alpha}-N_{\vec{q}I}^{\beta\alpha'}N_{\vec{q}I}^{\beta'\alpha}\right) \\
& +2e^{-2i\vec{k}\cdot\vec{a}_{\beta'\alpha}}\left(N_{\vec{q}R}^{\beta\alpha'}M_{\vec{q}R}^{\beta'\alpha}+N_{\vec{q}I}^{\beta\alpha'}M_{\vec{q}R}^{\beta'\alpha}-N_{\vec{q}R}^{\beta\alpha'}M_{\vec{q}I}^{\beta'\alpha}-N_{\vec{q}I}^{\beta\alpha'}M_{\vec{q}I}^{\beta'\alpha}\right) \\
& +2e^{-2i(\vec{k}+\vec{q})\cdot\vec{a}_{\beta'\alpha}}\left(N_{\vec{q}R}^{\beta\alpha'}M_{-\vec{q}R}^{\alpha\beta'}+N_{\vec{q}I}^{\beta\alpha'}M_{-\vec{q}R}^{\alpha\beta'}+N_{\vec{q}R}^{\beta\alpha'}M_{-\vec{q}I}^{\alpha\beta'}+N_{\vec{q}I}^{\beta\alpha'}M_{-\vec{q}I}^{\alpha\beta'}\right) \\
& +2e^{-2i(\vec{k}+\vec{q})\cdot\vec{a}_{\alpha'\beta}}\left(M_{-\vec{q}R}^{\alpha'\beta}N_{\vec{q}R}^{\beta'\alpha}-M_{-\vec{q}I}^{\alpha'\beta}N_{\vec{q}R}^{\beta'\alpha}-M_{-\vec{q}R}^{\alpha'\beta}N_{\vec{q}I}^{\beta'\alpha}+M_{-\vec{q}I}^{\alpha'\beta}N_{\vec{q}I}^{\beta'\alpha}\right) \\
& +e^{-2i(\vec{k}+\vec{q})\cdot\vec{a}_{\alpha'\beta}}e^{-2i\vec{k}\cdot\vec{a}_{\beta'\alpha}}\left(M_{-\vec{q}R}^{\alpha'\beta}M_{\vec{q}R}^{\beta'\alpha}-M_{-\vec{q}I}^{\alpha'\beta}M_{\vec{q}R}^{\beta'\alpha}-M_{-\vec{q}R}^{\alpha'\beta}M_{\vec{q}I}^{\beta'\alpha}+M_{-\vec{q}I}^{\alpha'\beta}M_{\vec{q}I}^{\beta'\alpha}\right) \\
& +e^{-2i(\vec{k}+\vec{q})\cdot\vec{a}_{\alpha'\beta}}e^{-2i(\vec{k}+\vec{q})\cdot\vec{a}_{\beta'\alpha}}\left(M_{-\vec{q}R}^{\alpha'\beta}M_{-\vec{q}R}^{\alpha\beta'}-M_{-\vec{q}I}^{\alpha'\beta}M_{-\vec{q}R}^{\alpha\beta'}+M_{-\vec{q}R}^{\alpha'\beta}M_{-\vec{q}I}^{\alpha\beta'}-M_{-\vec{q}I}^{\alpha'\beta}M_{-\vec{q}I}^{\alpha\beta'}\right) \\
& +2e^{-2i\vec{k}\cdot\vec{a}_{\alpha'\beta}}\left(M_{\vec{q}R}^{\beta\alpha'}N_{\vec{q}R}^{\beta'\alpha}+M_{\vec{q}I}^{\beta\alpha'}N_{\vec{q}R}^{\beta'\alpha}-M_{\vec{q}R}^{\beta\alpha'}N_{\vec{q}I}^{\beta'\alpha}-M_{\vec{q}I}^{\beta\alpha'}N_{\vec{q}I}^{\beta'\alpha}\right) \\
& +e^{-2i\vec{k}\cdot\vec{a}_{\alpha'\beta}}e^{-2i\vec{k}\cdot\vec{a}_{\beta'\alpha}}\left(M_{\vec{q}R}^{\beta\alpha'}M_{\vec{q}R}^{\beta'\alpha}+M_{\vec{q}I}^{\beta\alpha'}M_{\vec{q}R}^{\beta'\alpha}-M_{\vec{q}R}^{\beta\alpha'}M_{\vec{q}I}^{\beta'\alpha}-M_{\vec{q}I}^{\beta\alpha'}M_{\vec{q}I}^{\beta'\alpha}\right) \\
& +e^{-2i\vec{k}\cdot\vec{a}_{\alpha'\beta}}e^{-2i(\vec{k}+\vec{q})\cdot\vec{a}_{\beta'\alpha}}\left(M_{\vec{q}R}^{\beta\alpha'}M_{-\vec{q}R}^{\alpha\beta'}+M_{\vec{q}I}^{\beta\alpha'}M_{-\vec{q}R}^{\alpha\beta'}+M_{\vec{q}R}^{\beta\alpha'}M_{-\vec{q}I}^{\alpha\beta'}+M_{\vec{q}I}^{\beta\alpha'}M_{-\vec{q}I}^{\alpha\beta'}\right)\Big] ,
\end{aligned}
$$

which cannot really be simplified (except for the term in $N_{\vec{q}I}^{\beta\alpha'}N_{\vec{q}R}^{\beta'\alpha}$ which is equivalent to the one in $-N_{\vec{q}R}^{\beta\alpha'}N_{\vec{q}I}^{\beta'\alpha}$, as it is shown in the next section of the Appendix) because there is not a expression in general that relates $M_{-\vec{q}R(I)}^{\beta\alpha}$ with $M_{\vec{q}R(I)}^{\alpha\beta(0)}$.

## C.5 TrLog2 at the M point

Since

$$
N_{\vec{Q}_iR}^{\beta\alpha}=N_{\vec{Q}_iR}^{\alpha\beta}\,,\qquad N_{\vec{Q}_iI}^{\beta\alpha}=-N_{\vec{Q}_iI}^{\alpha\beta}\,,\qquad M_{\vec{Q}_iR}^{\beta\alpha}=e^{2i\vec{Q}_i\cdot\vec{a}_{\alpha\beta}}M_{\vec{Q}_iR}^{\alpha\beta}\,,\qquad M_{\vec{Q}_iI}^{\beta\alpha}=-e^{2i\vec{Q}_i\cdot\vec{a}_{\alpha\beta}}M_{\vec{Q}_iI}^{\alpha\beta}\,,
$$

and $\vec{Q}_i$ is equivalent to $-\vec{Q}_i$, we can work first in simplifying $\mathcal{V}$:

$$\begin{aligned}\mathcal{V}^{\alpha'\beta}(\vec{k},\vec{k}+\vec{Q}_i) &= \frac{1}{2}(1-\delta_{\alpha'\beta})\Big[2\left(N^{\beta\alpha'}_{\vec{Q}_iR}+N^{\beta\alpha'}_{\vec{Q}_iI}\right)+e^{-2i(\vec{k}+\vec{Q}_i)\cdot\vec{a}_{\alpha'\beta}}\left(M^{\alpha'\beta}_{-\vec{Q}_iR}-M^{\alpha'\beta}_{-\vec{Q}_iI}\right)\\ &\qquad +e^{-2i\vec{k}\cdot\vec{a}_{\alpha'\beta}}\left(M^{\beta\alpha'}_{\vec{Q}_iR}+M^{\beta\alpha'}_{\vec{Q}_iI}\right)\Big]\\ &= \frac{1}{2}(1-\delta_{\alpha'\beta})\Big[2\left(N^{\beta\alpha'}_{\vec{Q}_iR}+N^{\beta\alpha'}_{\vec{Q}_iI}\right)+e^{2i(\vec{k}+\vec{Q}_i)\cdot\vec{a}_{\beta\alpha'}}e^{2i\vec{Q}_i\cdot\vec{a}_{\beta\alpha'}}\left(M^{\beta\alpha'}_{\vec{Q}_iR}-M^{\beta\alpha'}_{\vec{Q}_iI}\right)\\ &\qquad +e^{2i\vec{k}\cdot\vec{a}_{\beta\alpha'}}\left(M^{\beta\alpha'}_{\vec{Q}_iR}+M^{\beta\alpha'}_{\vec{Q}_iI}\right)\Big]\\ &= (1-\delta_{\alpha'\beta})\Big[\left(N^{\beta\alpha'}_{\vec{Q}_iR}+N^{\beta\alpha'}_{\vec{Q}_iI}\right)+e^{2i\vec{k}\cdot\vec{a}_{\beta\alpha'}}\left(M^{\beta\alpha'}_{\vec{Q}_iR}+M^{\beta\alpha'}_{\vec{Q}_iI}\right)\Big]\,.\end{aligned}$$

For the last equality it has been used that $e^{2i\vec{Q}_i\cdot\vec{a}_{\beta\alpha'}}=\pm1$, so $e^{4i\vec{Q}_i\cdot\vec{a}_{\beta\alpha'}}=1$ always. Analogously,

$$\begin{aligned}\mathcal{V}^{\beta'\alpha}(\vec{k}+\vec{Q}_i,\vec{k}) &= \frac{1}{2}(1-\delta_{\beta'\alpha})\Big[2\left(N^{\beta'\alpha}_{\vec{Q}_iR}-N^{\beta'\alpha}_{\vec{Q}_iI}\right)+e^{-2i\vec{k}\cdot\vec{a}_{\beta'\alpha}}\left(M^{\beta'\alpha}_{\vec{Q}_iR}-M^{\beta'\alpha}_{\vec{Q}_iI}\right)\\ &\qquad +e^{-2i(\vec{k}+\vec{Q}_i)\cdot\vec{a}_{\beta'\alpha}}\left(M^{\alpha\beta'}_{-\vec{Q}_iR}+M^{\alpha\beta'}_{-\vec{Q}_iI}\right)\Big]\\ &= \frac{1}{2}(1-\delta_{\beta'\alpha})\Big[2\left(N^{\beta'\alpha}_{\vec{Q}_iR}-N^{\beta'\alpha}_{\vec{Q}_iI}\right)+e^{-2i\vec{k}\cdot\vec{a}_{\beta'\alpha}}\left(M^{\beta'\alpha}_{\vec{Q}_iR}-M^{\beta'\alpha}_{\vec{Q}_iI}\right)\\ &\qquad +e^{-2i(\vec{k}+\vec{Q}_i)\cdot\vec{a}_{\beta'\alpha}}e^{2i\vec{Q}_i\cdot\vec{a}_{\beta'\alpha}}\left(M^{\beta'\alpha}_{\vec{Q}_iR}-M^{\beta'\alpha}_{\vec{Q}_iI}\right)\Big]\\ &= (1-\delta_{\beta'\alpha})\Big[\left(N^{\beta'\alpha}_{\vec{Q}_iR}-N^{\beta'\alpha}_{\vec{Q}_iI}\right)+e^{-2i\vec{k}\cdot\vec{a}_{\beta'\alpha}}\left(M^{\beta'\alpha}_{\vec{Q}_iR}-M^{\beta'\alpha}_{\vec{Q}_iI}\right)\Big]\,.\end{aligned}$$

Now we can substitute these expressions into (5.26) with the objective of obtaining (5.32).

$$\begin{aligned}\mathrm{Tr}\big((G_0V)^2\big) =& \sum_{\vec{k}\vec{k}'}\sum_{\alpha\alpha'}\sum_{\beta\beta'}G_0^{\alpha\alpha'}(\vec{k})\mathcal{V}^{\alpha'\beta}(\vec{k},\vec{k}')G_0^{\beta\beta'}(\vec{k}')\mathcal{V}^{\beta'\alpha}(\vec{k}',\vec{k})\\ =& \sum_{\vec{k}i}\sum_{\alpha\alpha'}\sum_{\beta\beta'}G_0^{\alpha\alpha'}(\vec{k})\mathcal{V}^{\alpha'\beta}(\vec{k},\vec{k}+\vec{Q}_i)G_0^{\beta\beta'}(\vec{k}+\vec{Q}_i)\mathcal{V}^{\beta'\alpha}(\vec{k}+\vec{Q}_i,\vec{k})\\ =& \sum_{\vec{k}i}\sum_{\alpha\alpha'}\sum_{\beta\beta'}(1-\delta_{\alpha'\beta})(1-\delta_{\beta'\alpha})G_0^{\alpha\alpha'}(\vec{k})G_0^{\beta\beta'}(\vec{k}+\vec{Q}_i)\\ &\Big[\left(N^{\beta\alpha'}_{\vec{Q}_iR}+N^{\beta\alpha'}_{\vec{Q}_iI}\right)+e^{2i\vec{k}\cdot\vec{a}_{\beta\alpha'}}\left(M^{\beta\alpha'}_{\vec{Q}_iR}+M^{\beta\alpha'}_{\vec{Q}_iI}\right)\Big]\\ &\Big[\left(N^{\beta'\alpha}_{\vec{Q}_iR}-N^{\beta'\alpha}_{\vec{Q}_iI}\right)+e^{-2i\vec{k}\cdot\vec{a}_{\beta'\alpha}}\left(M^{\beta'\alpha}_{\vec{Q}_iR}-M^{\beta'\alpha}_{\vec{Q}_iI}\right)\Big]\\ =& \sum_{\vec{k}i}\sum_{\alpha\alpha'}\sum_{\beta\beta'}(1-\delta_{\alpha'\beta})(1-\delta_{\beta'\alpha})G_0^{\alpha\alpha'}(\vec{k})G_0^{\beta\beta'}(\vec{k}+\vec{Q}_i)\\ &\Big[\left(N^{\beta\alpha'}_{\vec{Q}_iR}N^{\beta'\alpha}_{\vec{Q}_iR}+N^{\beta\alpha'}_{\vec{Q}_iI}N^{\beta'\alpha}_{\vec{Q}_iR}-N^{\beta\alpha'}_{\vec{Q}_iR}N^{\beta'\alpha}_{\vec{Q}_iI}-N^{\beta\alpha'}_{\vec{Q}_iI}N^{\beta'\alpha}_{\vec{Q}_iI}\right)\\ &+e^{-2i\vec{k}\cdot\vec{a}_{\beta'\alpha}}\left(N^{\beta\alpha'}_{\vec{Q}_iR}M^{\beta'\alpha}_{\vec{Q}_iR}+N^{\beta\alpha'}_{\vec{Q}_iI}M^{\beta'\alpha}_{\vec{Q}_iR}-N^{\beta\alpha'}_{\vec{Q}_iR}M^{\beta'\alpha}_{\vec{Q}_iI}-N^{\beta\alpha'}_{\vec{Q}_iI}M^{\beta'\alpha}_{\vec{Q}_iI}\right)\\ &+e^{2i\vec{k}\cdot\vec{a}_{\beta\alpha'}}\left(M^{\beta\alpha'}_{\vec{Q}_iR}N^{\beta'\alpha}_{\vec{Q}_iR}+M^{\beta\alpha'}_{\vec{Q}_iI}N^{\beta'\alpha}_{\vec{Q}_iR}-M^{\beta\alpha'}_{\vec{Q}_iR}N^{\beta'\alpha}_{\vec{Q}_iI}-M^{\beta\alpha'}_{\vec{Q}_iI}N^{\beta'\alpha}_{\vec{Q}_iI}\right)\\ &+e^{2i\vec{k}\cdot\vec{a}_{\beta\alpha'}}e^{-2i\vec{k}\cdot\vec{a}_{\beta'\alpha}}\left(M^{\beta\alpha'}_{\vec{Q}_iR}M^{\beta'\alpha}_{\vec{Q}_iR}+M^{\beta\alpha'}_{\vec{Q}_iI}M^{\beta'\alpha}_{\vec{Q}_iR}-M^{\beta\alpha'}_{\vec{Q}_iR}M^{\beta'\alpha}_{\vec{Q}_iI}-M^{\beta\alpha'}_{\vec{Q}_iI}M^{\beta'\alpha}_{\vec{Q}_iI}\right)\Big]\,.\end{aligned}$$

Now, let us see how it is possible to simplify some of the terms. First of all, let us see how the term in $N^{\beta\alpha'}_{\vec{q}I}N^{\beta'\alpha}_{\vec{q}R}$ is equivalent to the one in $-N^{\beta\alpha'}_{\vec{q}R}N^{\beta'\alpha}_{\vec{q}I}$, which means showing that

$$
\begin{aligned}
T_{N_I N_R} &= \sum_{\vec{k}i} \sum_{\alpha\alpha'} \sum_{\beta\beta'} (1-\delta_{\alpha'\beta})(1-\delta_{\beta'\alpha}) G_0^{\alpha\alpha'}(\vec{k}) G_0^{\beta\beta'}(\vec{k}+\vec{Q}_i) N^{\beta\alpha'}_{\vec{Q}_i I} N^{\beta'\alpha}_{\vec{Q}_i R} \\
&= -\sum_{\vec{k}i} \sum_{\alpha\alpha'} \sum_{\beta\beta'} (1-\delta_{\alpha'\beta})(1-\delta_{\beta'\alpha}) G_0^{\alpha\alpha'}(\vec{k}) G_0^{\beta\beta'}(\vec{k}+\vec{Q}_i) N^{\beta\alpha'}_{\vec{Q}_i R} N^{\beta'\alpha}_{\vec{Q}_i I} \ .
\end{aligned}
$$

To show this I will start from the first equality, where we can use that, since we are summing over all of the sublattice indices, we can relabel $\alpha \leftrightarrow \beta$ and $\alpha' \leftrightarrow \beta'$:

$$
T_{N_I N_R} = \sum_{\vec{k}i} \sum_{\alpha\alpha'} \sum_{\beta\beta'} (1-\delta_{\alpha'\beta})(1-\delta_{\beta'\alpha}) G_0^{\beta\beta'}(\vec{k}) G_0^{\alpha\alpha'}(\vec{k}+\vec{Q}_i) N^{\alpha\beta'}_{\vec{Q}_i I} N^{\alpha'\beta}_{\vec{Q}_i R} \ .
$$

Now, in order to have the terms in the Green functions the same, we can first shift the momentum transferred $\vec{Q}_i \to \vec{Q}_i$, and then shift the momentum $\vec{k} \to \vec{k}+\vec{Q}_i$, which we can do because we are summing over all momenta:

$$
T_{N_I N_R} = \sum_{\vec{k}i} \sum_{\alpha\alpha'} \sum_{\beta\beta'} (1-\delta_{\alpha'\beta})(1-\delta_{\beta'\alpha}) G_0^{\beta\beta'}(\vec{k}+\vec{Q}_i) G_0^{\alpha\alpha'}(\vec{k}) N^{\alpha\beta'}_{-\vec{Q}_i I} N^{\alpha'\beta}_{-\vec{Q}_i R} \ .
$$

Finally, to match the correct sublattice indices, we can use (C.5), so that we find that the two terms are indeed the same:

$$
T_{N_I N_R} = -\sum_{\vec{k}i} \sum_{\alpha\alpha'} \sum_{\beta\beta'} (1-\delta_{\alpha'\beta})(1-\delta_{\beta'\alpha}) G_0^{\beta\beta'}(\vec{k}+\vec{Q}_i) G_0^{\alpha\alpha'}(\vec{k}) N^{\beta'\alpha}_{\vec{Q}_i I} N^{\beta\alpha'}_{\vec{Q}_i R} \ .
$$

The same steps and transformations can be used to show it for one of the terms that has an exponential prefactor:

$$
\begin{aligned}
T_{N_I M_R} &= \sum_{\vec{k}i} \sum_{\alpha\alpha'} \sum_{\beta\beta'} (1-\delta_{\alpha'\beta})(1-\delta_{\beta'\alpha}) G_0^{\alpha\alpha'}(\vec{k}) G_0^{\beta\beta'}(\vec{k}+\vec{Q}_i) e^{-2i\vec{k}\cdot\vec{a}_{\beta'\alpha}} N^{\beta\alpha'}_{\vec{Q}_i I} M^{\beta'\alpha}_{\vec{Q}_i R} \\
&= \sum_{\vec{k}i} \sum_{\alpha\alpha'} \sum_{\beta\beta'} (1-\delta_{\alpha'\beta})(1-\delta_{\beta'\alpha}) G_0^{\beta\beta'}(\vec{k}) G_0^{\alpha\alpha'}(\vec{k}+\vec{Q}_i) e^{-2i\vec{k}\cdot\vec{a}_{\alpha'\beta}} N^{\alpha\beta'}_{\vec{Q}_i I} M^{\alpha'\beta}_{\vec{Q}_i R} \\
&= \sum_{\vec{k}i} \sum_{\alpha\alpha'} \sum_{\beta\beta'} (1-\delta_{\alpha'\beta})(1-\delta_{\beta'\alpha}) G_0^{\beta\beta'}(\vec{k}+\vec{Q}_i) G_0^{\alpha\alpha'}(\vec{k}) e^{2i(\vec{k}+\vec{Q}_i)\cdot\vec{a}_{\beta\alpha'}} N^{\alpha\beta'}_{-\vec{Q}_i I} M^{\alpha'\beta}_{-\vec{Q}_i R} \\
&= -\sum_{\vec{k}i} \sum_{\alpha\alpha'} \sum_{\beta\beta'} (1-\delta_{\alpha'\beta})(1-\delta_{\beta'\alpha}) G_0^{\beta\beta'}(\vec{k}+\vec{Q}_i) G_0^{\alpha\alpha'}(\vec{k}) e^{2i\vec{k}\cdot\vec{a}_{\beta\alpha'}} N^{\beta'\alpha}_{\vec{Q}_i I} M^{\beta\alpha'}_{\vec{Q}_i R} \ .
\end{aligned}
$$

An analogous procedure can be followed to show that the rest of the terms are equal to the one with the fields in opposite order, simplifying the expression of $\mathrm{Tr}\big((G_0 V)^2\big)$ to be:

$$
\begin{aligned}
\mathrm{Tr}\big((G_0V)^2\big) =& \sum_{\vec{k}i}\sum_{\alpha\alpha'}\sum_{\beta\beta'}(1-\delta_{\alpha'\beta})(1-\delta_{\beta'\alpha})G_0^{\alpha\alpha'}(\vec{k})G_0^{\beta\beta'}(\vec{k}+\vec{Q}_i) \\
& \Big[\Big(N^{\beta\alpha'}_{\vec{Q}_iR}N^{\beta'\alpha}_{\vec{Q}_iR}+2N^{\beta\alpha'}_{\vec{Q}_iI}N^{\beta'\alpha}_{\vec{Q}_iR}-N^{\beta\alpha'}_{\vec{Q}_iI}N^{\beta'\alpha}_{\vec{Q}_iI}\Big) \\
& +2e^{-2i\vec{k}\cdot\vec{a}_{\beta'\alpha}}\Big(N^{\beta\alpha'}_{\vec{Q}_iR}M^{\beta'\alpha}_{\vec{Q}_iR}+N^{\beta\alpha'}_{\vec{Q}_iI}M^{\beta'\alpha}_{\vec{Q}_iR}-N^{\beta\alpha'}_{\vec{Q}_iR}M^{\beta'\alpha}_{\vec{Q}_iI}-N^{\beta\alpha'}_{\vec{Q}_iI}M^{\beta'\alpha}_{\vec{Q}_iI}\Big) \\
& +e^{-2i\vec{k}\cdot(\vec{a}_{\beta'\alpha}-\vec{a}_{\beta\alpha'})}\Big(M^{\beta\alpha'}_{\vec{Q}_iR}M^{\beta'\alpha}_{\vec{Q}_iR}+2M^{\beta\alpha'}_{\vec{Q}_iI}M^{\beta'\alpha}_{\vec{Q}_iR}-M^{\beta\alpha'}_{\vec{Q}_iI}M^{\beta'\alpha}_{\vec{Q}_iI}\Big)\Big] \\
=& \sum_{i}\sum_{\alpha\alpha'}\sum_{\beta\beta'}\Big[C_{NN}^{\beta\alpha'\beta'\alpha}(\vec{Q}_i)\Big(N^{\beta\alpha'}_{\vec{Q}_iR}N^{\beta'\alpha}_{\vec{Q}_iR}+2N^{\beta\alpha'}_{\vec{Q}_iI}N^{\beta'\alpha}_{\vec{Q}_iR}-N^{\beta\alpha'}_{\vec{Q}_iI}N^{\beta'\alpha}_{\vec{Q}_iI}\Big) \\
& +C_{MM}^{\beta\alpha'\beta'\alpha}(\vec{Q}_i)\Big(M^{\beta\alpha'}_{\vec{Q}_iR}M^{\beta'\alpha}_{\vec{Q}_iR}+2M^{\beta\alpha'}_{\vec{Q}_iI}M^{\beta'\alpha}_{\vec{Q}_iR}-M^{\beta\alpha'}_{\vec{Q}_iI}M^{\beta'\alpha}_{\vec{Q}_iI}\Big) \\
& +C_{NM}^{\beta\alpha'\beta'\alpha}(\vec{Q}_i)\Big(N^{\beta\alpha'}_{\vec{Q}_iR}M^{\beta'\alpha}_{\vec{Q}_iR}+N^{\beta\alpha'}_{\vec{Q}_iI}M^{\beta'\alpha}_{\vec{Q}_iR}-N^{\beta\alpha'}_{\vec{Q}_iR}M^{\beta'\alpha}_{\vec{Q}_iI}-N^{\beta\alpha'}_{\vec{Q}_iI}M^{\beta'\alpha}_{\vec{Q}_iI}\Big)\Big] ,
\end{aligned}
$$

with

$$
\begin{aligned}
C_{NN}^{\beta\alpha'\beta'\alpha}(\vec{Q}_i) =& (1-\delta_{\alpha'\beta})(1-\delta_{\alpha\beta'})\sum_{\vec{k}}G_0^{\alpha\alpha'}(\vec{k})G_0^{\beta\beta'}(\vec{k}+\vec{Q}_i) , \\
C_{MM}^{\beta\alpha'\beta'\alpha}(\vec{Q}_i) =& (1-\delta_{\alpha'\beta})(1-\delta_{\alpha\beta'})\sum_{\vec{k}}G_0^{\alpha\alpha'}(\vec{k})G_0^{\beta\beta'}(\vec{k}+\vec{Q}_i)e^{-2i\vec{k}\cdot(\vec{a}_{\beta'\alpha}-\vec{a}_{\beta\alpha'})} , \\
C_{NM}^{\beta\alpha'\beta'\alpha}(\vec{Q}_i) =& 2(1-\delta_{\alpha'\beta})(1-\delta_{\alpha\beta'})\sum_{\vec{k}}G_0^{\alpha\alpha'}(\vec{k})G_0^{\beta\beta'}(\vec{k}+\vec{Q}_i)e^{-2i\vec{k}\cdot\vec{a}_{\beta'\alpha}} .
\end{aligned}
$$

Furthermore, logic tells us that all of the terms that are a product of a real and an imaginary field should be zero, since the free energy needs to be real. Let us see a way to show that said terms are indeed zero.

$$
\begin{aligned}
\text{Imaginary terms} = \sum_{i}\sum_{\alpha\alpha'}\sum_{\beta\beta'}\Big[& 2C_{NN}^{\beta\alpha'\beta'\alpha}(\vec{Q}_i)N^{\beta\alpha'}_{\vec{Q}_iI}N^{\beta'\alpha}_{\vec{Q}_iR}+2C_{MM}^{\beta\alpha'\beta'\alpha}(\vec{Q}_i)M^{\beta\alpha'}_{\vec{Q}_iI}M^{\beta'\alpha}_{\vec{Q}_iR} \\
& +C_{NM}^{\beta\alpha'\beta'\alpha}(\vec{Q}_i)\Big(N^{\beta\alpha'}_{\vec{Q}_iI}M^{\beta'\alpha}_{\vec{Q}_iR}-N^{\beta\alpha'}_{\vec{Q}_iR}M^{\beta'\alpha}_{\vec{Q}_iI}\Big)\Big] .
\end{aligned}
$$

First we can transpose the fields using (C.5):

$$
\begin{aligned}
\text{Imaginary terms} = \sum_{i}\sum_{\alpha\alpha'}\sum_{\beta\beta'}\Big[& -2C_{NN}^{\beta\alpha'\beta'\alpha}(\vec{Q}_i)N^{\alpha'\beta}_{\vec{Q}_iI}N^{\alpha\beta'}_{\vec{Q}_iR} \\
& -2e^{2i\vec{Q}_i\cdot\vec{a}_{\alpha'\beta}}e^{2i\vec{Q}_i\cdot\vec{a}_{\alpha\beta'}}C_{MM}^{\beta\alpha'\beta'\alpha}(\vec{Q}_i)M^{\alpha'\beta}_{\vec{Q}_iI}M^{\alpha\beta'}_{\vec{Q}_iR} \\
& -e^{2i\vec{Q}_i\cdot\vec{a}_{\alpha\beta'}}C_{NM}^{\beta\alpha'\beta'\alpha}(\vec{Q}_i)\Big(N^{\alpha'\beta}_{\vec{Q}_iI}M^{\alpha\beta'}_{\vec{Q}_iR}-N^{\alpha'\beta}_{\vec{Q}_iR}M^{\alpha\beta'}_{\vec{Q}_iI}\Big)\Big] ,
\end{aligned}
$$

And now we can relabel $\beta \leftrightarrow \alpha', \beta' \leftrightarrow \alpha$ to recover the initial indices that the fields had before:

$$
\begin{aligned}
\text{Imaginary terms} = \sum_{i}\sum_{\alpha\alpha'}\sum_{\beta\beta'}\Big[& -2C_{NN}^{\alpha'\beta\alpha\beta'}(\vec{Q}_i)N^{\beta\alpha'}_{\vec{Q}_iI}N^{\beta'\alpha}_{\vec{Q}_iR} \\
& -2e^{2i\vec{Q}_i\cdot(\vec{a}_{\beta\alpha'}+\vec{a}_{\beta'\alpha})}C_{MM}^{\alpha'\beta\alpha\beta'}(\vec{Q}_i)M^{\beta\alpha'}_{\vec{Q}_iI}M^{\beta'\alpha}_{\vec{Q}_iR} \\
& -e^{2i\vec{Q}_i\cdot\vec{a}_{\beta'\alpha}}C_{NM}^{\alpha'\beta\alpha\beta'}(\vec{Q}_i)\Big(N^{\beta\alpha'}_{\vec{Q}_iI}M^{\beta'\alpha}_{\vec{Q}_iR}-N^{\beta\alpha'}_{\vec{Q}_iR}M^{\beta'\alpha}_{\vec{Q}_iI}\Big)\Big] .
\end{aligned}
$$

We can see that all the terms have changed sign under these manipulations. Hence, if we could show that

$$C_{NN}^{\beta\alpha'\beta'\alpha}(\vec{Q}_i) = C_{NN}^{\alpha'\beta\alpha\beta'}(\vec{Q}_i) \ , \tag{C.15a}$$

$$C_{MM}^{\beta\alpha'\beta'\alpha}(\vec{Q}_i) = e^{2i\vec{Q}_i\cdot(\vec{a}_{\beta\alpha'}+\vec{a}_{\beta'\alpha})} C_{MM}^{\alpha'\beta\alpha\beta'}(\vec{Q}_i) \ , \tag{C.15b}$$

$$C_{NM}^{\beta\alpha'\beta'\alpha}(\vec{Q}_i) = e^{2i\vec{Q}_i\cdot\vec{a}_{\beta'\alpha}} C_{NM}^{\alpha'\beta\alpha\beta'}(\vec{Q}_i) \ , \tag{C.15c}$$

we would be showing that those terms are zero. This can be done numerically, results of which can be found in Fig. C.1 at the upper vH point. Since we find that the matrices resulting from the matrix elements on both sides of each equation are the same, we conclude that the corresponding terms in the free energy vanish. It was also verified at different chemical potentials, although for simplicity, in C.1 only the calculations for the upper vH point are shown.

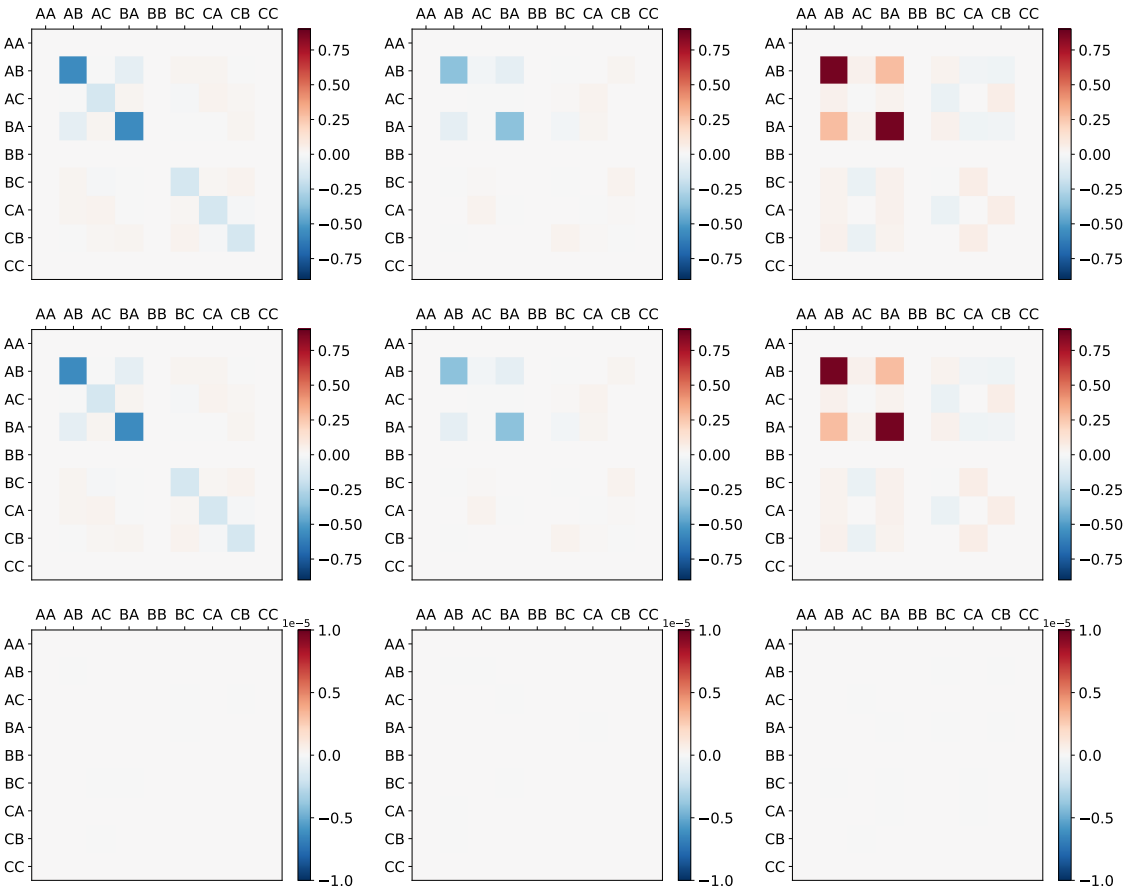


Figure C.1: Comparison of the matrices arising from the two different ways of defining the matrix elements, as shown in (C.15), for $\mu = 0$. (a)-(c) represent the graphical representation of the matrices with the matrix elements in the left-hand-sides of (C.15) and (d)-(f) the right-hand-sides, respectively. (g)-(i) show the difference between the two.

As a result, the final expression for the second order term of the TrLog expansion at the $M$ point is

$$\begin{aligned}\mathrm{Tr}\big((G_0V)^2\big) = \sum_i \sum_{\alpha\alpha'} \sum_{\beta\beta'} \Big[ & C_{NN}^{\beta\alpha'\beta'\alpha}(\vec{Q}_i)\left(N_{\vec{Q}_iR}^{\beta\alpha'}N_{\vec{Q}_iR}^{\beta'\alpha} - N_{\vec{Q}_iI}^{\beta\alpha'}N_{\vec{Q}_iI}^{\beta'\alpha}\right) \\ & + C_{MM}^{\beta\alpha'\beta'\alpha}(\vec{Q}_i)\left(M_{\vec{Q}_iR}^{\beta\alpha'}M_{\vec{Q}_iR}^{\beta'\alpha} - M_{\vec{Q}_iI}^{\beta\alpha'}M_{\vec{Q}_iI}^{\beta'\alpha}\right) \\ & + C_{NM}^{\beta\alpha'\beta'\alpha}(\vec{Q}_i)\left(N_{\vec{Q}_iR}^{\beta\alpha'}M_{\vec{Q}_iR}^{\beta'\alpha} - N_{\vec{Q}_iI}^{\beta\alpha'}M_{\vec{Q}_iI}^{\beta'\alpha}\right)\Big] ,\end{aligned}$$

with

$$\begin{aligned}C_{NN}^{\beta\alpha'\beta'\alpha}(\vec{Q}_i) =& (1-\delta_{\alpha'\beta})(1-\delta_{\alpha\beta'})\sum_{\vec{k}} G_0^{\alpha\alpha'}(\vec{k})G_0^{\beta\beta'}(\vec{k}+\vec{Q}_i) ,\\ C_{MM}^{\beta\alpha'\beta'\alpha}(\vec{Q}_i) =& (1-\delta_{\alpha'\beta})(1-\delta_{\alpha\beta'})\sum_{\vec{k}} G_0^{\alpha\alpha'}(\vec{k})G_0^{\beta\beta'}(\vec{k}+\vec{Q}_i)e^{-2i\vec{k}\cdot(\vec{a}_{\beta'\alpha}-\vec{a}_{\beta\alpha'})} ,\\ C_{NM}^{\beta\alpha'\beta'\alpha}(\vec{Q}_i) =& 2(1-\delta_{\alpha'\beta})(1-\delta_{\alpha\beta'})\sum_{\vec{k}} G_0^{\alpha\alpha'}(\vec{k})G_0^{\beta\beta'}(\vec{k}+\vec{Q}_i)e^{-2i\vec{k}\cdot\vec{a}_{\beta'\alpha}} .\end{aligned}$$

## C.6 Numerical details

The momentum grid was chosen so that in the calculation of the coefficients the greater error made between probed grid sizes was smaller than $10^{-4}$ as depicted in Fig. C.2. The chosen coefficient to calculate was $C_{NN}$.

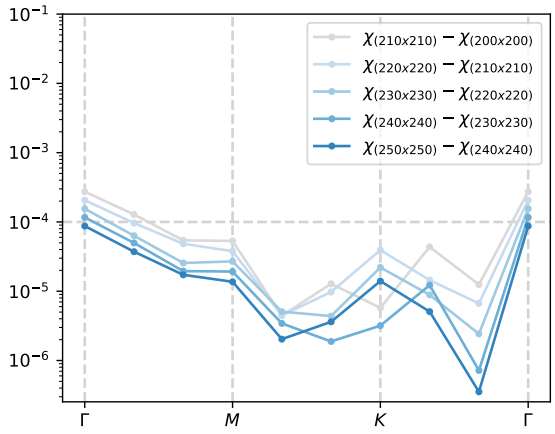


Figure C.2: Comparison of the error made between different chosen k-grid sizes when calculating the coefficient $C_{NN}$.

A similar calculation was made for the bare susceptibility, the results of which are found in Fig. C.3. There is also a comparisson between the usual grid size, $250 \times 250$, the one used for calculating Fig. **??**(b), which shows that the qualitative information obtained from the figure is still valid.

The calculated bare susceptibility at $\mu = 0.08$ can also be compared to the one calculated in Ref. [29], shown in Fig. C.4. The only difference seems to be a factor of 2, which could come from a spin sum.

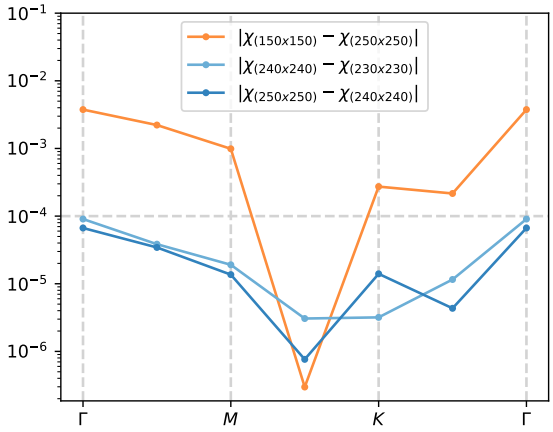


Figure C.3: Comparison of the error made between different chosen k-grid sizes when calculating the bare susceptibility $\chi_0$ from (5.29).

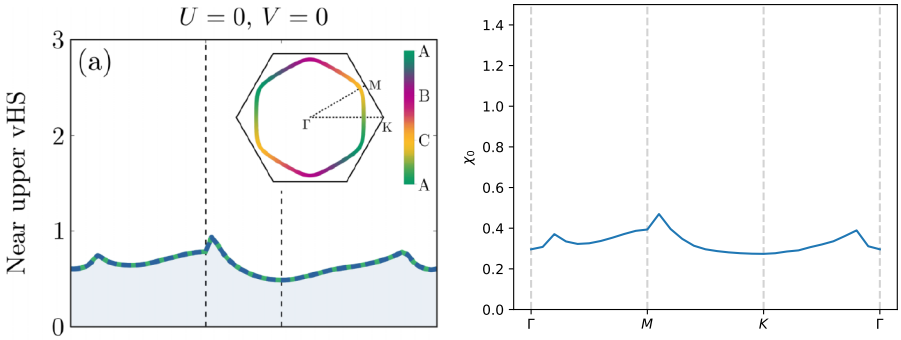


Figure C.4: Comparison of the bare susceptibility at $\mu = 0.08$ calculated in Ref. [29] (left) and my calculation (right).

# Bibliography


[1] Ortiz, B. R. *et al.* New kagome prototype materials: discovery of $KV_3Sb_5, RbV_3Sb_5$, and $CsV_3Sb_5$. *Phys. Rev. Mater.* **3**, 094407 (2019).

[2] Ortiz, B. R. *et al.* Fermi Surface Mapping and the Nature of Charge-Density-Wave Order in the Kagome Superconductor $CsV_3Sb_5$. *Phys. Rev. X* **11**, 041030 (2021).

[3] Neupert, T., Denner, M. M., Yin, J.-X., Thomale, R. & Hasan, M. Z. Charge order and superconductivity in kagome materials. *Nat. Phys.* **18**, 137–143 (2022).

[4] Jiang, H.-M., Liu, M.-X. & Yu, S.-L. Impact of the orbital current order on the superconducting properties of the kagome superconductors. *Phys. Rev. B* **107**, 064506 (2023).

[5] Park, T., Ye, M. & Balents, L. Electronic instabilities of kagome metals: Saddle points and Landau theory. *Phys. Rev. B* **104**, 035142 (2021).

[6] Zhao, H. *et al.* Cascade of correlated electron states in a kagome superconductor CsV3Sb5. *arXiv* (2021). `2103.03118`.

[7] Ortiz, B. R. *et al.* Superconductivity in the $\mathbb{Z}_2$ kagome metal $KV_3Sb_5$. *Phys. Rev. Mater.* **5**, 034801 (2021).

[8] Ortiz, B. R. *et al.* $CsV_3Sb_5$: A $\mathbb{Z}_2$ Topological Kagome Metal with a Superconducting Ground State. *Phys. Rev. Lett.* **125**, 247002 (2020).

[9] Buiarelli, L. Private communication (2023).

[10] Yin, Q. *et al.* Superconductivity and Normal-State Properties of Kagome Metal RbV3Sb5 Single Crystals. *Chin. Phys. Lett.* **38**, 037403 (2021).

[11] Kenney, E. M., Ortiz, B. R., Wang, C., Wilson, S. D. & Graf, M. J. Absence of local moments in the kagome metal KV3Sb5 as determined by muon spin spectroscopy. *J. Phys.: Condens. Matter* **33**, 235801 (2021).

[12] Jiang, Y.-X. *et al.* Unconventional chiral charge order in kagome superconductor KV3Sb5. *Nat. Mater.* **20**, 1353–1357 (2021).

[13] Luo, H. *et al.* Electronic nature of charge density wave and electron-phonon coupling in kagome superconductor KV3Sb5. *Nat. Commun.* **13**, 1–8 (2022).

[14] Liang, Z. *et al.* Three-Dimensional Charge Density Wave and Surface-Dependent Vortex-Core States in a Kagome Superconductor $CsV_3Sb_5$. *Phys. Rev. X* **11**, 031026 (2021).

[15] Wang, Z. *et al.* Electronic nature of chiral charge order in the kagome superconductor $CsV_3Sb_5$. *Phys. Rev. B* **104**, 075148 (2021).

[16] Shumiya, N. *et al.* Intrinsic nature of chiral charge order in the kagome superconductor $RbV_3Sb_5$. *Phys. Rev. B* **104**, 035131 (2021).

[17] Mielke, C. *et al.* Time-reversal symmetry-breaking charge order in a kagome superconductor. *Nature* **602**, 245–250 (2022).

[18] Altland, A. & Simons, B. D. *Condensed Matter Field Theory* (Cambridge University Press, Cambridge, England, UK, 2010).

[19] Tan, H., Liu, Y., Wang, Z. & Yan, B. Charge Density Waves and Electronic Properties of Superconducting Kagome Metals. *Phys. Rev. Lett.* **127**, 046401 (2021).

[20] Ratcliff, N., Hallett, L., Ortiz, B. R., Wilson, S. D. & Harter, J. W. Coherent phonon spectroscopy and interlayer modulation of charge density wave order in the kagome metal $CsV_3Sb_5$. *Phys. Rev. Mater.* **5**, L111801 (2021).

[21] Christensen, M. H., Birol, T., Andersen, B. M. & Fernandes, R. M. Theory of the charge density wave in $AV_3Sb_5$ kagome metals. *Phys. Rev. B* **104**, 214513 (2021).

[22] Lin, Y.-P. & Nandkishore, R. M. Chiral twist on the high-$T_c$ phase diagram in moir\'e heterostructures. *Phys. Rev. B* **100**, 085136 (2019).

[23] Lin, Y.-P. & Nandkishore, R. M. Complex charge density waves at Van Hove singularity on hexagonal lattices: Haldane-model phase diagram and potential realization in the kagome metals $AV_3Sb_5$ ($A$=K, Rb, Cs). *Phys. Rev. B* **104**, 045122 (2021).

[24] Kiesel, M. L., Platt, C. & Thomale, R. Unconventional Fermi Surface Instabilities in the Kagome Hubbard Model. *Phys. Rev. Lett.* **110**, 126405 (2013).

[25] Xiang, Y. *et al.* Twofold symmetry of $c$-axis resistivity in topological kagome superconductor $CsV_3Sb_5$ with in-plane rotating magnetic field. *arXiv* (2021). 2104.06909.

[26] Christensen, M. H., Birol, T., Andersen, B. M. & Fernandes, R. M. Loop currents in $AV_3Sb_5$ kagome metals: multipolar and toroidal magnetic orders. *arXiv* (2022). 2207.12820.

[27] Denner, M. M., Thomale, R. & Neupert, T. Analysis of Charge Order in the Kagome Metal $AV_3Sb_5$ ($A = \mathrm{K}, \mathrm{Rb}, \mathrm{Cs}$). *Phys. Rev. Lett.* **127**, 217601 (2021).

[28] Kiesel, M. L. & Thomale, R. Sublattice interference in the kagome Hubbard model. *Phys. Rev. B* **86**, 121105 (2012).

[29] Rømer, A. T., Bhattacharyya, S., Valentí, R., Christensen, M. H. & Andersen, B. M. Superconductivity from repulsive interactions on the kagome lattice. *Phys. Rev. B* **106**, 174514 (2022).